MATHEMATICAL MODELLING OF THE DYNAMICS OF GRANULAR MATERIALS IN A ROTATING CYLINDER

Thesis submitted to

THE COCHIN UNIVERSITY OF SCIENCE AND TECHNOLOGY

in partial fulfillment of the requirements

for the degree of

DOCTOR OF PHILOSOPHY

in

SCIENCE

by

V. HEMA
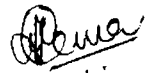
under the supervision of

Dr. S. SAVITHRI

REGIONAL RESEARCH LABORATORY (CSIR)

Thiruvananthapuram

November 2003

Declaration

I, Hema V., do hereby declare that the matter embodied in this thesis entitled "**Mathematical Modelling of the Dynamics of Granular Materials in a Rotating Cylinder**" is the result of the investigations carried out by me in the Computational Modelling and Simulation Unit of the Regional Research Laboratory (CSIR), Thiruvananthapuram, under the guidance of **Dr. S. Savithri**, and that the same has not been submitted elsewhere for any other degree.

In keeping with the general practice of reporting scientific observations, due acknowledgement has been made wherever the work described is based on the findings of other investigators.

Hema V.

Dr. S. Savithri
Scientist

CERTIFICATE

This is to certify that the work outlined the thesis entitled "**Mathematical Modelling of the Dynamics of Granular Materials in a Rotating Cylinder**" is an authentic record of the research work carried out by **V. Hema** under my supervision in partial fulfillment of the requirements for the degree of **Doctor of Philosophy** of the **Cochin University of Science and Technology** and further that no part thereof has been submitted elsewhere for any other degree.

Dr. S. Savithri

(Supervisor)

Acknowledgements

I wish to express my deep sense of gratitude to my supervisor Dr. S. Savithri for her guidance and sincere involvement throughout my Ph. D work, right from suggesting the problem till the completion of the work. Her sharp observations and innovative ideas were intellectually enlightening and were of valuable help in setting out the proper direction of the work. Personally, her devotion to work was a great source of inspiration to me, and her attitude was always pleasant and friendly. She was always available for discussions and lent me a patient hearing every time. Without her wholehearted support in every aspect of the work, it would not have been possible for me to complete the work in time. I am very much indebted to her for whatever I have achieved in my research tenure.

I am very grateful to Dr. G. D. Surender, Deputy Director, RRL for all the help I received from him. I benefited immensely from his vast knowledge, intellectual superiority and expertise in the field during the course of work and while preparing the draft of the thesis. I am grateful for his encouragement and willingness to help, which were a motivation for me in my work and my academic life.

I acknowledge with thanks the numerous help received from Dr. Roschen Sasikumar, Head, Computational Modelling and Simulation, in both scientific and personal matters. She helped me in brushing up my scientific spirit and was always ready to clear even my small doubts with sincere involvement.

I remember with thanks Mrs. Elizabeth Jacob, Scientist, for her support and friendly attitude during my tenure at RRL. I acknowledge with thanks the timely help and support received from Dr. C. Chandrasekhara Bhat, Dr. M. Ravi, Dr. T. R. Ramamohan and Dr. P. Shanmugham.

My sincere thanks to Dr. B. C. Pai, Director, RRL for his support and encouragement right from the beginning of my research. I also thank Dr. G. Vijay Nair, former Director, RRL for his support.

Abstract

A fundamental understanding of mixing and blending of granular materials in horizontal rotating cylinders will be beneficial to a wide range of industries: pharmaceuticals, metallurgy, ceramics, composites, polymers, food processing and agriculture. Yet, in relation to its industrial prevalence, the understanding of granular mixing lags considerably when compared to that of liquid mixing.

Granular bed motion in the transverse cross section of a horizontal rotating cylinder is fundamental in determining advective heat transfer as well as axial flow of the bed material; but to date studies have been mainly empirical aimed at determining the macroscopic bed motion but devoid of detailed information of granular bed dynamics at a microscopic level.

The current study is therefore aimed at the development of a theoretical simulation tool based on Discrete Element Method (DEM) to interpret granular dynamics of solid bed in the cross section of the horizontal rotating cylinder at the microscopic level and subsequently apply this model to establish the transition behaviour, mixing and segregation.

The simulation of the granular motion developed in this work is based on solving Newton's equation of motion for each particle in the granular bed subjected to the collisional forces, external forces and boundary forces. At every instant of time, the forces are tracked and the positions, velocities and accelerations of each particle is

The software code for this simulation is written in VISUAL FORTRAN 90. After checking the validity of the code with special tests, it is used to investigate the transition behaviour of granular solids motion in the cross section of a rotating cylinder for various rotational speeds and fill fraction.

This work is hence directed towards a theoretical investigation based on Discrete Element Method (DEM) of the motion of granular solids in the radial direction of the horizontal cylinder to elucidate the relationship between the operating parameters of the rotating cylinder geometry and physical properties of the granular solid.

The operating parameters of the rotating cylinder include the various rotational velocities of the cylinder and volumetric fill. The physical properties of the granular solids include particle sizes, densities, stiffness coefficients, and coefficient of friction. Further the work highlights the fundamental basis for the important phenomena of the system namely; (i) the different modes of solids motion observed in a transverse cross-section of the rotating cylinder for various rotational speeds, (ii) the radial mixing of the granular solid in terms of active layer depth (iii) rate coefficient of mixing as well as the transition behaviour in terms of the bed turnover time and rotational speed and (iv) the segregation mechanisms resulting from differences in the size and density of particles.

The transition behaviour involving its six different modes of motion of the granular solid bed is quantified in terms of Froude number and the results obtained are validated with experimental and theoretical results reported in the literature. The transition from slumping to rolling mode is quantified using the bed turnover time and a linear relationship is established between the bed turn over time and the inverse of the rotational speed of the cylinder as predicted by Davidson et al.[2000]. The effect of the rotational speed, fill fraction and coefficient of friction on the dynamic angle of repose are presented and discussed. The variation of active layer depth with respect to fill fraction and rotational speed have been investigated. The results obtained through

simulation are compared with the experimental results reported by Van Puyvelde *et. al.* [2000] and Ding *et al.* [2002].

The theoretical model has been further extended, to study the mixing and segregation in the transverse direction for different particle sizes and their size ratios. The effect of fill fraction and rotational speed on the transverse mixing behaviour is presented in the form of a mixing index and mixing kinetics curve. The segregation pattern obtained by the simulation of the granular solid bed with respect to the rotational speed of the cylinder is presented both in graphical and numerical forms. The segregation behaviour of the granular solid bed with respect to particle size, density and volume fraction of particle size has been investigated. Several important macro parameters characterising segregation such as mixing index, percolation index and segregation index have been derived from the simulation tool based on first principles developed in this work.

CONTENTS

LIST OF FIGURES

LIST OF TABLES

CHAPTER 1

INTRODUCTION

1.1 Granular materials: A fascinating field

Granular materials are large conglomerations of discrete microscopic particles of varying size, shape and material properties, which displace from one another and interact only at the contact points. Granular materials are obiquitous; a few examples include food products such as rice, corn and breakfast cereal flakes, building materials (sand, gravel and soil) and chemicals (coal, plastics and pharmaceuticals). They play an important role in several of our industries such as mining, agriculture, civil engineering and pharmaceutical engineering. They are also important in geological processes where landslides and erosion occur on a larger scale.

The behaviour of granular materials is determined by the material and geometric properties of the particles at the contact points. Depending on these conditions the granular materials exhibit properties reminiscent of the various states of matter; they may be deformed as solids, may have flowability similar to liquids or compressibility like that of gases. For example, a sand pile at rest with a slope lower than the angle of repose, behaves like a solid: the material remains at rest even though gravitational forces create macroscopic stresses on its surface. If the pile is tilted several degrees above the angle of repose, grains start to flow. However, this flow is clearly not that of an ordinary fluid because it only exists in a boundary layer at the pile's surface with no movement in the bulk.

A distinguishing feature of granular flows over other flows of solid-fluid mixtures is that in granular flows, the direct interaction of particles plays an important

role in the flow mechanics. The dynamics of granular materials are highly dissipative and a significant fraction of the energy dissipation and momentum transfer in granular flows occur when particles are in contact with each other or with a boundary. Unlike the flows of solid-liquid mixtures, the temperature has no effect on grain motion since external forces such as gravity dominate the behaviour. Further the frictional interactions between the individual grains are highly nonlinear and, for static friction, even discontinuous. Also the particle size in a granular system is comparable to the length scale of flow variation; for example, the patterns such as waves resulting from the flow of granular materials occur on scales only 10-100 times that of the individual grain. Due to these unique properties exhibited by granular systems they are usually considered as an additional state of matter in its own right.

The unusual and unique character exhibited by granular material systems have led to a resurgence of interest within several scientific and engineering disciplines ranging from physics, soil mechanics and chemical engineering (Jaeger and Nagel [1992]; Behringer [1993, 1995]; Bideau and Hansen [1993]; Jaeger *et al.* [1994, 1996a, 1996b]; Mehta [1994]; Hayakawa *et al.* [1995]).

The science of granular media has a long history. Much of the engineering literature has been devoted to understanding how to deal with these materials. Notable contributions in the literature include Coulomb [1773], who proposed the ideas of static friction; Faraday [1831], who discovered the convective instability in a vibrated container filled with powder, and Reynolds [1885], who introduced the notion of dilatancy, which implies that a compacted granular material must expand in order for it to undergo shear.

Finally, there is another vitally important reason for the recent activity in this field. As mentioned above, many of our industries rely on transporting and storing granular materials. These include the pharmaceutical industry which relies on the processing of powders and pills, agriculture and the food processing industry where

seeds, grains and foodstuffs are transported and manipulated, as well as all construction based industries. Similarly, manufacturing processes in the automotive industry rely on casting large metal parts in carefully packed beds of sand. Thus it is important to develop appropriate technology for handling and controlling granular materials effectively, and this still remains as an area not yet fully explored.

1.2 Why study granular materials?

A good understanding of the physics of granular materials is desirable in designing efficient processing and handling systems. The significance of this is apparent when one considers the following statistics:

- In chemical industry approximately one-half of the products and at least three-quarters of the raw materials are in granular form (Neddermann [1992]).

- Ennis *et al.* [1994] estimate that $61 billion in the chemical industry is linked to particle technology.

- Approximately 1.3% of the U.S. electrical power production goes toward grinding particles or ores (Ennis *et al.* [1994]).

- Landslides cause a minimum of $1.5 billion dollars of property damage and at least 25 fatalities in the United States annually.

- Each year over 1,000 silos, bins, and hoppers fail in North America (Knowlton *et al.* [1994]).

- In Mexico, 5 million tons of corn is handled each year, 30% of which is lost due to poor handling systems.

In the chemical industry alone, it is estimated that half the products and three-quarters of the raw materials are in the form of particulates (Neddermann [1992]) and also enormous costs are associated with handling these materials. For example, a

straightforward process such as crushing ores uses approximately 1.3% of the U.S. annual energy consumption. Estimates show that around 60% of the capacity of many of the industrial plants is wasted due to problems related to the transport of these materials from part of the factory floor to another (Ennis *et al.* [1994]). A recent study of 40 solids processing plants in U.S. and Canada showed that 80% of the plants experienced solids handling problems and most of the plants were slow coming on-line. Furthermore, once operational, handling problems continued resulting in achieving only 40% to 50% that of its desired performance (Knowlton *et al.* [1994]). *In order to avoid such problems and to properly design systems involving particulates, there needs to be a better understanding of the mechanics and dynamics of granular materials. Hence, even a small improvement in our understanding of how granular media behave should have a profound impact on industry. Unfortunately there remains a poor understanding of how to model and simulate flow of granular materials. Most of the particulate handling knowledge is empirical and a scientific approach to analyzing these flows does not yet exist fully.*

1.3   Granular Mixing and Segregation

Three mechanisms have been recognized as important in solids mixing (Lacey [1954]) namely, (i) convection, (ii) diffusion and (iii) shear. In any particular process one or more of these three basic mechanisms may be responsible for the course of the operation. In convective mixing, masses or group of particles transfer from one location to another while in diffusion mixing individual particles are distributed over a surface developed within the mixture. In shear mixing, groups of particles are mixed through the formation of slipping planes developed within the mass of the mixture, but this is often considered as part of a convective mechanism. A combination of the mechanisms described above promotes mixing in diverse types of mixers.

Solids mixing, also known as blending, is a common processing operation used in the manufacture of products such as ceramics, plastics, fertilizers, detergents, pharmaceuticals, food products, building materials, and cosmetics. The intent of mixing operations is to produce products of uniform quality and content and also to control the rates of heat and mass transfer and chemical reactions. Industrial devices designed to mix solids include tumblers, convective mixers, gravity flow mixers, and fluidized mixers.

However, the movement of particles during a mixing operation can also result in another manifestation known as segregation, which may retard, or even reverse, the mixing process (Henein *et al.* [1983a, 1983b], Nityanand [1986]). When particles differing in physical properties, particularly size and/or density, are mixed, mixing is accompanied by a tendency to segregate. Thus, in any mixing operation mixing and de-mixing may occur concurrently and the intimacy of the resulting mix depends on the predominance of the former over the latter. Apart from the properties already mentioned, surface properties, flow characteristics, friability, moisture content, and tendency to cluster or agglomerate, may also influence the tendency to segregate. The similar the ingredients are in size, shape and density, the easier the mixing operation is and the more intimate the final mix. Once the mixing and de-mixing mechanism reach a state of equilibrium, the condition of the final mix is determined and further mixing will not induce improved result.

The importance of segregation on the degree of homogeneity achieved in solids mixing cannot be over- emphasized. Any tendency for segregation to occur must be recognized when selecting solids mixing equipment. Segregation in a mixture of dry solids is readily detected by use of a heap test. A well-mixed sample of the solids is poured through a funnel so as to form a conical heap. Samples taken from the central core and from the outside edge of the cone should have essentially the same compositions if segregation is not to be a problem. When the two samples have

significantly different sizes or densities, it can be assumed that segregation would occur unless a very careful choice of equipment is made. It is generally accepted that the efficiency of a mixing process must be related to both the flow properties of the components, and to the selection or design of the mixer.

In some cases the phenomenon of segregation is exploited in order to separate or remove particles with different properties. Devices utilizing this phenomenon include vibratory sieves and Humphreys spirals and Reichert cones. In most instances, however, segregation is undesirable since it counteracts the intent of mixing operations. Even if a collection of particulates is well-mixed, subsequent transport and handling along conveyor belts or in railroad cars, for example, often results in segregation of the constituents. This is of particular concern for the pharmaceutical and ceramics industries where homogeneous blends of solids are critical.

A common approach to solids blending is to use the *tumbling blender*, which is essentially a hollow vessel attached to a horizontal rotating shaft. Tumblers are perhaps the most common among solid processing and mixing devices. In addition to mixing, this type of apparatus impacts such applications as drying kilns, ball mills, and coating processes. In any tumbler, the bulk of the granular material moves as a solid body, while the surface layer forms the down-surface flow. It is within this region of downward flow that mixing and segregation occurs.

Considerable efforts have been made to design mixing processes that maximize homogeneity and minimize mixing times. However, progress in understanding flow and mixing of granular materials has been hindered by the lack of understanding of their constitutive behaviour. In recent years, many constitutive relations have been proposed to model granular flows. Most of these theories are limited to a situation of either a rapid flow or a quasi-static flow. However, the flow

pattern within tumbling mixers generally consists of a rapid flowing region and a non-deforming region that usually contains a large part of the material to be mixed and therefore a scientific approach to investigate granular mixing in tumbling blenders is not yet possible.

1.4 Need for the present study

Granular flow in rotating cylinders is encountered in practical applications such as drying, mixing, and separation of particulate materials. Hence a fundamental understanding of mixing and blending of granular materials in horizontal rotating cylinders can be beneficial to a wide range of industries, namely; pharmaceuticals, metallurgy, ceramics, composites, polymers, food processing and agriculture, to name a few. Yet, in relation to its industrial relevance, the understanding of mixing of granular materials lags considerably behind that of liquid mixing (Ottino [1989]). Even though fundamental solids mixing mechanisms have been widely studied by investigators over the years (Lacey [1954]; Hogg *et al.* [1966]; Bridgwater *et al.*,[1985], Bridgwater [1995]), a synthesis of these fundamentals into a coherent mixing description has been elusive. In fact, despite a substantial amount of work during the past few years aimed at understanding granular mechanics (Henein. *et al.* [1983a, 1983b]); Nityanand *et al.*, [1986]; Jaeger and Nagel [1992]; Jaeger *et al.* [1996a, 1996b]) and powder mixing (Fan *et al.* [1990]; Poux. *et al.* [1991]) we do not yet have a full understanding of even the simplest case, namely; the mixing mechanism of two identical powders in a slowly rotated container.

Hence our research is focused on granular mixing in tumbling mixers, the simplest prototype being a horizontal cylinder, partially filled with granular material and rotated about its axis. Tumbling mixers are widely used in industry and current design practices are primarily based on empirical data. The goal of this work is to build a numerical simulation tool, which will help to evolve better designs for

equipment as well as improved industrial practice. *One of the objectives of the work is to arrive at a mathematical model for the dynamics of mixing and use it to simulate real-world systems, which in turn can be used for a rational approach to design.*

Engineers and physicists interested in complex non-Newtonian behaviour of granular flows have developed several continuum theories (Ottino [1989], Khakhar *et al.* [1997a, 1997b]). However, it is difficult to measure bulk properties such as stress, strain, and void fraction, which are necessary to develop a continuum theory, and hence continuum approach has achieved only limited success in mixing problems. Similarly, the other approaches to modelling granular flow, such as those based on statistical mechanics and cellular automata (Baxter and Behringer [1990,1991]), while useful in certain regimes, are not general enough for all types of granular flow, and have not been successfully used as a predictive tool in granular mixing.

The success of molecular dynamic simulations for gas and liquid systems has motivated the use of the Discrete Element Methods (DEM) (Cundall and Strack [1979]; Walton and Braun [1993]; Tsuji [1993]; Mishra and Rajamani [1992]; Ristow [1994]) in modelling granular flows. These methods consider the granular material as a collection of a large number of discrete solid particles, which move independently from each other according to the deterministic laws of Newtonian mechanics. The advantage of these methods over the continuum models is their ability to simulate a wide range of granular flows with different particle sizes, shapes, and physical properties. The major drawback of the discrete models is the excessive run time for relatively small number of particles even with state of the art computers. When the number of particles is of the same order as in real flows of fine materials, the computation time becomes extremely long. Therefore, it is expensive or impossible to apply the discrete particle simulation to the case of fine powder.

Hence this work is directed towards a theoretical investigation based on Discrete Element Method (DEM) of the motion of granular solids in the radial direction of the horizontal cylinder to elucidate the relationship between the operating parameters of the rotating cylinder geometry and physical properties of the granular solid. ·

The operating parameters of the rotating cylinder include the various rotational velocities of the cylinder and volumetric fill. The physical properties of the granular solids proposed to investigate include particle sizes, densities, stiffness coefficients, and coefficient of friction. Finally the thesis will also investigate the following three factors of the system namely;

- *The different modes of solids motion observed in a transverse cross-section of the rotating cylinder for various rotational speeds,*
- *The radial mixing of the granular solid as well as the transition behaviour in terms of the bed turnover time and rotational speed*
- *Segregation mechanisms resulting from differences in the size and density of particles.*

1.5 Layout of the thesis

Chapter 2 contains a state of art of literature review of the transverse solids bed motion in a rotating cylinder. A comprehensive overview of all experimental and theoretical studies related to the granular solids motion in rotating cylinders is presented. The advantages and disadvantages of the various theoretical and computer aided simulation methods are also discussed.

A detailed description of the mathematical model based on Discrete Element Method is provided in **Chapter 3**. The different types of contact forces available in the literature are discussed. Then formulation suitable for the dynamics of granular material motion in radial direction of the horizontal rotating cylinder is presented along with appropriate contact forces. The flow chart of the algorithm along with initial configuration generation is presented. This chapter concludes with a discussion on the validation of the software code DEMCYL developed for the present study.

Chapter 4 discusses the numerical results obtained by the simulation tool developed in Chapter 3 for a rotating cylinder of inner radius 1.5 m. The results obtained are presented both at the micro-level and macro-level. The micro dynamic analysis of the granular flow behaviour is presented in terms of the kinetic energy of the system and the radial position of the granular particles and as velocity vector plots. At the macro level, the effect of the rotational speed, fill fraction and coefficient of friction on the dynamic angle of repose are presented and discussed. Also the different types of the transverse solids motion with respect to changes in the rotational speed of the cylinder is presented in terms of the bed turnover time. The Active layer depth with respect to fill fraction and rotational speed are presented. The results obtained through simulation are compared with the experimental results of Van Puyvelde *et. al.* [2000] and Ding *et al.* [2002].

An analysis of mixing and segregation in the transverse direction for different particle sizes and their size ratios is carried out in **Chapter 5**. The effect of fill fraction and rotational speed on the transverse mixing behaviour is presented in the form of a mixing index and mixing kinetics curve. The segregation pattern obtained by the simulation of the granular solid bed with respect to the rotational speed of the cylinder is presented. The segregation behaviour of the granular solid bed with respect to particle size, density and volume fraction of particle size has been investigated. From the results of the numerical experiments through computer

simulation, the macro parameters such as mixing index, percolation index and segregation index are obtained.

A summary of the significant results and the scope for future investigations in this area are presented in the concluding **Chapter 6**.

simulation, the macro parameters such as mixing index, percolation index and segregation index are obtained.

A summary of the significant results and the scope for future investigations in this area are presented in the concluding **Chapter 6**.

CHAPTER 2

A LITERATURE REVIEW ON THE TRANSPORT PHENOMENA OF THE GRANULAR BED MOTION IN A ROTATING CYLINDER

2.1 Introduction

Rotating cylinders play a prominent role in the processing of granular materials in metallurgical and chemical industries in which operations such as reduction of iron oxide, calcination of limestone and petroleum coke are carried out. The widespread usage of rotating cylinders in processing can be attributed to such factors as its ability to handle varied feed stocks having large variations in particle sizes and ability to maintain distinct environments; for example reducing conditions within the solid bed coexisting with an oxidizing atmosphere in the freeboard (a unique feature of the rotating reactor that is not easily achieved in other reactors) in the direct reduction of minerals.

In order to improve the performance of the processes taking place inside the rotating cylinder, a better understanding of the transport phenomena in the granular medium inside the rotating cylinder is required. During particle motion, solid particles inside the cylinder undergo various processes like heat exchange, drying, heating, chemical reaction etc. Hence it is very essential to have a fundamental understanding of the processes occurring inside a rotating cylinder, so that it can be designed to function under optimum process conditions.

Since the present work focuses on granular bed motion in the radial direction of a rotating cylinder, this chapter presents a comprehensive review of the literature relating to solid bed motion in the radial direction of the horizontal rotating cylinder. Commencing with a description of the general dynamics of the solid bed movement in a rotating cylinder, a detailed review of the theoretical and experimental studies related to transverse solid bed motion, mixing and segregation behaviour is presented.

2.2 Dynamics of granular motion in rotating cylinders

In normal industrial practice, rotating cylinders partially filled with granular solids having a volumetric hold-up of 10% to 50% of the total volume of the cylinder are used. The cylinder is inclined along its axial length at a few degrees to the horizontal and is rotated along its horizontal axis as shown in Figure 2.1. Horizontally rotating cylinders are slightly tilted along their axis to facilitate the movement of solid particles.
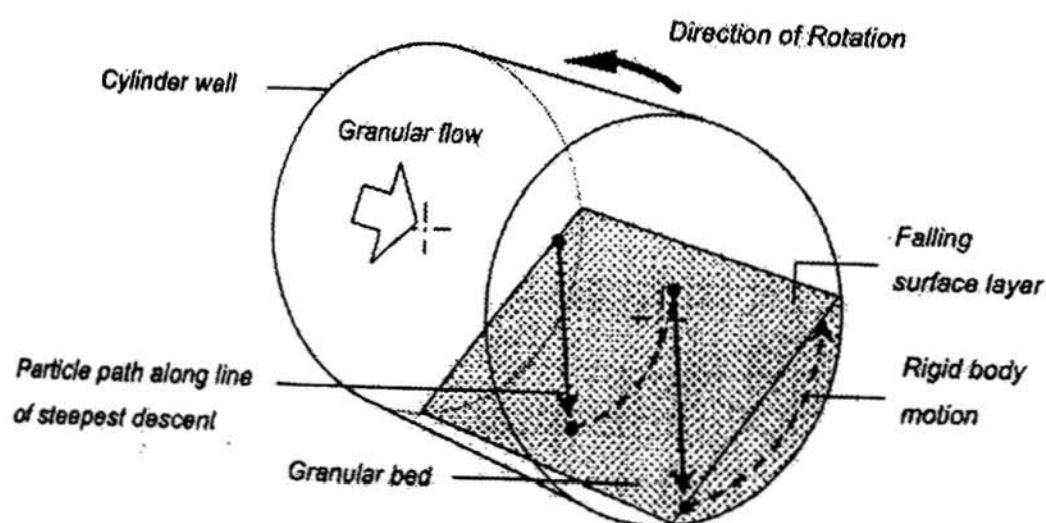
Figure 2.1: Schematic view of granular bed motion in a rotating cylinder
(Spurling, [2000])

The movement of parti cles inside the solid bed can be resolved into two components, namely, (i) in the transverse direction and (ii) in the axial direction The transverse movement of the granular medium is perpendicular to the cylinder axis and is responsible for the homogeneity of the solid bed, whereas the axial movement of particles takes care of the shape of the solid bed and the residence time of the particles inside the various zones. The granular materials are slowly conveyed along the cylinder length as a result of continuous circulation and force of gravity down the slope. Earlier works by Sullivan *et al.* [1927], Seaman [1951] and Boateng [1993] show that the axial motion of the particles is mainly due to transverse movement, since for every particle turnover in the radial cross section there is an axial material advance. Eventhough there is a linkage between particle motion in the transverse direction and particle velocity in the axial direction, the literature deals with these two types of bed motion as independent phenomena. Only in recent past an attempt has been made to quantitatively link the axial velocity to the transverse motion (Perron and Bui [1990]).

2.3 Granular bed motion along the cylinder axis

The bulk motion of a granular bed under steady state operating conditions in a rotating cylindrical reactor has been experimentally investigated by several groups of researchers using laboratory and pilot plant scale devices, commencing with the work of Sullivan *et al.* [1927] and Seaman [1951]. The movement of solid particles in the axial direction determines the residence time, which is an important parameter for the design of rotating cylindrical reactors. The first attempt to study the residence time of solid particles in a rotating cylinder was made by Sullivan *et al.* [1927]. Earlier researchers made attempts to predict the mean axial velocity and residence time of the granular materials focusing mainly on the angle of repose of the solid bed, horizontal slope of the rotating cylinder and the angular velocity of the cylinder. Seaman [1951]

proposed a theoretical analysis for the relationship for residence time determined by axial solids velocity namely;

$$V_S = 0.955 \frac{R\omega\beta}{\sin\varepsilon} \tag{2.1}$$

where β is the slope of the cylinder, R is inner radius of the cylinder, ε is the dynamic angle of repose and ω is the angular velocity of the cylinder.

Perron and Bui [1990] summarized various relations connecting the mean solids axial velocity to slope of the cylinder, rotational speed, loading and dynamic or static angle of repose. By applying a dimensional analysis on the velocity profile for the bed cross-section, they proposed a new formula to predict axial velocity; namely,

$$V_S = R\beta\omega \left[\frac{L^{\frac{\psi}{\pi}} R^{-1-\frac{\psi}{\pi}}}{R} \left(H^2 \cos\varepsilon + 2H\sqrt{2HR - H^2} \sin\varepsilon \right) \left(\frac{1 - \cos\frac{\theta}{2}}{1 + \frac{2\tan\frac{\theta}{2}}{\theta}} \right) \right] \tag{2.2}$$

In this equation, H is the actual bed depth, θ is the bed depth in angular measure, and ψ and π are exponents determined by dimensional analysis. This expression is unique in that rather than yielding only a mean axial velocity it allows quantitative predictions for local axial velocity through its inclusion of various local parameters: for example, the local transverse velocity profile. However, the validity of the expression has not been clearly established even at the laboratory or pilot scales, and the problems of scale-up to the industrial level still remains formidable.

Nonetheless the most commonly used correlation is still that proposed by Seaman [1951].

Sai *et al.* [1990, 1992] conducted experiments in rotating cylinder containing ilmenite particles to study the residence time distribution of low density particles, hold-up and bed depth profile and their study supported the conclusion of Sullivan *et al.* [1927]. Chatterjee *et al.* [1983] has also reported the same observation. *All these studies are based on the assumption that the system is under steady state and only a single type of material is used for deriving the empirical relationships.*

A number of industrial situations give rise to transient behaviour in the solids motion, such as start-up, irregularities in the granular feed rate and fluctuations in the physical properties of the granular solid. In order to devise an effective control strategy, and successful process models, it is therefore important to understand the unsteady solids motion resulting from sudden changes in the operating variables, namely the rotation speed, the solids feed rate, and the slope of the kiln axis. There is little published work dealing with the dynamic case except for a small set of laboratory scale experimental measurements of the variation in the discharge rate of solids with time following a step change in each of the operating variables, as reported by Sriram and Sai [1999]. They validated the equations of Perron and Bui [1990] for different experimental conditions covering the steep changes in the feed rate of solids. Ang *et al.* [1998] developed an empirical equation for the residence distribution for a binary feed mixture of solid particles.

Recently Spurling [2000] has carried out an extensive study, both theoretical and experimental, of the motion of a rolling bed of sand flowing through a laboratory scale cylinder inclined along its length and slowly rotating about its axis, to study the effect of the discharge dam geometry on the steady state hold-up profile. Also, experimental measurements have been made of the discharge flow rate and axial

hold-up profile as functions of time following a step up or down in one of three variables; viz., (i) the mass feed rate, (ii) the rotation speed, and (iii) the axis of inclination, and has been verified with the work of Sai *et al.* [1992] and Sriram and Sai [1999].

2.4 Granular bed motion in the transverse plane

The motion of a bed of granular solids in the transverse plane of a rotated cylinder can take different forms, as described by Henein *et al.* [1983a]. As the cylinder rotation speed is increased from zero, six distinct modes of bed behaviour viz., slipping, slumping, rolling, cascading, cataracting and centrifuging are observed, as shown schematically in Figure 2.2
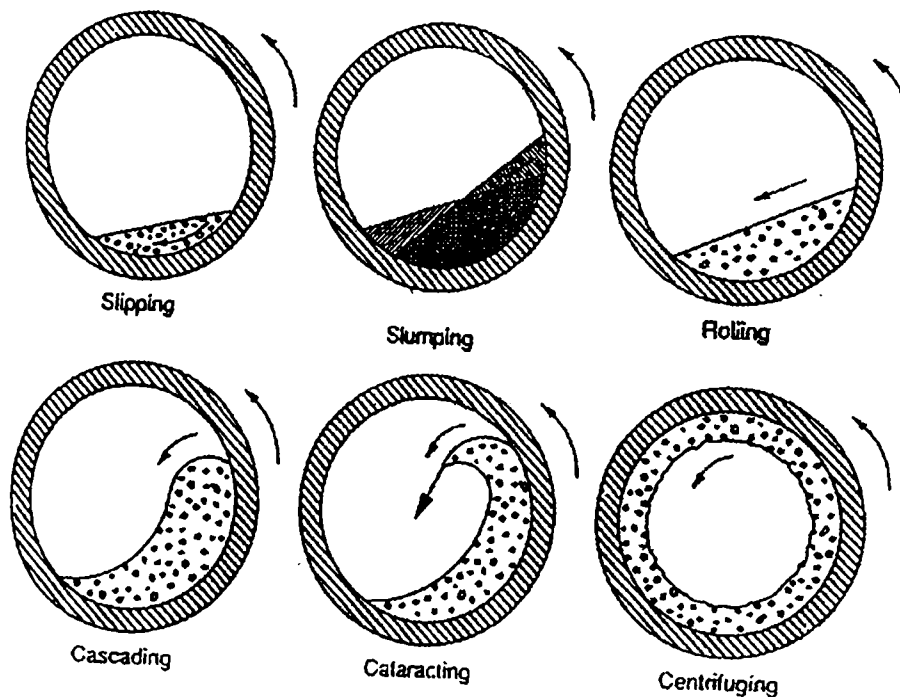
Figure 2.2: Schematic view of the different modes of solids motion
(Boateng, [1993])

2.4.1 Slipping Mode

At very low rotational speeds, especially when the friction between the granular bed and the cylinder wall is low, the granular bed behaves as a rigid body. The bed motion is observed to take one of two forms (i) the granular bed remains at rest and the granular solid continuously slides at the wall, or (ii) the granular solid repeatedly moves upward with the cylinder until the bed surface reaches a maximum inclination and then slips at the wall back to a minimum inclination and then resumes rotation.

2.4.2 Slumping Mode

In this mode, the granular solid is lifted like a rigid body by the cylinder wall such that the inclination of the bed surface increases continuously until it reaches an upper angle of repose, then detaches from the upper surface of the bed, and falls as a discrete avalanche toward the lower half of the bed. Following the avalanche the inclination of the surface of the granular solid drops to an angle of repose that is less than the static angle of repose of the granular solid. The slumping frequency is observed to increase with increasing rotation speed, eventually leading to the rolling mode. The change between the slumping and rolling modes of bed motion is not always clearly defined, rather the bed behaviour is found to go through a transition in which the bed changes unpredictably between rolling and slumping behaviour.

2.4.3 Rolling Mode

The bulk of the bed rotates as a rigid body about the cylinder axis at the same rotation speed as the cylinder wall. On the bed surface there appears a thin layer of continuously falling particles forming a plane free surface that is inclined at the dynamic angle of repose of the granular solid to the horizontal plane. Solid particles

mix more effectively in the rolling mode. In the rolling mode, bed material can be divided into two distinct regions, namely a 'passive region or plug flow region' where the particles are carried upward by the cylinder wall, and a relatively thin 'active region or cascading layer' where the particles flow down the slipping upper bed surface as shown in Figure 2.3. In the passive region, granular mixing is negligible and the mixing mainly occurs in the active region. At higher mixer rotational speeds, the continuous flow *rolling regime* is obtained, in which a thin layer of particles flows down the free surface while the remaining particles rotate as a fixed bed. Transverse mixing in this case depends on the dynamics and results from the shearing and collisional diffusion within the layer.
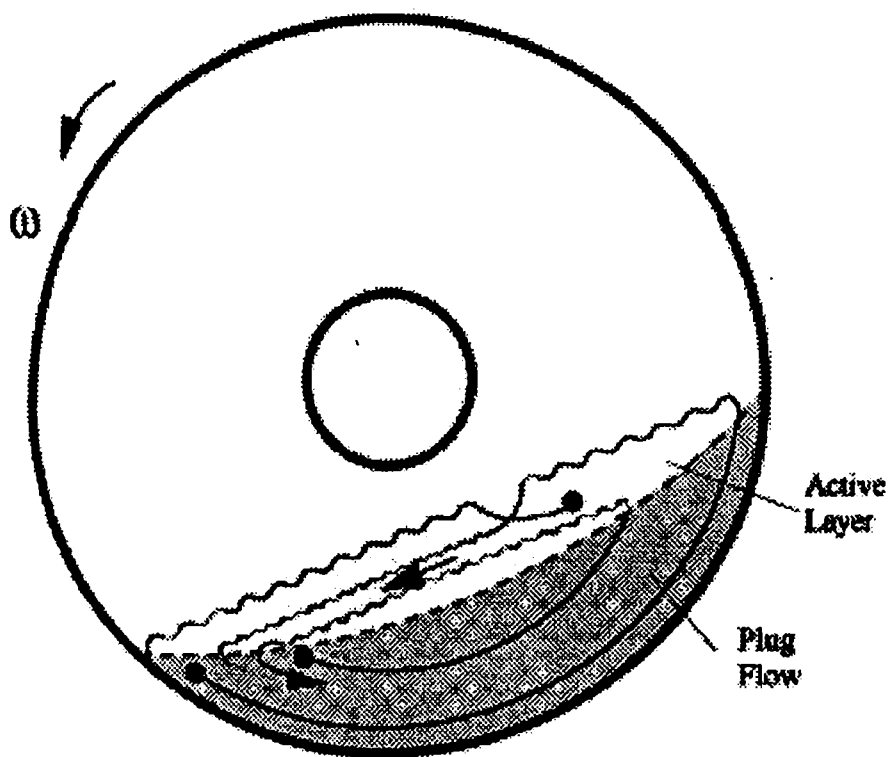
Figure 2.3: Rolling bed motion: top plane- active (shear) layer; bottom plane - plug flow (non-shearing region), (Boateng, [1993])

2.4.4 Cascading Mode

As the rotation speed is increased further, the particles in the upper corner of the rolling bed are lifted higher before detaching from the cylinder wall, and the bed surface assumes a crescent shape in the cylinder cross-section. This mode of material motion is termed as cascading mode.

2.4.5 Cataracting Mode

On further increasing the rotational speed, centrifugal forces become increasingly important in the motion of particles along the bed surface, the curvature of the cascading surface becomes highly pronounced and particles are projected into the freeboard space from the upper corner of the bed.

2.4.6 Centrifuging Mode

At a Froude number of unity, the granular solid is confined to the inner wall of the cylinder by centrifugal forces. According to Nityanand *et al.* [1986], the critical rotational speed at which a particle at the cylinder wall starts centrifuging can be calculated from the equation

$$n_c = \frac{30}{\pi} \sqrt{\frac{2g}{D}} \tag{2.3}$$

where g is the acceleration due to gravity and D is the diameter of the cylinder.

2.5 Dynamics of granular material motion

Rutgers [1965] has provided a criterion for the dynamic similarity of the rotating cylinder by quantifying the transverse bed motion in terms of rotational Froude number,

$$Fr = \frac{\omega^2 R}{g} \qquad (2.4)$$

where ω is the rotational speed of the cylinder, R is the inner radius of the cylinder and g is the acceleration due to gravity. The slipping, slumping and rolling modes of bed motion have been investigated experimentally by a number of authors, including Henein *et al.* [1983a, 1983b] and McTait [1998]. The change from the slumping to the rolling mode of bed motion was found to occur at a rotational Froude number between 1×10^{-4} and 1×10^{-3} by Henein *et al.* [1983a] and between 1×10^{-5} and 1×10^{-4} by McTait [1998]. Also the mode of bed motion was found to be uniquely determined by (i) the hold-up as a fraction of the cylinder volume, (ii) the rotation speed, (iii) the cylinder diameter, and (iv) the particle size and shape. It was found that the transition from a slumping to a rolling bed occurred at a lower rotational Froude number for the cases of (i) a higher fractional hold-up, (ii) particles of spherical rather than irregular shape, (iii) smaller particles, (iv) cylinders of larger diameter, and (v) granular solids with a lower static angle of repose.

McTait [1998] used sand and glass ballotini, of mean particle size 0.6 and 0.22 mm respectively, rotated in cylinders of diameter 0.105, 0.194, 0.288 and 0.5 m with either smooth or rough walls. The bed motion was classified from observations made through a transparent end plate of the cylinder and the slumping mode of

motion was charecterised from the digital images captured by a video camera. It was found that the transition between the slumping and rolling modes of bed motion occurred at a higher rotation speed for a cylinder with rough walls. The scale-up parameters proposed by Henein *et al.* (1983a) were tested against the experimental observations.

Rajchenbach [1990] identified hysteresis in the transition between slumping and rolling modes of bed motion in a granular bed of 0.3 mm diameter glass spheres, rotated in a cylinder of diameter 190 mm. When the rotational speed was increased, the transition from slumping to rolling took place at a rotational speed of 0.5 rpm, whereas when the rotation speed was decreased, the transition from rolling to slumping occurred at a lower rotation speed of 0.25 rpm.

Henein *et al.* [1983b] proposed mathematical models governing the transition between various modes of motion such as (i) slipping to slumping (ii), slipping to rolling, (iii), slumping to rolling and (iv) rolling to cascading. It was proposed that the transition from slumping to rolling would take place when the time taken for the shear wedge to slump down the bed surface was equal to the time required for the surface of the bed to increase from the lower to the upper angle of repose.

Ding *et al.*, [2001] used non-invasive PEPT (Positron Emission Particle Tracking) technique to follow the particle trajectory and velocity in the rolling mode. A mathematical model based on the thin-layer approximation was proposed to describe solids motion in the active layer. Reasonable agreement was obtained between the model predictions and experiments. A new parameter termed as the *solids exchange coefficient* was proposed to characterize particle exchange between the passive and active regions. A theoretical expression for this parameter was also derived. This expression, upon application of the thin-layer approximation, reduces to give an explicit relationship between the solids exchange coefficient and cylinder

operating parameters such as rotational speed and fill percentage, as well as the bed material rheological properties. The solids exchange coefficient was also shown to give a possible scale-up rule for rotating cylinders operated in a rolling mode.

Mellmann [2001] has reviewed the results on transverse bed motion and developed mathematical models to predict the transitions between different forms of transverse motion of granular solid bed. His predictions for the transition behaviours based on the values of the Froude number are presented in Table 2.1. He has also represented the transverse motion of bed materials as a bed behaviour diagram where the wall friction coefficient and the Froude number are plotted against the filling degree and it represents the ranges of individual forms of motion and their limits.

Table 2.1: Different modes of solids motion in terms of Froude Number (Mellmann [2001])

Types of motion	Froude number
Slipping	$0 < Fr < 10^{-4}$
Slumping	$10^{-5} < Fr < 10^{-3}$
Rolling	$10^{-4} < Fr < 10^{-2}$
Cascading	$10^{-3} < Fr < 10^{-1}$
Cataracting	$10^{-1} < Fr < 1$
Centrifuging	$Fr \geq 1$

2.6 Particle mixing and segregation in transverse plane

Since particle mixing is maximum in the rolling mode, studies related to mixing and segregation have been reported mainly for the rolling regime in transverse direction. Also it has been found that the active layer is predominantly responsible for

the mixing and segregation of solids (Henein *et al.* [1983a, 1983b], Boateng and Barr [1996,1997], Boateng [1993], Chakraborty *et al.* [2000]).

The mixing and segregation of particles in a horizontal cylinder, partially filled with granular solid and slowly rotated about its axis, has been investigated experimentally by a large number of authors, commencing with the work of Oyama [1939], Weidenbaum and Bonilla [1955] and Roseman and Donald [1962]. In general, experiments were performed in a cylinder that was closed at both ends and rotated in batch mode, at a rotation speed resulting in the slumping, rolling or cascading modes of bed motion.

Experimental measurements of radial mixing of mono-sized particles of equal density in a slumping bed has been reported by Clement *et al.* [1995] and Metcalfe *et al.* [1995], and in a rolling bed by Khakhar *et al.* [1997a]. Clement *et al.* [1995] used a video camera to track the motion of a single particle of diameter 1.5 mm in a short cylinder of diameter 160 mm and depth 15 mm. The particle was found to move at random between different radial positions in the bed. Metcalfe *et al.* [1995] investigated the radial mixing of table salt of mean diameter 0.6 mm, rotated in a short cylinder of diameter 144 mm and length 24 mm. A simple model for the mixing process was proposed which involves (i) a geometric part corresponding to transport of the slumping wedge from the top to the bottom of the bed, and (ii) a dynamic part, assuming random mixing within the wedge. Good agreement was found between the model and experiment, but the model was found to consistently overestimate the mixing rate.

Khakhar *et al.* [1997a] used a video camera to investigate radial mixing in a thin cylinder, of diameter 69 mm and length 15 mm, between different colours of (i) angular sugar crystals of diameter 1 mm, and (ii) spherical sugar balls of diameter 1.8 mm. The rate of mixing per revolution was found to increase as the hold-up was

decreased and to be higher for spherical particles. A continuum model for mixing based on an Eulerian model for granular flow, was derived in which the particle motion was assumed to have a random diffusional component perpendicular to the direction of flow. The model was found to be in reasonable qualitative agreement with experimental observations for a range of values of hold-up.

A number of authors have reported that differences in the size, density and shape of particles would result in particle segregation in the falling layer of the circulating bed. According to Henein *et al.* [1983a, 1983b], Nityanand *et al.* [1986] segregation is a combination of three mechanisms, namely, (i) percolation, (ii) vibration and (iii) flow segregation. Particle percolation is the process where by smaller particles in a mixture trickle through the voids in a bed of larger particles, thus forming a mixture with larger particles on top and smaller particles on bottom. This type of segregation is a function of the packing characteristics of the bed, particle size and shape. According to Bridgwater [1976], when there is a difference in particle size, there is a chance for percolation to occur. Segregation by vibration typically occurs when a mixture of coarse and fine particles is subjected to prolonged vibration. As a result of the vibrations the smaller particles segregate to the bottom while the larger particles would segregate to the top. Segregation by flow occurs when granular solids are set in motion over an inclined surface. Coarse particles travel down an inclined surface further than fine particles and spherical particles flow easier than angular particles.

During percolation, more dense particles are found to filter downwards through the layer while larger, less dense, particles are displaced upwards. Hence it was proposed that percolation occurs because there is a larger probability of smaller more dense particles falling downwards into voids between particles at lower positions in the flowing layer. Particle segregation in the shear layer was found to produce segregation patterns in the axial and radial directions. In the radial direction,

a horizontal core of finer or denser particles was found to form in the granular bed, whereas in axial segregation either (i) alternate bands of coarse and fine, or light and heavy, particles formed down the length of the granular bed, or (ii) bands of fine, or light, particles formed adjacent to the ends of the cylinder and in a horizontal core along the length of the bed. The rate of radial segregation was found to be of an order of magnitude faster than axial segregation, leading to the conclusion that axial segregation progressed with the radially segregated bed as its initial condition.

Nityanand *et al.* [1986] have investigated radial segregation in binary and ternary mixtures of spherical acrylic beads of diameter 4, 6.4 and 9 mm, rotated in a cylinder of diameter 0.2 m or 0.4 m, to produce the rolling mode of bed motion. The effect of varying the following experimental parameters was investigated: (i) the hold-up, between 23 % and 52 % of the cylinder volume, (ii) the rotation speed, between 1.4 and 100 rpm, and (iii) the mass fraction of fines in the mixture, between 10 % and 49 %. The granular bed was initially well mixed, and measurements of the segregation process were made using a high speed video camera through a transparent end plate to the cylinder. It was found that:

- The smallest size of particles segregated to form a central core, of similar shape to the bed cross-section, just below a falling layer of coarse particles, and the size of the core was found to be proportional to the mass fraction of the finest component in the granular bed.

- In a ternary mixture, the annulus of granular solid around the core was found to be a well mixed mixture of beads with diameters 6.4 mm and 9.5 mm respectively.

- In all cases the segregation process was found to reach equilibrium within a single turnover of the granular bed. The segregation rate was quantified by

counting the rate at which the finer beads were depleted from a control volume, defined to be equal to the outer annulus of the segregated bed

- The segregation kinetics was found to be zero order, independent of the hold-up, and the rate of segregation was found to be higher for (i) a larger cylinder diameter, (ii) a higher rotation speed and (iii) a larger ratio of the largest and smallest particle sizes.

Pollard and Henein [1989] reported similar measurements for 3 narrow size ranges of irregular limestone particles with a mean particle size of 2.8, 4.6 and 6 mm. The behaviour of the granular bed was found to be similar to that described for spherical particles, except that the segregated core was found to contain a small fraction of larger particles. Henein *et. al.* [1985, 1987] investigated radial segregation by sampling the composition of the granular bed in a cylinder of diameter 0.4 m rotated to produce the slumping or rolling mode of bed motion. It was found that the bulk density of a binary mixture of two particle sizes had a minimum value for a certain ratio of the two components, and the density of the segregated core was shown to be close to this value for a granular bed composed of a binary mixture of limestone particles.

Khakhar *et al.* [1997b] investigated radial segregation between spherical particles of steel and glass, both about 1.6 mm in diameter, but with a weight ratio of about 3.8, in a cylinder of diameter 75 mm. The effect of varying two experimental variables was investigated: (i) the number fraction of the dense particles, and (ii) the hold-up. It was found that the dense particles formed a central core of similar shape to the bed cross-section irrespective of the hold-up. The core size was found to increase, and the boundary of the core to become more sharply defined, as the number fraction of dense particles was increased.

There is little experimental evidence to quantify the effect of particle shape on radial segregation, or segregation in a granular solid made up of many different particle sizes, and in the limit, a continuous particle size distribution.

A number of authors have proposed quantitative models for granular flow, mixing and segregation in the cross-section of a cylinder. McCarthy *et al.* [1996] extended the model of Metcalfe *et al.* [1995], for a slumping bed, by using particle dynamics to model the effect of segregation on rearrangement of granular solids inside a falling wedge, but no attempt was made to validate the model experimentally. Boateng and Barr [1996, 1997], Boateng [1993] and Khakhar *et al.* [1997a, 1997b] derived Eulerian models for particle mixing in the rolling mode and reported good quantitative and qualitative agreement with their experimental observations.

The velocity profile across the rolling bed at mid chord has been measured by Nakagwa *et al.*,[1993], using magnetic resonance imaging and by Boateng [1993], using a fibre optic method. The results of both the authors agree considerably. It has been commonly assumed that the velocity profile in the active layer was symmetric about the mid chord. But Boateng [1993] observed that for larger cylinders the velocity profiles become skewed. Henein *et al.* [1983 a, b] noted that the active layer depth decreased for smaller particles; decreased with increasing bed depth and increased with the rotational velocity. Boateng [1993] found that the proportion of active layer increased with increasing velocity and decreased with increased cylinder loading.

The model of Yang and Farouk [1997] predicted that the active layer thickness increased for finer particles. This was not consistent with the results of Henein *et al.* [1983a, 1983b] and could be due to the use of different experimental materials and/or conditions. Boateng and Barr [1997] studied the effect of the end zone on the active layer velocity and proportion. They showed that near the end piece

of a cylinder the angle of repose of the material was enhanced and this resulted in a significantly higher velocities in the active layer at the end piece compared to velocities in the bulk.

Hogg and Fuerstenau [1972] described the mixing in the transverse section of a rolling bed as a combination of the convective and diffusive mixing mechanisms, Lehmberg *et al.* [1977] measured the dynamics of mixing of solids in an experimental cylinder but did not quantify the mixing rate. Their experiments involved a 310 mm cylinder and they mixed 0.80 mm sand, which consisted of a batch of approximately 90% white and 10% black. They used a rotational velocity of 2 rpm and found that the bed became fully mixed 42 seconds after the rotation was started.

Pershin and Mineav [1989] simulated the mixing in a transverse section of a rolling bed using a concentric layer model. This model considered mixing when material moved from one sub layer to the next and only one transaction was allowed per bed rotation. This model had the obvious drawback of assuming that mixing depended only on the number of rotations and not on the dimensions of the bed. Furthermore, this model focused on material moving closer to the center of the bed such as is the case for segregation.

Woodle and Munro [1993] studied the mixing rate from a statistical point of view and found the rate of mixing to be constant until the bed became fully mixed. There was a random fluctuation in this fully mixed value due to random distributions of the material. They used cylinder loadings of 3% to 15% for 12mm particles and found that the bed became fully mixed in 17 to 46min.

Boateng and Barr [1996, 1997] and Boateng [1993] devised a model of mixing and segregation using granular mechanics. The focus of their work was on the fully segregated bed and heat transfer from the gas phase to the bed, which had

important implications for calcining in rotary kilns but was not useful to predict the dynamic mixing behaviour in a rotating cylinder. The modelling of both the mixing rate and the final amount of mixing of solids have been proposed by Van Puyvelde et al. [2000a,2000b] based on the dynamic data collected from experimental results of Van Puyvelde et al. [1999].

As can be seen from the above review, several models has been proposed in the literature but each model is limited by its individual experimental conditions. Numerous variables in the models, such as cylinder size, the material size and type, the rotational velocity and the analysis method make it difficult to compare the results of one model with those of the other. This difficulty is further enhanced by the lack of a full disclosure of experimental conditions.

2.7 Modelling the flow of granular materials

According to Hogue and Newland [1994], the methods to simulate the behaviour of granular materials may be classified by two approaches, namely; Continuum Mechanics Method (CMM) or Macroscopic Modelling and Discrete Element Methods (DEM) or Microscopic Modelling.

2.7.1 Macroscopic modelling or Continuum theory

Primary challenge in granular flow modelling is not in setting up the conservation equations for mass, momentum and energy but in establishing the stress/strain relationship for the particulate mass as this relationship depends on the flow regime and vice versa. Davies [1986] has compared the observed behaviour of granular materials, subjected to shear stress, to other common types of flow behaviour as shown in Figure 2.4.
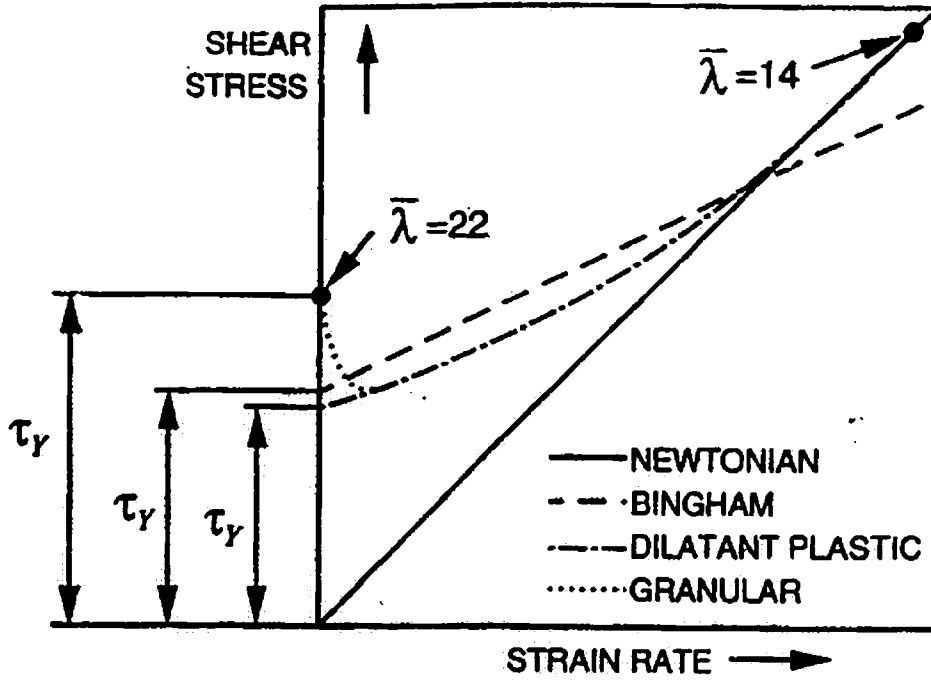
Figure 2.4: Comparison of granular flow behaviour with other type flows (Davies, [1986])

The figure 2.4 shows the shear stress as a fraction of a dilation factor $\bar{\lambda}$, defined as,

$$\frac{1}{\left[\dfrac{v^*}{v}\right]^{\frac{1}{3}} - 1} \tag{2.5}$$

where, v is the volume concentration of solids, v^* is the minimum possible void fraction that the material can maintain. For granular materials in static condition, the particles flow together into a rigid grid, which means that some degree of stress can be sustained without inducing flow. However as the stress approaches some critical level, the particles begin to ride up on one another and the grid commences dilation (Boateng and Barr [1996,1997]). At the critical stress, the dilation, $\bar{\lambda}$, reaches a

maximum and the material begin to flow. Once this occurs the shear stress shows an incipient steep decline with increasing strain rate and it is this initial behaviour, which distinguishes granular flow from that of other flows. Beyond a certain rate of strain, the stress begins to increase again and the relation between the shear stress and the rate of strain turns non-linear. These fundamental aspects of the flow behaviour of granular materials or bulk solids similar to that in rotary kilns have been reviewed by Savage [1979].

The mechanisms of momentum transfer and hence stress generation for granular flows include the following;

- Static stresses resulting from the rubbing between particles, which is independent of strain rate.
- Translational stresses resulting from the movement of particles to regions having different velocity.
- Collisional stresses resulting from inter-particle collision, which result in transfer of both momentum and kinetic energy.

The relative importance of these three mechanisms will depend on both the volume concentration of solids within the solids bed, i.e., the dilatancy factor, $\bar{\lambda}$, and the rate of strain. The static contribution dominates at high particle concentration and low strain rates. In this situation, the particles are in close contact and the shear stresses are of the quasi-static, rate independent Coulomb-type as described in soil mechanics literature (de Jong [1964], Spencer [1964], Mandl and Luque [1970] and Roscoe [1970]).

Conversely at low particle concentrations and high strain rates, the mean free path of the particles is large compared to particle diameters and interchange of particles between adjacent layers moving at different mean transport velocities may

dominate stress generation, analogous to turbulent viscosity in fluid flow. At moderate particle concentration and high strain rate, collision between particles will dominate stress generation because in this situation there are rarely any void spaces of sufficient size for the interchange of particles over significant distance. The case pertaining to low and moderate particle concentration has been termed as the grain inertia regime (Bagnold [1954]) and under these conditions the dynamics of the actual particle collision becomes important.

Reviews of continuum methods are widely available in the literature (Runesson and Nilsson [1986], Polderman *et al*. [1987], Johnson and Jackson [1987], Savage and Lun [1988[, Savage [1988], Campbell [1990], Gu *et al*. [1992], Adams and Briscoe [1993], Abu Zaid and Ahmadi [1993]). Khakhar *et al*., [1997a, 1997b] analyzed the flow behaviour macroscopically using continuum model by taking averages across the active layer to obtain average velocity variation along the layer.

2.7.2   Microscopic modelling or discrete element modelling

The discrete element method (DEM) is based on the Lagrangian approach for the simulation of the motion of granular material on the microscopic level of particles. It means that DEM can be used to calculate quantities that are difficult to obtain experimentally and can be used to improve continuum mechanics method. With the development of powerful computing machines and various numerical techniques more and more attempts have been made to study granular flows using discrete element methods (Kenji Yamane *et al*., [1995], Chakraborty *et al*., [2000], Rajamani *et al*., [2000]). The DEM can be divided into three main classes

- Statistical Mechanics models
- Classical Newtonian dynamics models
- Hybrid models

Statistical Mechanics models: Statistical mechanics models use stochastic components in particle displacements, for example the Monte Carlo method (Devillard, [1990), Camp and Allen [1996]), the cellular automata method (Baxter and Behringer [1990]) or the random walk approach (Caram and Hong [1991]).

Monte Carlo method was first introduced into the field of granular materials to study the size segregation of binary mixtures undergoing vertical vibrations (Rosato et al., 1987]. But this method has several limitations, for example; (i) no physical time scale enters the model since the collision time is assumed to be zero (ii) the normal restitution coefficient has to be zero in order to minimize the potential energy during each particle move. It is therefore difficult to relate the physical material properties to the random walk process which might be the reason why this method has not attracted much attention in the field of granular materials in recent years.

The use of *cellular automaton* models to study granular materials dates back to the introduction of the concept of *self-organized criticality*, where sandpile avalanche statistics were used (Bak et al., 1987]. In these models, space is discretized into cells which have the size of the particles and can either be occupied or empty. The particle dynamics is modeled by specifying a set of particle collision rules which apply when certain conditions are fulfilled, e.g. the local surface angle (slope) exceeds a threshold value. Theses rules were later refined by deriving them from experiments to study the outflow rate (Baxter and Behringer, 1990], stagnation zones (Baxter and Behringer, 1991] and the segregation process during particle outflow from two-dimensional hoppers (Fitt and Wilmott, 1992]. But as with most models working on lattices, the surface angle is mostly given by the topology of the underlying lattice and only identical particles were studied so far. A direct connection of the update time and the physical time is also missing which greatly reduces the scope of the *cellular automaton* approach. It has been argued (Baumann, 1997] that

the discretization of the particle velocities leads to contradictions with experimental results and to unphysical behaviour.

Random walk model by Caram and Hong, [1991] focuses on the overall geometry of highly packed granular particles through which voids diffuse under the influence of gravity (Hong, [1993]). It is based on a random walk process on a discrete lattice and was mostly used to study the particle outflow from two-dimensional hoppers (Caram and Hong, 1992]. The model involves many simplifications and has certain limitations: (i) the void diffusivity which enters the model is not correlated to any physical or geometrical quantity, (ii) the voids maintain their integrity as they move upwards whereas they disperse in real granular systems and (iii) stresses do not appear in the model but play a crucial role

Classical Newtonian dynamics models: Classical Newtonian dynamics models use equations of particle dynamics derived form Classical Newtonian mechanics for each particle. These models can be divided into two groups namely;

- Event-driven methods (EDM)
- Time-driven methods (TDM)

The event driven method (EDM) or hard sphere method is based on instantaneous collisions, which means that the state of the particles is updated only when the event occurs, i.e., when the particles collide. Energy dissipation during collisions is defined by the coefficient of restitution, which can be set according to Newton's law of restitution, or Poisson's hypothesis. However, the principle of energy conservation may be violated under certain conditions by Newton's law and Poisson's hypotheses (Hogue and Newland [1994]). This method has been used to study simple shear flow of frictional spheres (Lun and Bent, [1994]), one-dimensional

particle dynamics with energy input (Du et al., 1995] and the collision process in two dimensions (McNamara and Young, 1996]. But for large particle numbers and low restitution coefficient, the system can undergo an infinite number of collisions in finite time leading to a kind of clustering termed as *inelastic collapse* and this has been found in one-dimensional (McNamara and Young, 1992] and two-dimensional systems (McNamara and Young, 1993]. In such cases the *event driven* algorithm breaks down and requires further refinement to take care of the inelastic collapse.

Time driven methods (TDM) or soft sphere method (pioneered by Cundall and Strack [1979]), is best suited when the time of collision between real particles is larger than the time of the mean free path of the particles. In this case the current state of the particles at a particular time is updated after a fixed time step, which is smaller than the smallest time of impacts. The state of the particles is obtained by the time integration of the Newton's equations of motion for the translational and rotational motion for each particle in the granular medium. The inter-particle forces acting on the system are of key importance, apart from the external forces like the frictional force, damping force and the gravitational force. At every time step, the forces and momentum acting on each particle is tracked and the velocities and accelerations are assumed to be constant during that time step. Only the collisions and the contact forces affect the neighbouring particles. Particles are treated as contacting elastic bodies which may overlap with each other. Contact forces depend on the overlap geometry, materials properties and the dynamics of the particles.

A characteristic feature of the soft sphere model is that they are capable of handling multiple particle contacts, which is of importance when modelling quasi-static systems like granular flows in rotating cylinder. Hence this method is chosen for the present work to study the dynamics of granular material motion in a rotating cylinder. A good review of soft sphere method or discrete element simulation, is presented by Algis Dzingys and Bernhard Peters [2001], Cleary [1998a, 1998b,

1998c, 2000, 2001], Mishra and Rajamani [1992]. Ristow [1996], Dury and Ristow [1998] have used molecular dynamics simulation for simulating granular flows and presented a good review of this method.

Hybrid models combine ideas of statistical mechanics and Classical Newtonian Dynamics models. The particle motion is simulated using hard sphere approach using pseudo-random coefficients of restitution for energy dissipation.

2.8 Experimental work

In recent years experimental techniques such as Positron Emission Topography (PET), Positron Emission Particle Tracking (PEPT), Magnetic Resonance Imaging (MRI) and Gamma Ray Tomography (GRT) have been used to study the granular dynamics in rotating cylinders.

2.8.1 Positron Emission Topography:

The Positron Emission Topography (PET) has now become a widely used technique in medicine, and was developed at Birmingham University by Hawkesworth *et al.* [1991], Parker *et. al.* [1993, 1994]. PET is a technique in which, radioisotopes that emit positrons are injected into the system under consideration say, a rotating cylinder. Positrons are similar to electrons, but they have a positive charge, whereas electron has a negative charge. The collision of a positron and an electron in the system results in the emission of gamma rays, which can be detected and used to note the location of activities of each particle inside the cylinder. The newer models of positron emission topography scanners allow for more accurate and fast performance.

2.8.2   Positron Emission Particle Tracking:

Positron emission particle tracking (PEPT) is a technique for following the motion of a radioactively labeled tracer particle. It uses a radio nuclide which decays by positron emission and detects the back-to-back鄐ays produced when a positron annihilates with an electron. The tracer position is calculated by triangulation from a small number of back to back ray pairs, to within 2 mm 20 times per second for a slow moving tracer particle, and to within 5 mm 250 times per second for a tracer moving at speeds greater than 1 m/s. The鄐鄐ays are very penetrating and allows non-invasive tracking in actual engineering structures.

The PEPT technique has been used by a number of authors to investigate granular flow and mixing in various kinds of processing equipment including: (a) Lodige mixer (Broadbent *et al.*, [1993]), (b) partially filled horizontal cylinder slowly rotated about its axis, (Parker *et al.*, [1997]), (c) planetary mixer, consisting of a vertical cylinder stirred by a vertical blade, (Hiseman *et al.*, [1997]), (d) ploughshare mixer, (Jones and Bridgwater [1998]) and (e) horizontal cylinder stirred by a single flat blade, (Laurent et al. [2000]).

2.8.3   Magnetic Resonance Imaging:

Magnetic Resonance Imaging commencing with the work of Nakagawa *et al.* [1993], a number of authors have reported the results of Magnetic Resonance Imaging (MRI) measurements of granular flows. The technique allows non-invasive measurement of the particle velocity, concentration and velocity fluctuations. The technique works well at all positions in the sample and does not require mechanical markers and has no preferred orientation of measurement.

2.8.4 Gamma Ray Tomography:

In Gamma Ray Tomography, gamma rays or X-rays are scattered back to a detector array for producing an image. Since the X-ray response to scattering differs from that of absorption and transmission, reflected images can reveal details that shadow images miss. In addition, reflection mode only requires access to one surface. This can have advantages where the high-density bulk of an object obliterates all transmission shadows but a volume of interest is near one surface. The gamma ray tomography system for the measurement of radial voidage consists of a 67.5 microcurie 137Cs gamma source (disc source of 2 cm diameter), sodium iodide (NaI) with thallium (Tl) activated scintillation detectors (BICRON, 5 in number), a photo-multiplier tube, a preamplifer, a multi-channel (5 channels) analyser, data acquisition systems (para electronics) and related hardware and software. In the multi-channel counter, each channel generates an amplified energy pulse for a corresponding input pulse. These amplifed generated pulses lie between the base line energy (E) and the base line window energy (E dE) in window mode operation.

2.9 Conclusion

This Chapter provides a thorough literature survey on the transport phenomena of the granular bed motion in a horizontal rotating cylinder. Literature on the axial solid bed movement is surveyed first, followed by a detailed description of the different modes of motion of the granular solid bed in the transverse plane. The transition behaviour as predicted by Henein *et al.* [1983a, 1983b], Ding *et al.* [2002] and Mellmann [2001] is discussed at length. From the discussions it has been observed that transition behaviour depends mainly on the rotational speed, fill fraction, particle size and cylinder diameter. There is no unified empirical relation of these variables, which predicts the transition behaviour exactly.

Literature on particle mixing and segregation during the rolling mode of the granular solid bed is presented next followed by the description of the mechanism of particle segregation. The works of Henein *et al.* [1983a, 1983b], Nityanand *et al.* [1986], Metcalfe *et al.* [1995] are discussed in detail. It has been observed that the effect of particle shape on radial segregation and the segregation in a granular solid made up of many different particle sizes has not been studied yet.

This is followed by the modelling studies related to the flow of granular materials both on macroscopic scale and on microscopic scale. Several models have been proposed in the literature, but each model is validated only with the corresponding individual experiments, and has not been validated with other set of experiments or with other models.

Finally the experimental techniques   used to measure the particle positions, velocities, accelerations etc. of granular particles is presented. Hence based on the literature it has been concluded that a unified model without any empirical relations of the process variables is necessary for granular dynamics in a horizontal rotating cylinder, to predict the dynamics in a more realistic way and to study the effect of various process variables like rotational speed, fill fraction etc.

CHAPTER 3

THEORETICAL MODEL: DISCRETE ELEMENT METHOD

3.1 Introduction

In this chapter we introduce the problem and outline our strategy for solving it. It is clear from the literature review presented in the earlier chapter that the most appropriate method to model granular motion in rotating cylinder is the *Discrete Element Method or soft sphere method* since it is capable of handling multiple particle contacts, which is particularly important when modelling quasi-static systems like granular flows in rotating cylinder. Hence the soft sphere method is chosen for the present work to study the dynamics of granular material motion in a rotating cylinder. This chapter describes the general principles of Discrete Element Method.

The Discrete Element Method (DEM) is based on the Lagrangian approach. Hence it is possible to simulate the motion of granular material at the microscopic level, which in turn can be used to obtain fundamental informatics that are difficult to obtain experimentally or through macroscopic modelling. In the discrete element method, the particle position, orientation, translational and angular velocity are assumed as independent variables. They are obtained by integrating a system of fully deterministic classical equations based on Newtonian dynamics for each particle. For this purpose, explicit expressions have to be evaluated for all the forces acting on and between the particles.

Some of the forces between the particles have their origin based on the deformation experienced by particles when they are in contact with their neighbouring particles. An overlap area of the particles pressed against each other generally provides a good approximation as shown in Figure 3.1.

real deformation of particles

h_{ij}

particle deformation as overlap
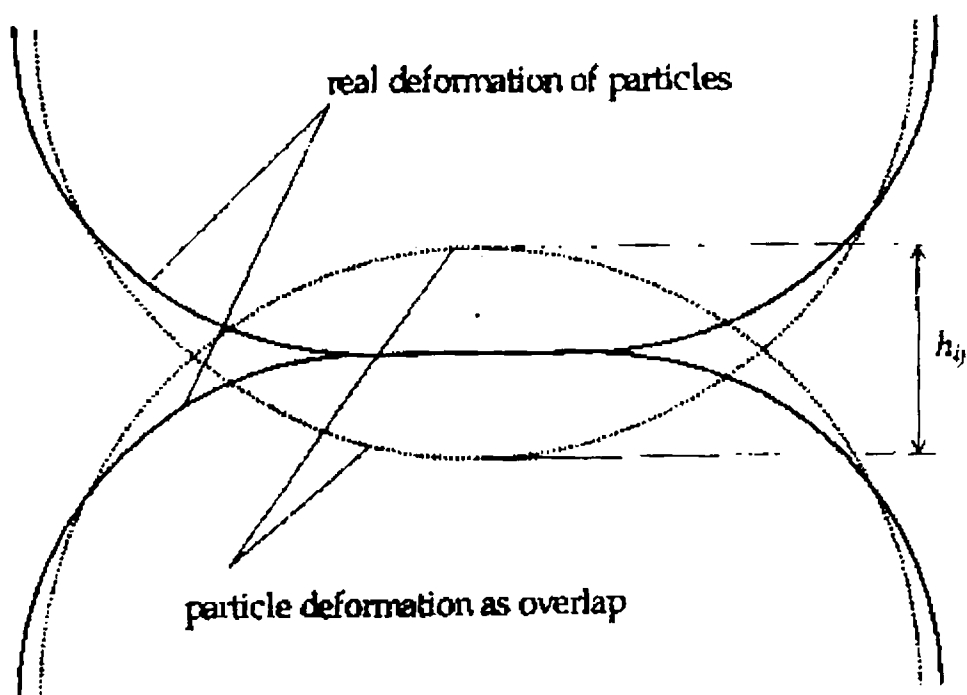
Figure 3.1: Elastic contact of two particles as overlap (Dziugys and Peters, [2001])

This assumption is valid since the deformation is much smaller than the particle size. Thus, the contact forces between them depend on the overlap geometry, the properties of the material and the relative velocity between the particles in the contact area. Hence in the perfect contact model, it is required to describe the effects of elasticity, energy loss through internal friction and surface friction and attraction on the contact surface for describing the contact force calculations, (Kohring [1995]).

3.2 Equations of particle motion

The equations of motion for each particle are derived from Newton's law of classical Newtonian dynamics. These include a system of equations for the translational motion of center of gravity and rotational motion around the center of gravity for each particle in the granular medium.

3.2.1 Translational motion

Translational motion of the center of gravity of a particle i can be fully described by a system of equations (Landau and Lifshitz, [1960])

$$m_i \frac{d^2 x_i}{dt^2} = m_i a_i = F_i \tag{3.1}$$

$$v_i = \frac{dx_i}{dt} \tag{3.2}$$

where v_i, a_i and x_i are vectors of velocity, acceleration and the position of the center of gravity m_i of the particle $i(i = 1,...N)$ respectively. N is the total number of particles in the granular material. Since the motion of particles is considered to be that of a rigid body, the sum of all forces F_i is assumed to act on the center of gravity of the particle:

$$F_i = F_{i,contact} + F_{i,gravity} + F_{i,external} \tag{3.3}$$

where $F_{i,contact}$ is the summation of direct contact forces between the particle i and all other particles that are in contact with particle i.

$$F_{i,contact} = \sum_{j=1, j \neq i}^{n_{ij}} F_{ij} \tag{3.4}$$

where F_{ij} is a force acting on the contact area of elastic impacts between the particles i and j, n_{ij} denotes the number of particles that are in contact with i. It should be noted here that Newton's third law of motion applies

$$F_{ij} = -F_{ji} \tag{3.5}$$

In general, contacting forces can also include inter-particle forces acting between charged particles. $F_{i,gravity}$ is the gravitational force acting on the particle:

$$F_{i,gravity} = m_i g = V_i \rho_i \, g \tag{3.6}$$

where, V_i is the particle volume, ρ_i is the particle density and g denotes the gravity acceleration vector.

$F_{i,external}$ corresponds to the total sum of all the external forces acting on the particle such as the fluid drag forces and fluid lift forces, which are prominent in solid-gas phase systems. If a particle is charged, then $F_{i,external}$ includes the external magnetic field also.

3.2.2 Rotational Motion

Rotational motion of the particle i around the center of gravity can be fully described by the following systems of equations (Landau and Lifshitz, [1960])

$$I_i \frac{d^2\theta_i}{dt^2} = T_i \tag{3.7}$$

$$\omega_i = \frac{d\theta_i}{dt} \tag{3.8}$$

where the θ_i and ω_i are the vectors of orientation and angular velocity. I_i is the inertial tensor of the particles and is expressed as $I_i = (I_{1i}, I_{2i}, I_{3i})$. The sum of all torques T_i acting on the particle i is given by

$$T_i = T_{i,contact} + T_{i,fluid} + T_{i,external} \tag{3.9}$$

where $T_{i,fluid}$ denotes the total torque caused by anti-symmetric fluid drag forces, $T_{i,external}$ denotes the summation of torques caused by other external forces and $T_{i,contact}$ is the summation of all the torques caused by the contact forces between the particles and is expressed as

$$T_{i,contact} = \sum_{j=1, j\neq i}^{N} T_{ij} = \sum_{j=1, j\neq i}^{N} d_{cij} \times F_{ij} \tag{3.10}$$

where dc_{ij} is the vector of relative contact positions

Orientation θ_i, angular velocity ω_i, torque T and inertia momentum I_i of two-dimensional particles can be treated as scalars. Therefore, the equations of rotational motion of the particle i around the center of gravity can be simplified as follows

$$I_i \frac{d^2\theta_i}{dt^2} = I_i u_i = T_i$$

$$\omega_i = \frac{d\theta_i}{dt}$$

For three-dimensional particles, however, the inertial moment must be calculated at every time step, according to the new orientation of the particle in the space. Therefore, it is convenient to use the space-fixed and body-fixed co-ordinate systems. The space-fixed (or laboratory) co-ordinate system is fixed in a laboratory space. The body-fixed (or local) co-ordinate system is a moving Cartesian co-ordinate system, which is fixed with the particle and whose axes are superposed by the principal axes of inertia (Algis Dzingys & Bernhard Peters [2001])

The inertial tensor always is diagonal $I_i = (I_{1i}, I_{2i}, I_{3i})$ in a body-fixed co-ordinate system. For spherical particles, $I_{1i} = I_{2i} = I_{3i} = I_i$, and body-fixed co-ordinates can be set in the same direction as space-fixed ones. Therefore, orientation is not used for spheres and the equations of motion can be written as

$$\frac{d\omega_i}{dt} = \frac{T_i}{I_i}.$$

(3.11)

3.3 Boundary conditions

The properties of granular flow are strongly dependent on the boundary conditions at the wall (Thompson and Grest, [1991]). Therefore the boundary conditions are very important for an adequate simulation of the granular material behaviour. Several types of boundary conditions can be employed:

(a) Walls that may be moving or stationary

(b) Inflow and outflow

(c) Periodic

Walls can be constructed using planes, spheres, cylinders or any other shape as big particles or by an array of small particles. In general, boundaries of the system such as walls are required for the motion of granular material or particles within enclosures, where the wall may have an important influence on the motion of a granular material due to wall-particle interaction. Furthermore, walls can move and rotate around a point of rotation. The rotation of wall particles, in particular is unavoidable in the present study, in which the motion of granular material on the rotating cylinder solely depends on the moving wall.

A rotating cylinder can be constructed by a cylinder or sphere with a negative radius. Collisions between particles and walls are defined by the material and geometry of the particles and walls, as in the case of collisions between particles. It is convenient to construct rough walls by an array of particles (Thompson and Grest, [1991]).

For the present formulation the following methodology is adapted; the system under consideration has been modelled by an ensemble of spheres possessing the

same material constants as that of the grains inside the container. The motion of the wall spheres is not affected by the impacts but is strictly governed by the continuous rotation of the cylinder. The calculation of contact forces between the particles and wall are defined in the same way as between particles.

3.4   Particle shape

In three dimensional co-ordinate systems, particles can be represented by spheres, ellipsoids, super quadrics, polyhedrons, etc. and for two dimensional co-ordinate system by disks, ellipses, polygons, polar forms etc. and by strings in one dimensional co-ordinate system. Reviews of various possible shapes of particles and some aspects of applications of shapes are presented in Haff [1993] and Ristow [1996]. It is not a difficult problem to construct particles of various shapes. The major problem however is to detect the contact between the neighbouring particles and to calculate the overlap area, intersection and contact points and normal and tangential contact vectors. For some of the analytical shapes, such as ellipsoids or super quadrics, analytical solutions may be found, However, for complicated shapes, considerable computational effort is needed.

The choice of sphere offers considerable simplification since the center of gravity of a sphere coincides with the geometrical center and the particle can be described only by its radius with no need of specifying the orientation (Lubachevsky [1991], Lubachevsky *et al.*, [1996], Kornilovsky *et al.*, [1996], Sadd *et al.*, [1993], Hoomans *et al.*, [1996], Luding *et al.* [1996], Kumaran [1997]).

This especially applies to molecular dynamics simulations, because it is quiet natural to describe an atom as a sphere (Grest *et al.*, [1989], Gilkman *et al.*, [1996]). The particle is described only with the radius and no orientation is needed. Campbell

and Brennen [1985] used a disk to simulate three dimensional cylinders oriented in the same direction and located in the same plane. *Hence for the present study, the particle shape is assumed to be spherical.*

3.5 General Scheme for the contact geometry

Let any two particles i and j be in contact with position vectors x_i and x_j with center of gravity lying at O_i and O_j having linear velocities v_i and v_j, angular velocities ω_i and ω_j respectively as shown in Figure 3.2. (Algis Dzingys and Bernhard Peters [2001]).
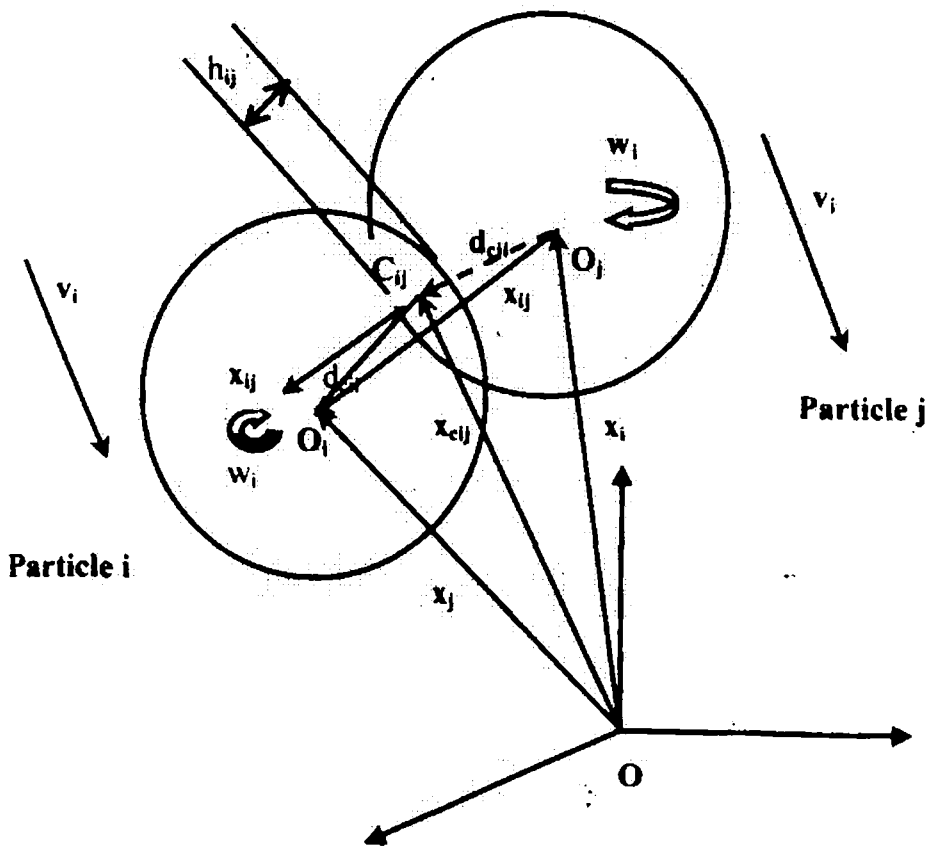
Figure 3. 2: Contact between two particles i and j.

The contact point C_{ij} is defined to be at the center of the overlap area with the position vector x_{cij}. The vector x_{ij} of the relative position point from the center of gravity of particle i to that of particle j is defined as $x_{ij} = x_i - x_j$.

The depth of overlap is h_{ij}. Unit vector in the normal direction of the contact surface through the center of the overlap area is denoted by n_{ij}. It extends from the contact points to the inside of the particle i as $n_{ij} = -n_{ji}$.

The vectors d_{cij} and d_{cji} are directed towards the contact point from the centers of particle i and particle j respectively and are represented as

$$d_{cij} = x_{cij} - x_i$$

and

$$d_{cji} = x_{cji} - x_j \tag{3.12}$$

Since the particle shape is assumed to be spherical, for spheres of any dimension the contact parameters can be written as follows:

$$h_{ij} = \begin{cases} R_i + R_j - |x_{ij}|, & |x_{ij}| < R_i + R_j \\ 0, & |x_{ij}| \geq R_i + R_j \end{cases} \tag{3.13}$$

$$n_{ij} = \begin{cases} 0, & x_{ij} = 0 \\ \dfrac{x_{ij}}{|x_{ij}|}, & x_{ij} \neq 0 \end{cases} \tag{3.14}$$

$$d_{c_{ij}} = -\left(R_i - \frac{h_{ij}}{2}\right)n_{ij}$$

(3.15)

where R_i is the radius of the particle.

The relative velocity of the contact point is defined as

$$v_{ij} = v_{cij} - v_{cji},$$

(3.16)

where,

$$v_{cij} = v_i + \omega_i \times d_{cij}$$

$$v_{cji} = v_j + \omega_j \times d_{cji}.$$

are the velocities of particle i and particle j respectively.

The normal and tangential components of the relative velocities are defined by

$$v_{n,ji} = \left(v_{ij} \cdot n_{ij}\right)n_{ij}$$

(3.17)

and

$$v_{t,ji} = v_{ij} - v_{n,ij}$$

(3.18)

In case of contact with partial slip, particles may slip relative to the distance $\delta_{t,ij}$ in tangential direction. $\delta_{t,ij}$ is the integrated slip in tangential direction after particles i and j came into contact and can be defined by the equation, (Algis Dzingys and Bernhard Peters [2001]).

$$\delta_{t,ij} = \left|\int v_{t,ij}(t)dt\right|$$

(3.19)

Here $\delta_{t,ij}$ is allowed to increase until the tangential force exceeds the limit imposed by static friction. The vector of tangential displacement $\delta_{t,ij}$ is defined to be perpendicular to the normal contact direction and located on the same line as $v_{t,ij}$. If the tangential component of the contact velocity $v_{t,ij}$ is not equal to zero, then the unit vector t_{ij} of the tangential contact direction is directed along $v_{t,ij}$. If $v_{t,ij}$ is equal to zero, t_{ij} has the same direction as that of the slip. Otherwise t_{ij} is equal to zero, if $v_{t,ij}$ and $\delta_{t,ij}$ are equal to zero, then

$$t_{ij} = \begin{cases} \dfrac{v_{t,ij}}{\left|v_{t,ij}\right|}, & v_{t,ij} \neq 0 \\[4mm] \dfrac{\delta_{t,ij}}{\left|\delta_{t,ij}\right|}, & v_{t,ij} = 0, \delta_{t,ij} \neq 0 \\[4mm] 0, & \text{otherwise} \end{cases} \qquad (3.20)$$

3.6 Inter particle contact forces

The contact force F_{ij} of a viscoelastic collision between two particles i and j acts on the contact surface and is convenient to calculate F_{ij} acting on an imaginary contact point C_{ij}. According to Kohring [1995] a model of inter-particle viscoelastic contact forces has to describe the following four effects:

- Particle elasticity
- Energy loss through internal friction
- Attraction on the contact surface
- Energy loss due to surface friction

F_{ij} can be expressed as the sum of normal and tangential components

$$F_{ij} = F_{n,ij} + F_{t,ij} \tag{3.21}$$

which is in their general form, would be a function of the relative normal (n_{ij}) and tangential (δ_{ij}) displacements of contact as well as the relative normal and tangential velocities, Sadd *et al.* [1993],

$$F_{n,ij} = F_{n,ij}(h_{ij}, v_{n,ij}, \delta_{t,ij}, v_{t,ij}) \tag{3.22}$$

$$F_{t,ij} = F_{t,ij}(h_{ij}, v_{n,ij}, \delta_{t,ij}, v_{t,ij}) \tag{3.23}$$

Algis Dziugys and Bernhard Peters [2001] have given a detailed survey of the various types of contact forces used for discrete element simulation along with their merits and demerits. *For the present theoretical formulation the contact forces between the spherical particles are modelled as springs, dash-pots and a friction slider as originally proposed by Cundall and Strack [1979].* The schematic representation of contact forces adopted for the theoretical formulation using spring, dash-pot and slider is shown in Figure 3.3 for particle-particle contact and particle-wall contact. The spring accounts for elastic repulsion, dash-pots express the damping effect, and friction sliders express the tangential friction force in the

presence of a normal force. The effect of these mechanical elements on particle motion appears through the stiffness k, the damping coefficient η and the friction coefficient μ.

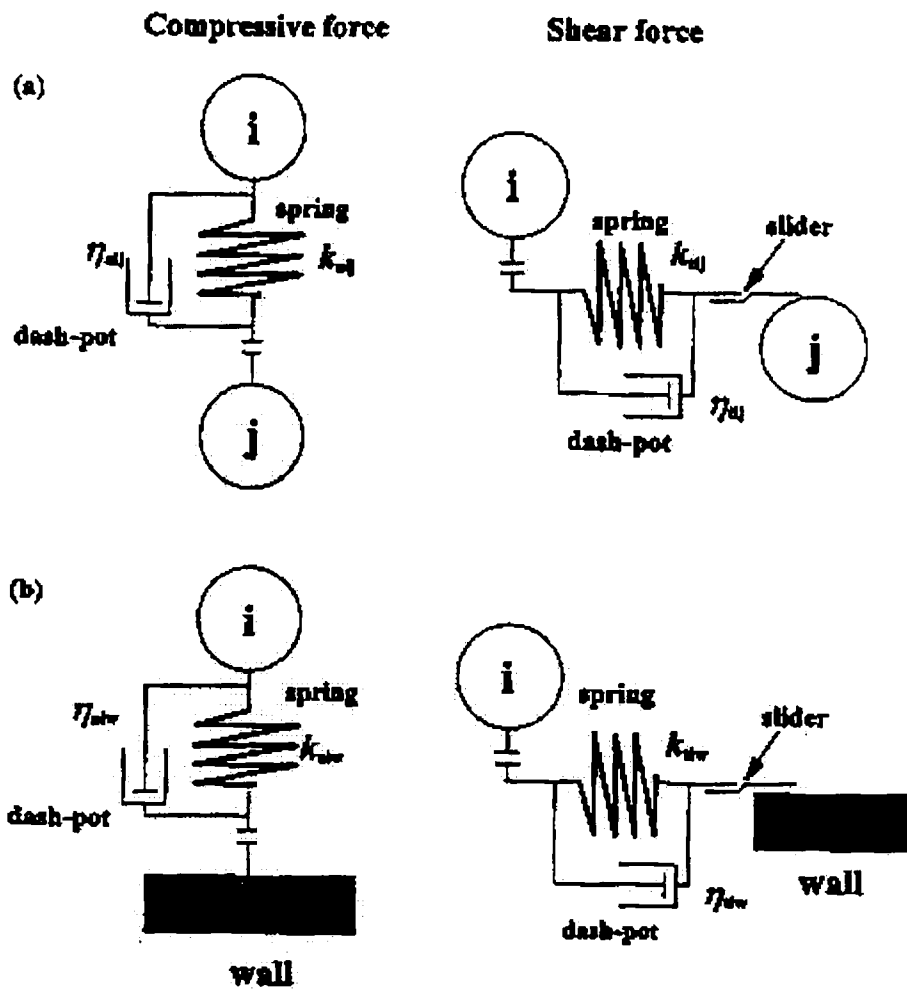**Compressive force** **Shear force**

(a)

(b)

Figure 3.3 : Schematic representation of contact forces

The normal components of contact forces between particles can be expressed as the sum of elastic repulsion, internal friction and the surface attraction forces.

$$F_{n,ij} = F_{n,ij,elastic} + F_{n,ij,viscous} \qquad (3.24)$$

Normal Elastic repulsion force, $F_{n,ij,elastic}$: This force is based on the linear Hooke's law of a spring with a spring stiffness constant $k_{n,ij}$ and is given by the expression,

$$F_{n,ij,elastic} = k_{n,ij} h_{ij} n_{ij} \qquad (3.25)$$

where h_{ij} is the depth of overlap between the contacting particles, n_{ij} is the normal component of the displacement between the particles i and j. The maximum overlap is dependent on the stiffness coefficient. Typically average overlaps of 0.1-1.0% are desirable requiring stiffness of the order of $10^5 - 10^7$ N/m (Cleary, 2000)

Normal energy dissipation force, $F_{n,ij,viscous}$: Energy is dissipated during real collisions between particles and, in general, it depends on the history of impact. A very simple and popular model is based on the linear dependency of force on the relative velocity of the particles at the contact point with a constant normal dissipation coefficient γ_n and is expressed as

$$F_{n,ij,viscous} = -\gamma_n m_{ij} v_{n,ij} \qquad (3.26)$$

where m_{ij} is the effective mass of the contacting particles i and j and is given by

$$m_{ij} = \frac{m_i m_j}{m_i + m_j} .$$

The tangential component force model is more complicated due to the consideration of static and dynamic frictional forces. Moreover these forces depend on the normal force and normal displacement. Further the model for static friction must include energy dissipation, because perpetual oscillations in tangential direction will be obtained during the time of static friction. In the literature two major approaches can be found to represent tangential contact forces namely; global and complex models. Global models describe all the phenomena of the tangential force through a single expression. Complex models describe static and dynamic friction by separate equations and the Coulomb criteria. Of course, the continuous particle interaction models require special models for tangential forces. The present theoretical formulation is based on the complex model approach where the evolution of tangential force $F_{t,ij}$ being divided into parts of static friction or dynamic friction. When the tangential force $F_{t,ij}$ is larger than the Coulomb-type cut-off limit, dynamic friction predominates. When $F_{t,ij}$ is lower than the limit, the model of static friction force $F_{t,ij,static}$ must be implemented. Such an approach can be modelled by

$$F_{t,ij} = \begin{cases} F_{t,ij,static} & \text{for } |F_{t,ij,static}| < |F_{t,ij,dynamic}| \\ F_{t,ij,dynamic} & \text{for } |F_{t,ij,static}| \geq |F_{t,ij,dynamic}| \end{cases} \qquad (3.27)$$

or, in a more convenient form for programming purposes, by

$$F_{t,ij} = -t_{ij} \min\left(|F_{t,ij,static}|, |F_{t,ij,dynamic}|\right) \qquad (3.28)$$

where t_{ij} is the unit vector of the tangential direction of the contact point.

The dynamic frictional force can be described by the following equation,

$$F_{t,ij,dynnamic} = -\mu \left| F_{n,ij} \right| t_{ij} \tag{3.29}$$

where μ is the dynamic friction coefficient

The static friction force is composed of contributions from both the tangential spring and energy dissipation terms and they are expressed as

$$F_{t,ij,static} = F_{t,ij,spring} + F_{t,ij,dissipation} \tag{3.30}$$

where the tangential spring force is defined as

$$F_{t,ij,spring} = -k_{t,ij} \delta_{t,ij} t_{ij}, \tag{3.31}$$

Here, $k_{t,ij}$ is the spring stiffness coefficient and $\delta_{t,ij}$ is the integrated slip in tangential direction after the particles i and j come into contact.

Friction model for energy dissipation in the tangential direction can be used in the energy dissipation in normal direction,

$$F_{t,ij,dissipation} = -\gamma_t m_{ij} v_{t,ij} \tag{3.32}$$

where γ_t is the shear dissipation coefficient and m_{ij} the effective mass of the contacting particles.

Based on the above description of the general formulation of the discrete element method the governing equations for the motion of granular material inside a rotating cylinder can be summarized as follows;

$$m_i \frac{d^2 x_i}{dt^2} = m_i a_i = F_i \tag{3.33}$$

$$v_i = \frac{dx_i}{dt} \tag{3.34}$$

$$I_i \frac{d^2 \theta_i}{dt^2} = T_i \tag{3.35}$$

$$\omega_i = \frac{d\theta_i}{dt} \tag{3.36}$$

Here

$$F_i = m_i g + F_{i,contact}$$

$$= m_i g + \sum_{j=1, j \neq i}^{N} F_{ij}$$

$$= m_i g + \sum_{\substack{j=1 \\ j \neq 1}}^{N} (F_{n,ij} + F_{t,ij})$$

$$= m_i g + \sum_{\substack{j=1 \\ j \neq 1}}^{N} F_{n,ij} + \sum_{\substack{j=1 \\ j \neq 1}}^{N} F_{t,ij} \tag{3.37}$$

and

$$T_i = T_{i,contact}$$

$$= \sum_{j=1, j \neq i}^{N} T_{ij}$$

$$= \sum_{j=1, j \neq i}^{N} d_{cij} \times F_{ij} \qquad (3.38)$$

where dc_{ij} is the vector pointing from the center of gravity of particle i to the contact point with particle j.

In the next section the procedure for solving these equations is presented.

3.7 Time integration:

Various time integration schemes can be used to solve the equations. The main requirements for a good scheme are given below:

- It should be stable

- It should satisfy the required accuracy

- It preferably should satisfy energy and momentum conservation

- It should not require excessive memory

- Time consuming calculation of inter-particle forces should be carried to the minimum possible extent-ideally once per time step, Δt

Some of the most popular schemes used in DEM by various authors include; first order Euler's scheme, Fourth-order Runge Kutta method (Ovensen *et al.*, [1996], Allen and Tildseley, [1987], Shida *et al.*, [1997]), velocity verlet scheme (Aoki and Akiyama [1995], Kopf *et al.*, [1997], Satoh [1995a, 1995b]), second order Adams-Bashforth scheme (Sundaram and Collins [1996]) and predictor-corrector schemes (Newmark and Asce, [1959]), Thompson and Grest [1991], Form *et al.* [1993], Lee and Hermann [1993]).

Van Gunsteren and Berendsen [1977] compared the Gear predictor-corrector, Runge-Kutta and verlet schemes for macromolecular simulations and concluded that Gear scheme is the best for small time steps and verlet algorithm for larger time steps. *Hence the 5th order Gear predictor-corrector scheme (Allen and Tildseley, [1987]) is used in this work to solve the equations, which is stable for second-order differential equations with global truncation error of* $O\left(\Delta t^{q+1-2}\right) = O\left(\Delta t^{q-1}\right)$.

3.7.1 Gear's Predictor-Corrector Algorithm

Generally predictor-corrector methods are composed of three steps, namely;

(i)   Prediction

(ii)   Evaluation

(iii)   Correction

Using the current particle position $x(t)$ and particle velocity $v(t)$, the new particle position and new particle velocity is updated using the following steps:

a) Predict the particle position $x(t + \Delta t)$ and particle velocity $v(t + \Delta t)$ at the end of each iteration

b) Evaluate the forces at $t + \Delta t$ using the predicted position

c) Correct the predicted values using some combination of the predicted and previous values of the particle position and particle velocity.

In fifth order Gear predictor-corrector algorithm the particle positions x, at time $t + \Delta t$ was predicted using a fifth–order Taylor series based on particle positions

and their derivatives at time t. The derivatives $\dot{x}_i(t), \ddot{x}_i(t), \dddot{x}_i(t), x_i^{(iv)}(t)$ and $x_i^{(v)}(t)$ are also predicted at each time $t + \Delta t$ by applying Taylor expansions at t:

$$x_i(t + \Delta t) = x_i(t) + \dot{x}_i(t)\Delta t + \ddot{x}_i(t)\frac{(\Delta t)^2}{2!} + \dddot{x}_i(t)\frac{(\Delta t)^3}{3!} + x_i^{(iv)}(t)\frac{(\Delta t)^4}{4!} + x_i^{(v)}(t)\frac{(\Delta t)^5}{5!}$$

$$\dot{x}_i(t + \Delta t) = \dot{x}_i(t) + \ddot{x}_i(t)\Delta t + \dddot{x}_i(t)\frac{(\Delta t)^2}{2!} + x_i^{(iv)}(t)\frac{(\Delta t)^3}{3!} + x_i^{(v)}(t)\frac{(\Delta t)^4}{4!}$$

$$\ddot{x}_i(t + \Delta t) = \ddot{x}_i(t) + \dddot{x}_i(t)\Delta t + x_i^{(iv)}(t)\frac{(\Delta t)^2}{2!} + x_i^{(v)}(t)\frac{(\Delta t)^3}{3!}$$

$$\dddot{x}_i(t + \Delta t) = \dddot{x}_i(t) + x_i^{(iv)}(t)\Delta t + x_i^{(v)}(t)\frac{(\Delta t)^2}{2!}$$

$$x_i^{(iv)}(t + \Delta t) = x_i^{(iv)}(t) + x_i^{(v)}(t)\Delta t$$

$$x_i^{(v)}(t + \Delta t) = x_i^{(v)}(t)$$

Then the inter particle forces acting on each particle at time $t + \Delta t$ is evaluated using the predicted particle positions. Applying the obtained evaluated forces at time $t + \Delta t$ and Newton's second law, the particle accelerations $\ddot{x}_i(t + \Delta t)$ can be determined. The difference between the predicted accelerations and evaluated accelerations is then computed;

$$\Delta \ddot{x}_i = \ddot{x}_i(t + \Delta t) - \ddot{x}_i^P(t + \Delta t)$$

The predicted particle positions and their derivatives are corrected using the difference $\Delta \ddot{x}_i$ obtained between the predicted accelerations and that given by the evaluated force.

In the Gear's Predictor Corrector algorithm, this difference term is used to correct all the predicted particle positions and their derivatives. The correction terms are given by;

$$x_i = x_i^P + \alpha_o \Delta R_2$$

$$\dot{x}_i \Delta t = \dot{x}_i^P \Delta t + \alpha_1 \Delta R_2$$

$$\frac{\ddot{x}_i (\Delta t)^2}{2!} = \frac{\ddot{x}_i^P (\Delta t)^2}{2!} + \alpha_2 \Delta R_2$$

$$\frac{\dddot{x}_i (\Delta t)^3}{3!} = \frac{\dddot{x}_i^P (\Delta t)^3}{3!} + \alpha_3 \Delta R_2$$

$$\frac{x_i^{(iv)} (\Delta t)^4}{4!} = \frac{x_i^{(iv)P} (\Delta t)^4}{4!} + \alpha_4 \Delta R_2$$

$$\frac{x_i^{(v)} (\Delta t)^5}{5!} = \frac{x_i^{(v)P} (\Delta t)^5}{5!} + \alpha_5 \Delta R_2$$

where,

$$\Delta R_2 = \frac{\Delta \ddot{x}_i (\Delta t)^2}{2!}$$

Values of parameters α_i (Allen and Tildseley, [1987]) for second order differential equations of predicting order q are presented in table 3.1.

Table 3.1 : Values of the parameter α_i

α_i	$q = 3$	$q = 4$	$q = 5$
α_0	$\dfrac{1}{6}$	$\dfrac{19}{120}$	$\dfrac{3}{16}$
α_1	$\dfrac{5}{6}$	$\dfrac{3}{4}$	$\dfrac{251}{360}$
α_2	1	1	1
α_3	$\dfrac{1}{3}$	$\dfrac{1}{2}$	$\dfrac{11}{18}$
α_4	-	$\dfrac{1}{12}$	$\dfrac{1}{6}$
α_5	-	-	$\dfrac{1}{60}$

The parameter α_i promotes numerical stability of the algorithm. The solution of equations (3.33) to (3.36) was carried out by a 5th order Gear Predictor-Corrector scheme (Allen and Tildseley, [1987]). The time step Δt of the integration was chosen such that the entire contact between the particles was resolved within 10 time steps at least.

The time step Δt, for the time integration of the particle position, velocity, orientation and angular velocity depends on the time of contact T_c, which can be expressed as

$$T_c = \pi \sqrt{\frac{m}{k}}$$

which is estimated based on the single degree of freedom system of mass m connected to the ground by a spring of stiffness k. Hence the time step must be sufficiently small to ensure a stable numerical scheme of time integration and Cundall and Strack [1979] proposed that the time step must be smaller than the critical time

step $\Delta T_c = \sqrt{\frac{m}{k}}$

3.8 Collision detection

One of the most difficult barriers concerning the DEM simulation is the enormous number of particles, which represents the actual system, due to the reason that as the number of particles increases, the computational time also increases. This problem is inherent in contact-dominated flows. For real life systems, the particle number is usually very large compared to any small-scale models. Therefore, in order to make the simulation technique a really practical notion, Tsuji, *et. al.*, [1993] presented a method where a group of particles where replaced with one big ball and calculated the contact forces only for these balls. He also found similarity laws between cases of large number and small number of particles.

Agrawala *et al.*,[1997] implemented a computational scheme termed "boxing" to reduce the number of particles that have to be tested for potential contact with each

entity. To do so, the entire space was divided into small boxes, and a set of pointers was used to store all the particles inside each box in a linked list called a contact list. Hence, tests for potential contacts are done only between particles in the same or in neighbouring boxes.

In this work, we have adapted a methodology to reduce the computational time by calculating a neighbour list for each particle i. The particle i is said to be the neighbour list of particle j, if the distance D between the centers of particles i and j, is less than 2.5 times the larger particle diameter. i.e., if $D \leq 2.5 \, dp$.

Two particles *i* and *j* are said to be in contact if the distance between their centers is less than or equal to the sum of the radii. Hence the particles that are in contact with particle *i* is determined by checking this criteria with the particles in the neigbour list of particle *i* only. This procedure reduces lot of computational time since simulation of *n* interacting particles using DEM involves $\frac{n(n-1)}{2}$ pair of contacts.

3.9 Input parameters

The input parameters needed to run the simulations can be divided into three groups viz.

- Geometrical data of the system under investigation
- The particle physical parameters
- The outputs required

The geometrical parameters of the system under study for the present simulation are the diameter, length, fill fraction and rotational speed of the cylinder. The

position of the cylinder wall is also defined by a set of particles with respect to a global coordinate system.

The particle physical properties are specified by their size distribution, density, stiffness parameters and damping parameters.

The outputs required depends on the type of information required such as the positions and velocities of the particle at different time intervals, the trajectories of a set of sample particles, the variation of normal, tangential forces and kinetic energy of the whole system with respect to time.

3.10 Implementation of the code

The major computational tasks of DEM at each time step can be summarized as follows:

- Finding the neighbour list for each particle
- Detection of contacts between a particle *i* and its neighbours
- Computation of contact forces from relative displacement between particles
- Summation of contact forces to determine the total unbalanced force
- Computation of acceleration from force
- Velocity and displacement by integrating the acceleration
- Updating the position of particles

Based on the theoretical formulation presented above, a software code called DEMCYL was written in Visual Fortran (version 6.6). which simulates the dynamics of granular material motion in a rotating cylinder. Visual Fortran is chosen as a programming language for the following reasons

- It is the most powerful structured programming language for scientific simulation.

- Improved flexibility like dynamic array concept, linking routines etc

The program currently runs on a Pentium IV machine with 256 MB RAM and Windows 2000 operating system. The maximum number of particles that can be used for this system is around 4000 since for each particle, the number of variables that has to stored is 12 and hence the array size becomes Number of particles X 12 and this array size has an significant effect on the program run time.

The program starts by reading all the input variables, and depending on the fill fraction and size distribution the number of particles is determined for each size. Since it is very difficult to generate a packed bed with a velocity distribution, the following methodology was adapted to generate the initial packed bed. First the particles are placed in an orthogonal grid and are assigned random initial velocities.

The particles are given different identities to identify their sizes and are shown in different colours during the output plots. Initially the particles do not experience any inter particle contact forces but experiences only the gravity force. But once the particles start colliding with each other the program computes the inter-particle contact forces. The total kinetic energy of the system is calculated and when the when the kinetic energy distribution dissipates to zero, the particles has to come to rest.

This data is stored as the initial configuration of the packed bed of particles along with the initial velocity distribution of particles. The cylinder wall is then allowed to rotate with a specified angular velocity and the program performs the computation at each time step. The program stores the position, velocity and force

information for all the particles and hence an enormous amount of memory is needed which increases tremendously with the increase in the number of particles.

The corresponding flow charts are given in Figures 3.4 and 3.5. The flow chart in Figure 3.4 shows the algorithm used for generating the initial packed bed and Figure 3.5 represents the flow chart showing the algorithm used for updating the particle position at every time step, after updating the neighbour list. The total force acting on each particle is calculated using the equations 3.37. Then the particle positions are updated using Gear predictor algorithm. The whole procedure is repeated till the required amount of time or till the system reaches steady state.

Once the program receives the stop signal, it stores the position, the velocity, acceleration, the neighbour list, kinetic energy of each particle at that instant of time as a separate file called "redata". A flag has been set in the "restart" option program. Once the program is restarted, depending on the value of the flag, the program either reads from the redata file or start from the initial distribution.

The code also has a provision to be stopped at intermediate values and it can be automatically restarted using the following procedure.
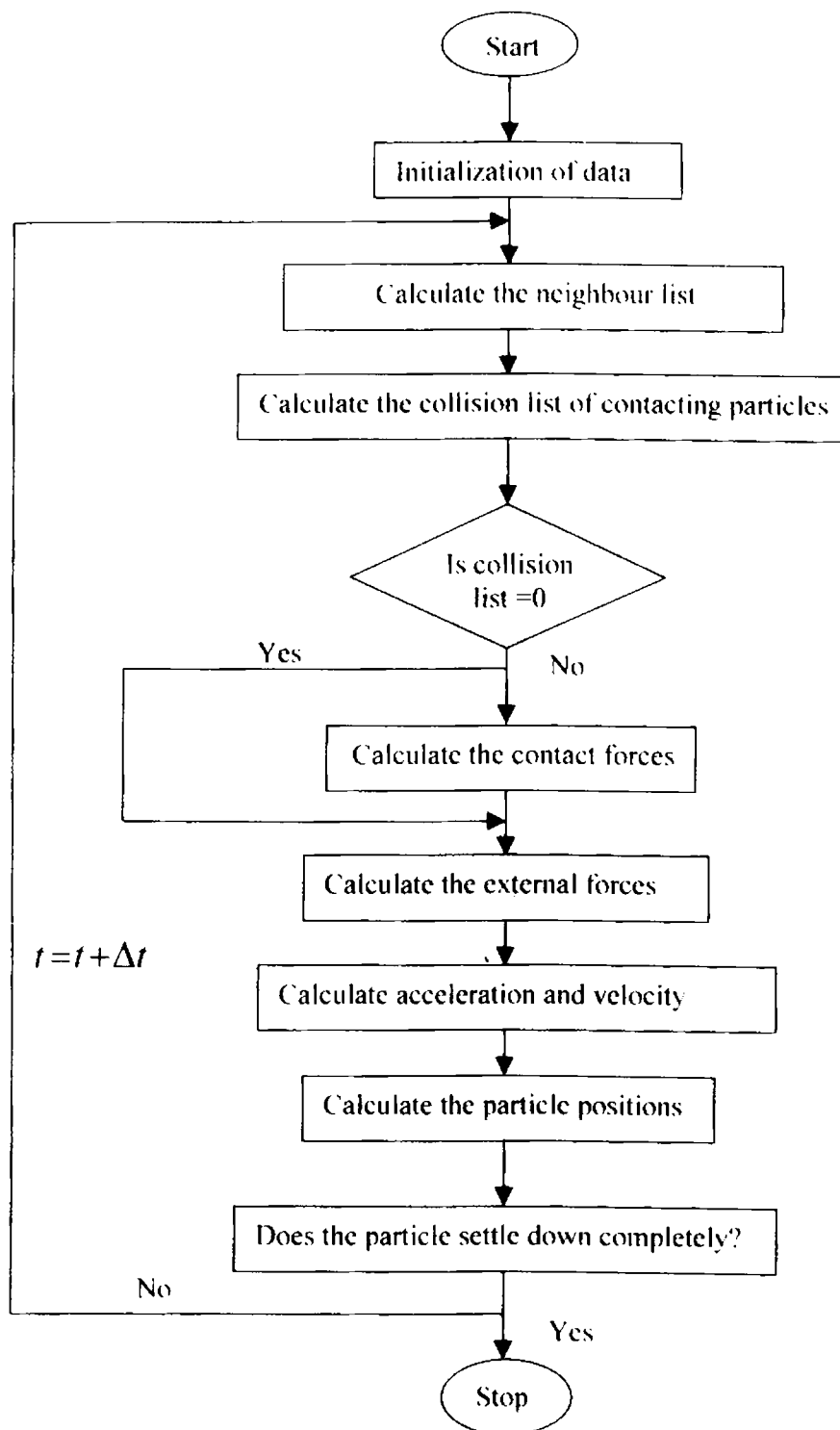
Figure 3.4: Flow chart showing the initial distribution of solid particles as a packed bed
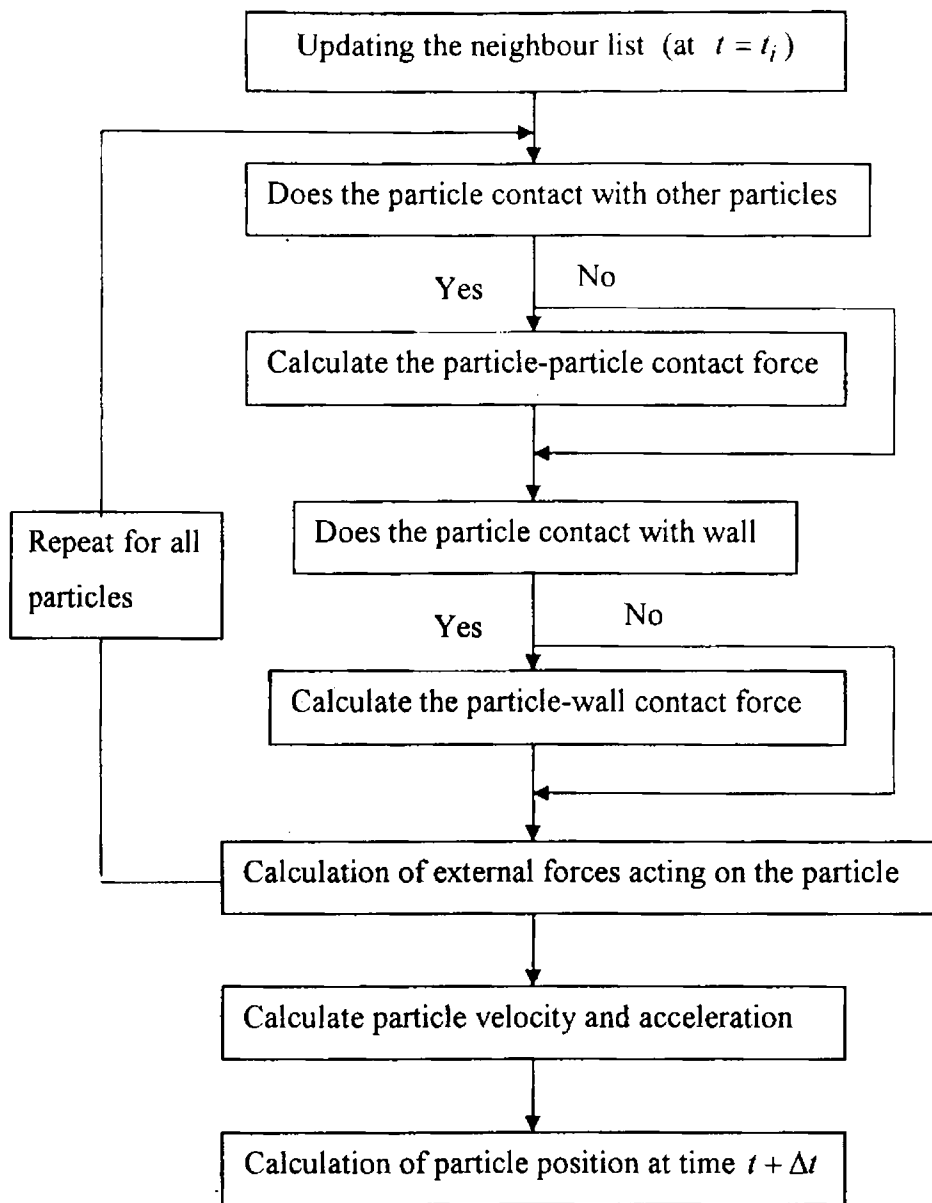
```
┌─────────────────────────────────────────────┐
│   Updating the neighbour list  (at  t = t_i )│
└─────────────────────────────────────────────┘
                      │
                      ▼
┌─────────────────────────────────────────────┐
│   Does the particle contact with other particles│
└─────────────────────────────────────────────┘

        Yes    │   No
               ▼
┌─────────────────────────────────────────────┐
│   Calculate the particle-particle contact force│
└─────────────────────────────────────────────┘
                      │
                      ▼
┌────────────────┐    ┌─────────────────────────────┐
│ Repeat for all │    │ Does the particle contact with wall│
│ particles      │    └─────────────────────────────┘
└────────────────┘
                    Yes    │   No
                           ▼
          ┌─────────────────────────────────────────┐
          │   Calculate the particle-wall contact force│
          └─────────────────────────────────────────┘
                              │
                              ▼
          ┌─────────────────────────────────────────────────┐
          │   Calculation of external forces acting on the particle│
          └─────────────────────────────────────────────────┘
                              │
                              ▼
          ┌─────────────────────────────────────────────────┐
          │   Calculate particle velocity and acceleration  │
          └─────────────────────────────────────────────────┘
                              │
                              ▼
          ┌─────────────────────────────────────────────────┐
          │   Calculation of particle position at time  t + Δt│
          └─────────────────────────────────────────────────┘
```

Figure 3.5:   Flow chart showing the calculation of particle positions at time $t + \Delta t$

3.11 Special Validation tests

There are two fundamental aspects to test the accuracy and predictability of a program model. First, the program must accomplish what is specified in the model and secondly how accurately the prediction of the model is validated with data from experiments. In order to decrease the chances of error, it is necessary to check the program using different types of validation tests [Asmar *et al.*, (2002)] as follows.

(i). Large runs to inspect the overall running of the program

(ii). Manual calculations to check small test runs

(iii). Special cases to inspect the implementation of individual program

(iv). Inspection of graphical output for the above to see if it looks sensible

(v). Inspection by an independent assessor

(vi). Use of specialist software for testing code against specifications.

DEMCYL was tested based on some of the above-mentioned strategies. Since the contact forces calculations are crucial for any DEM simulation some special tests are conducted to test the validity of the software code developed for this purpose.

3.11.1 Effect of normal elastic force in the vertical direction (Test 1)

This test simulates the free falling particle under gravity and also tests the particle-wall contact force. For this test, parameters corresponding to the tangential and damping forces are set zero and the effect of normal elastic force alone is studied. This test also confirms the particle-particle interaction since the wall is represented as a set of particles. The diameter of the particle is 6 cm and the dropping height chosen is 5 cm and the density of the particle is 1300 kg/m^3. The value of the normal stiffness parameter is 5x10^5 units. The particle is dropped from the same height

hitting the wall/particle, and the particle rebounds to its original height and the normal

elastic force reaches a peak during contact as shown in Figures 3.6 and 3.7
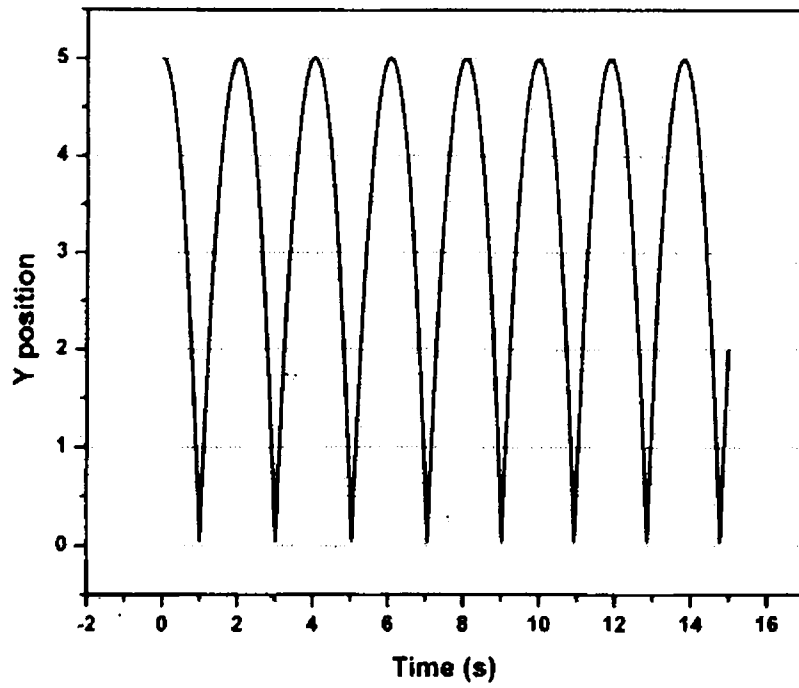
Figure 3.6 : y-position vs time
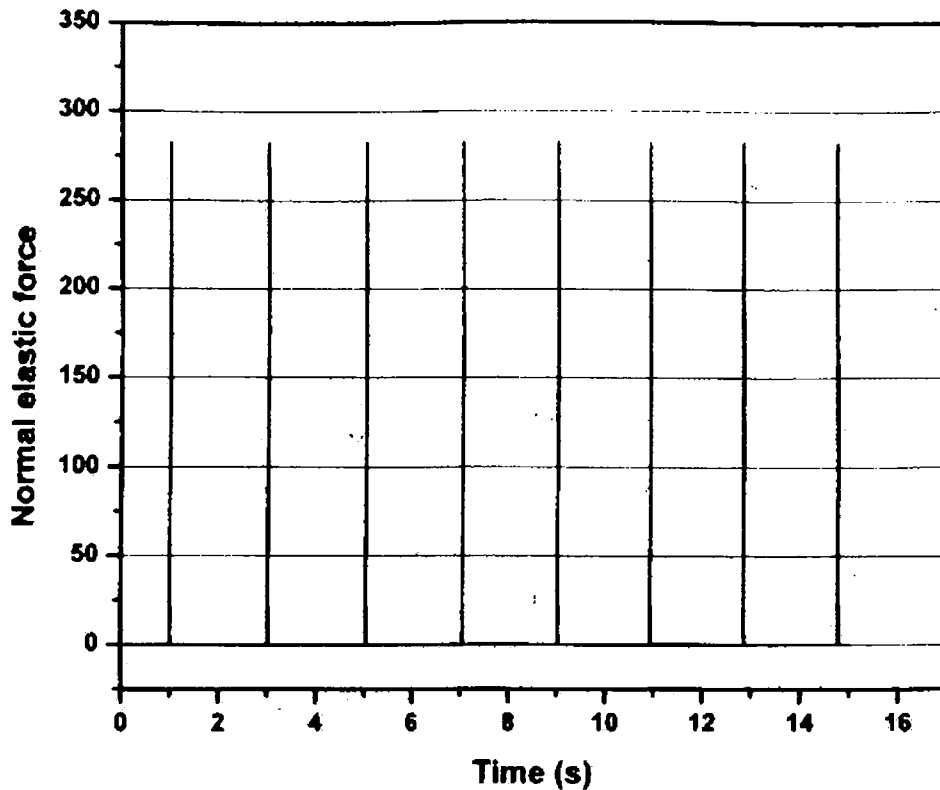
Figure 3. 7: Normal elastic force vs time

3.11.2 Effect of normal elastic force in the horizontal direction (Test2)

This test is identical to test1 but with one particle moving in the horizontal direction with initial velocity in x-direction. The gravitational, tangential and normal damping forces are set at zero. The parameters chosen are same as in test 1 and the initial velocity of the particle is taken as 1 m/s. Figure 3.8 shows the results for a particle with initial velocity in the x-direction. As can be seen, the particle rebounds horizontally between the walls with no loss of energy. There is no movement in the y-z directions and no rotation.
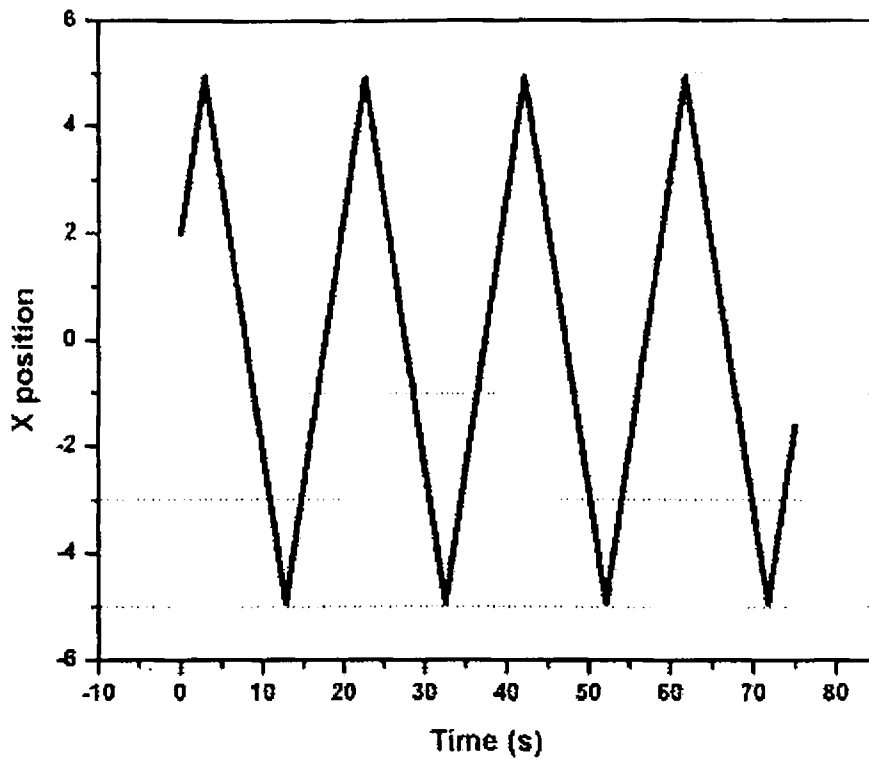
Figure 3.8: x-position vs time

3.11.3 Effect of normal damping force (Test 3)

This test is also similar to test 1 but with the normal damping force accounted for. The normal damping constant is taken as 100 s^{-1}. Figures 3.9 and 3.10 shows the effect of damping on the motion of the particle. The particle fails to reach the original height and its height decays due to damping effect. Also it can be seen form Figures the decline in the normal elastic force and damping force at consecutive contacts. There is no movement in the x-z directions and there is no rotation.
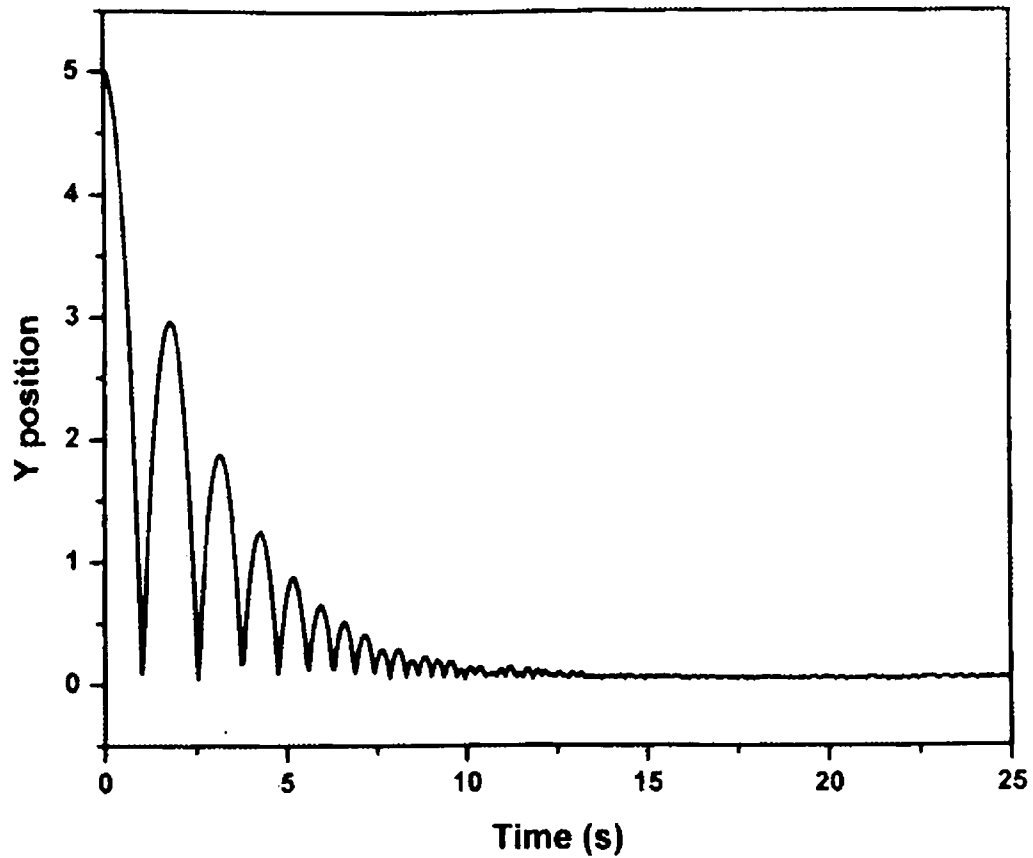
Figure 3.9: Y-position vs time

Further tests were also carried out to check the validity of tangential forces and the results are found to be in agreement with the expected outputs.

3.12 Conclusion

Since soft sphere approach is found to be the most appropriate method for modelling quasi-static systems like granular flows in rotating cylinder, the theoretical model based on Discrete Element Method (soft sphere approach) is presented in this

Chapter for simulating the dynamics of granular bed motion in the transverse plane of the horizontal rotating cylinder.

After introducing the general concepts of DEM, appropriate governing equations for the present system is presented along with the corresponding expressions for the normal and tangential contact forces. A strategy for finding the neighbour list and collision partners is explained. This is followed by the flow chart of the software code DEMCYL. Finally special validation tests have been carried to check the validity of the code developed. Hence the software code is tested for its accuracy and bugs and then results are generated for the dynamics of particle motion in a rotating cylinder. These results are presented in the next chapter.

CHAPTER 4

DYNAMICS OF GRANULAR SOLIDS MOTION IN THE TRANSVERSE PLANE OF ROTATING CYLINDER

4.1 Introduction

The motion of a bed of granular solids in the transverse plane of a rotating cylinder can exhibit a series of motions (Henein *et al.*,[1983a]), namely: slipping, slumping, rolling, cascading, cataracting and centrifuging which have been explained in detail in Chapter 2. The slipping, slumping and rolling modes of bed motion have been investigated experimentally by a number of authors, including Henein *et al.* [1983a] and McTait [1998]. The transition from slumping to the rolling mode of bed motion was found to occur at a rotational Froude number between 10^{-3} and 10^{-4} by Henein *et al.* [1983a] and between 10^{-4} and 10^{-5} by McTait [1998].

The specific mode of bed motion was also found to be uniquely determined by (i) the hold-up as a fraction of the cylinder volume, (ii) the rotation speed, (iii) the cylinder diameter, and (iv) the particle size and shape. It was found that the transition from a slumping to a rolling bed occurred at a lower rotational Froude number for (i) a higher fractional hold-up, (ii) particles having a spherical shape rather than an irregular shape, (iii) smaller particles, (iv) cylinders with larger diameter, and (v) granular solids with a lower static angle of repose. In a slumping bed, it was observed that the granular materials is lifted as a rigid body by the cylinder wall such that the inclination of the bed surface increases continuously until it reaches an upper angle of repose; then detaches from the upper surface of the bed, and falls as a discrete avalanche toward the lower half of the bed.

It can be observed from the literature that the work carried out by various investigators are mainly at a macroscopic level and further they have interpreted the process through empirical parameters derived from experiments. *No attention has been paid to the effect of the dynamic behaviour of the granular solids due to surface flow of granular solids, the effect of transient forces such as collision forces acting on the particles, the total kinetic energy of the system, particle velocities etc. These factors are crucial to generate a reliable model based on first principles for the purpose of design with negligible empirical input.*

In this chapter we use Discrete Element Method to obtain the relevant dynamic information on motion of granular solids subjected to rotational movement based on discrete element simulation. *Even though the software code DEMCYL is capable of solving three-dimensional motion of granular solids in a rotating cylinder, results in this chapter are aimed for a 2-dimensional situation viz., the simulation of granular solids in the transverse plane of the rotating cylinder. Since this approach provides adequate interpretation of the process without requiring unjustified computer time. We have restricted our analysis to 2-dimensional, since this would be adequate to gain enough information about the process while also reducing the computer time considerably.*

The dynamic information sought for includes the individual particle velocities, their trajectories, surface flow velocities, velocity vector plots, total kinetic energy and dynamic angle of repose. The two important process parameters considered in this chapter are fill fraction and rotational speed. The transition from slumping-rolling behaviour has been explained based on bed turnover time. The effect of the coefficient of friction on dynamic angle of repose, active layer depth as a function of rotational speed and fill fraction are also discussed.

4.2 Simulation of a packed bed of granular solids as an initial condition

The transverse plane of a horizontal cylinder is a circle. This is represented as a set of spherical particles at a distance equal to the cylinder radius from the origin of the Cartesian coordinate system chosen. The origin of the coordinate system is at the center of the circle as shown in Figure 4.1.
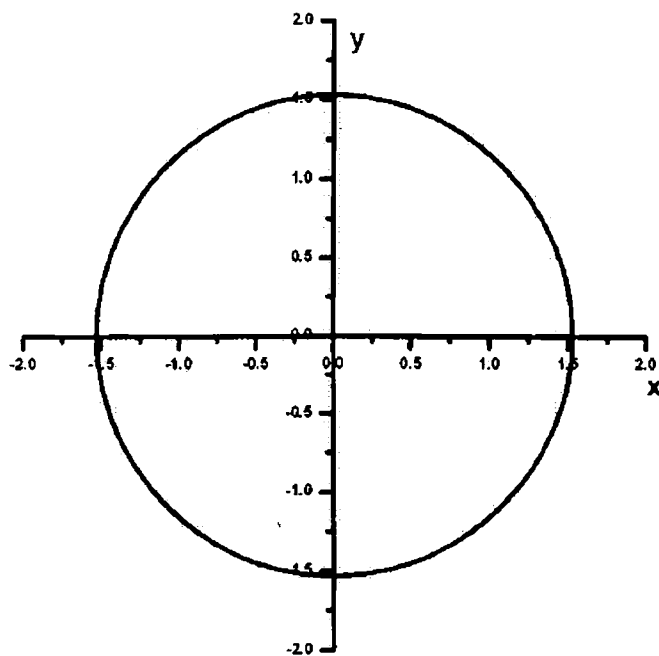
Figure 4.1   Coordinate system chosen for simulation

The initial condition, $t = 0$ of granular solids in the transverse plane of the rotating cylinder is assumed to be a packed bed of granular solids. Since the initial conditions of granular particles in a packed bed cannot be specified a priori, the calculations were carried out at two stages. Given the fill fraction, particle sizes

and their distribution, the number of particles for each size range was determined using equation (4.1)

$$np(i) = \frac{4\,fw_i A}{\pi\,d_p(i)^2}$$

(4.1)

where fw_i is the percentage of fraction of the particles of size $d_p(i)$ and A is the cross sectional area of the bed. An orthogonal grid is then generated with the size of the grid equal to the diameter of the largest particle and the particles are placed at the center of these grids so that they don't overlap over each other. Uniform sized particles are given a particular colour. Figure 4.2 shows one such initial distribution generated for two different sized particles at equal number concentrations.
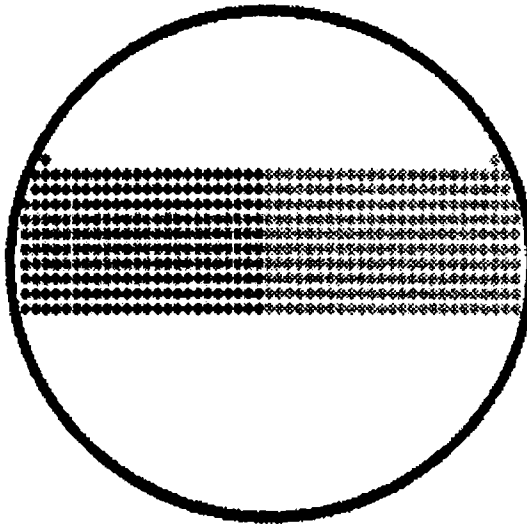
Figure 4.2: Initial Distribution of the particles

The initial velocities of individual particles were chosen randomly and the force of gravity is allowed to act on each particle. The time step was chosen according to the stability criteria explained in Chapter 3. Initially the particles fall under gravity since there is no contact force, but after some time the contact forces

also come into play. The bordering shape of the rotating cylinder, which first stops the pure vertical motion and secondly causes the particles to interact with each other, limits the motion of the particles. The total kinetic energy of the system is calculated as follows;

$$KE = \frac{1}{2} \sum_{i=1}^{N_p} m_i v_i^2$$
(4.2)

where m_i is the mass, v_i is the velocity and N_p is the total number of particles in the system. The simulation was continued till all the particles came to rest; that is until the total kinetic energy of the system becomes negligible as shown in Figures 4.3 (a) and (b). The location and linear and rotational velocities of particles at this stage are chosen as the initial conditions for the next stage of simulation.
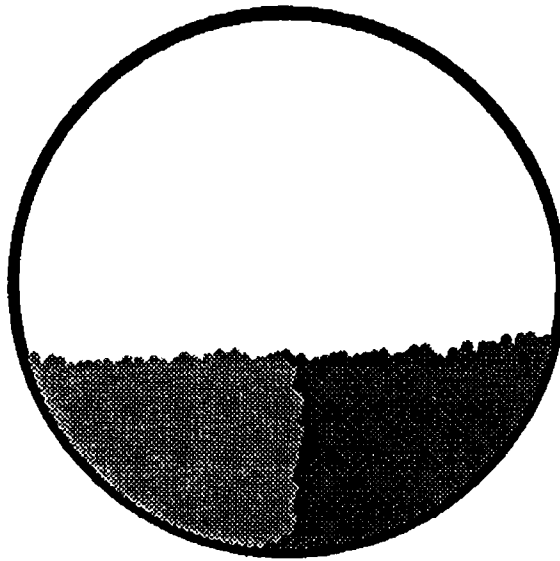
Figure 4.3(a): Initial Packed bed
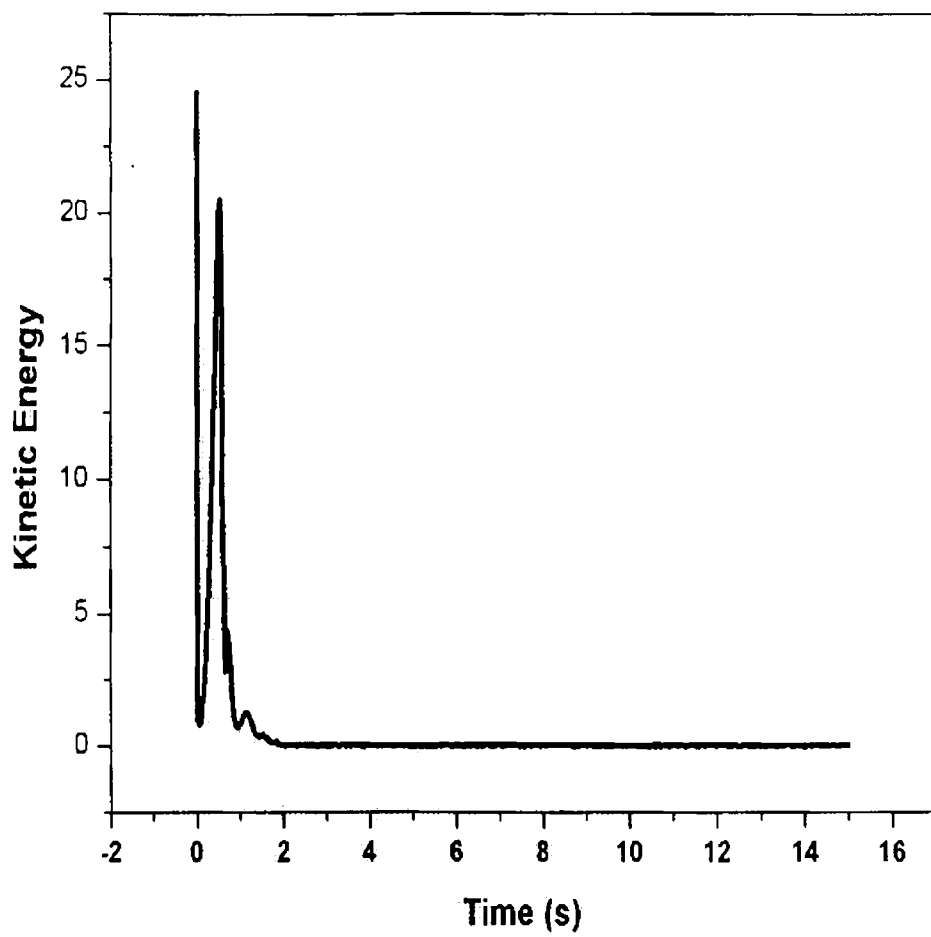
Figure 4.3(b): Total kinetic energy with respect to time

4.3 Simulation of granular solids in the transverse plane of the rotating cylinder

Starting with the initial conditions explained in Section 4.2, the cylinder wall is allowed to rotate at a specified rotational velocity. Various simulation parameters used in this work are summarized in Table 1.

Table 4.1: Process parameters

Parameter	Values
Radius (m)	1.5 m, 7.5×10^{-2} m
Rotational speed (rpm)	1 - 80
Particle radius (mm)	5-10
Particle density kg/m^3	1300
Fill fraction (%)	10% - 30%
Number of particles	500-3000
Normal spring constant (Pa)	5.0e+05
Normal energy dissipation coefficient (s^{-1})	100
Tangential energy dissipation coefficient (s^{-1})	20
Coefficient of Friction (-)	0.1-1.0

The spherical solid particles representing the wall of the cylinder undergo only rotational motion, and these particles contribute only to the contact force calculations of the particles in the solid bed. When the cylinder rotates, the particles in the solid bed undergo collisions with other granular particles as well as with the cylinder wall resulting in translational and rotational motion. The following parameters are obtained from the simulation results.

4.3.1 Dynamic angle of repose

The included angle made by the upper surface of the granular solid bed with the horizontal line of a rotating cylinder is defined as the *dynamic angle of repose*. Hence from the simulation data, the maximum and minimum values of x-position of the particles are found and a line is drawn joining these two points as

shown in Figure 4.4. The dynamic angle of repose Θ , can be then obtained as the angle that this line makes with the x-axis by employing the following equation

$$\tan \Theta = \frac{m_2 - m_1}{1 + m_1 m_2}$$

(4.3)

where m_1, m_2 are the slopes of the respective lines.
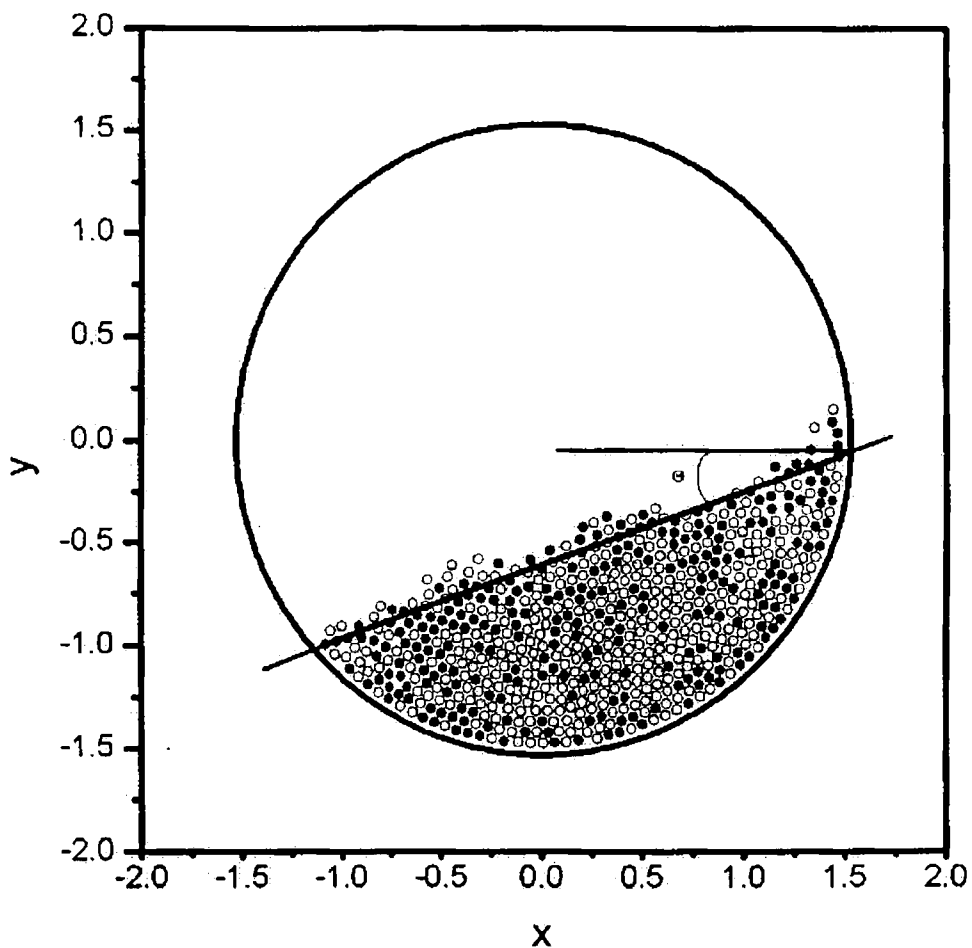
Figure 4.4   Dynamic angle of repose

4.3.2 Velocity profiles

The velocity profile of the particles at any instant is best exhibited by a vector plot indicating the magnitude and the direction of the velocities of the particles by small directed line segments. The x, y coordinates of the all the particles in the granular bed at time t and $t + \Delta t$ are stored in two different files.

The graphics software **ORIGIN 6.0** was used to draw the velocity vector plot using **XYXY option**, where the extreme X and Y columns determine the XY coordinate of the tail of the vector and the inner set of X and Y columns determine XY coordinate of the head of the vector. One such typical profile is shown in Figure 4.5.
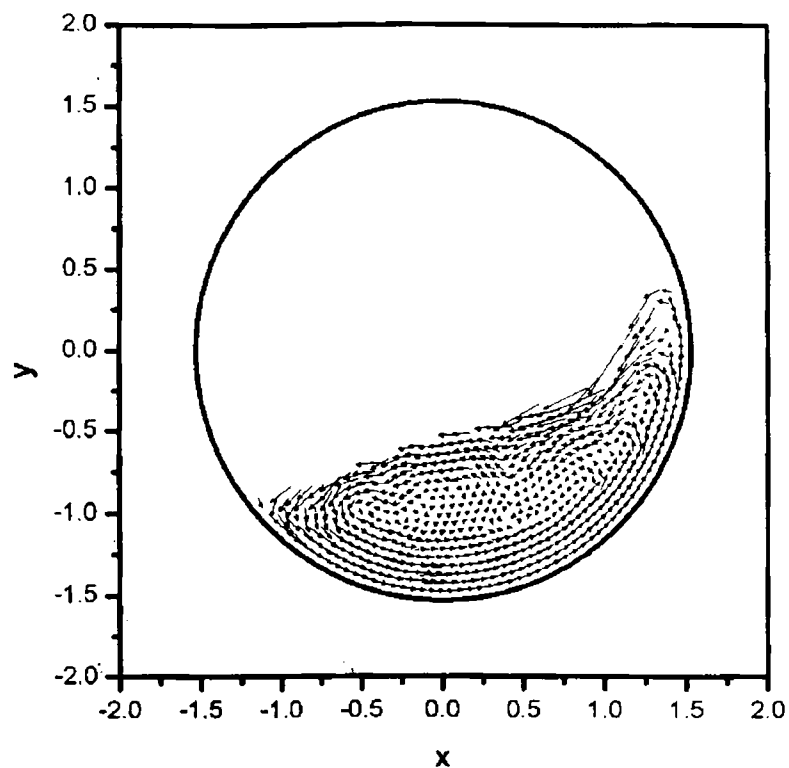
Figure 4.5: A typical vector plot

4.3.3 Surface velocity of the granular bed

The entire transverse plane of the rotating cylinder was divided into segments as shown in Figure 4.6. The average velocity for each sector was calculated as

$$v_x = \frac{1}{n_s} \sum_{i=1}^{n_s} v_{x_i}$$

$$v_y = \frac{1}{n_s} \sum_{i=1}^{n_s} v_{y_i} \qquad\qquad (4.4)$$

where v_{x_i}, v_{y_i} are the x and y component of the velocities of the individual granular particles inside each sector. The surface sectors are then identified and the velocities corresponding to these sectors are fixed as the surface velocities.
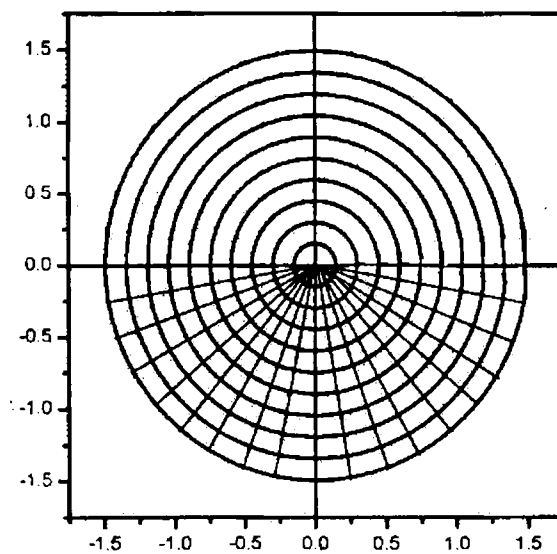
Figure 4.6   Discretization of the cross section into segments

4.3.4 Active layer depth

According to Henein et al [1983a], the rolling bed is characterized by two regions: the non-shearing plug flow region and the shearing active layer of particles cascading down the top surface. In the plug flow region, the particles rotate as a rigid body with a velocity, which varies linearly with distance from the

center of the cylinder. At the region near the free surface, particles cascade down due to rapid collisions and gravity. The demarcation between these two regions is a stagnation plane where particles are momentarily stationary before reversing the direction. Such demarcation is clearly shown in Figure 4.5. From the velocity profile plot the active layer is approximated as an area where the particles cascade down along the free surface and this is shown by the velocity vectors accelerating downwards

4.3.5 Evolution of kinetic energy of the system with respect to time

The amount of energy dissipated during collisions between particle-particle and particle-wall interactions plays a prominent role in characterizing the dynamics of granular motion. Dissipation of energy attributed to the particle distributions and velocity distributions include kinetic energy, potential energy etc. Since the kinetic energy plays an important role, a book keeping was carried out to store the fluctuations of kinetic energy as defined by equation 4.2. At every instant of time the kinetic energy was calculated for each particle and was averaged out with the total number of particles to get the total kinetic energy of the granular solid bed during the rotational motion of the cylinder.

4.4 Simulation of the various modes of the granular solid bed

Employing the procedures described in the previous sections, we simulated the dynamics of granular material motion with the diameter of the rotating cylinder set to 1.5 m. Results have generated for mono sized spherical particles having diameters 6 mm assuming an initial fill fraction of 20 % at various rotational speeds. Figures 4.7(a) to 4.7 (e) depict the six different modes of motion, namely slipping, slumping, rolling, cascading, cataracting and

centrifuging which were obtained through simulation by varying the rotational velocity of the rotating cylinder along with their corresponding velocity profiles.

(a)   (b)

(c)   (d)

(e)   (f)
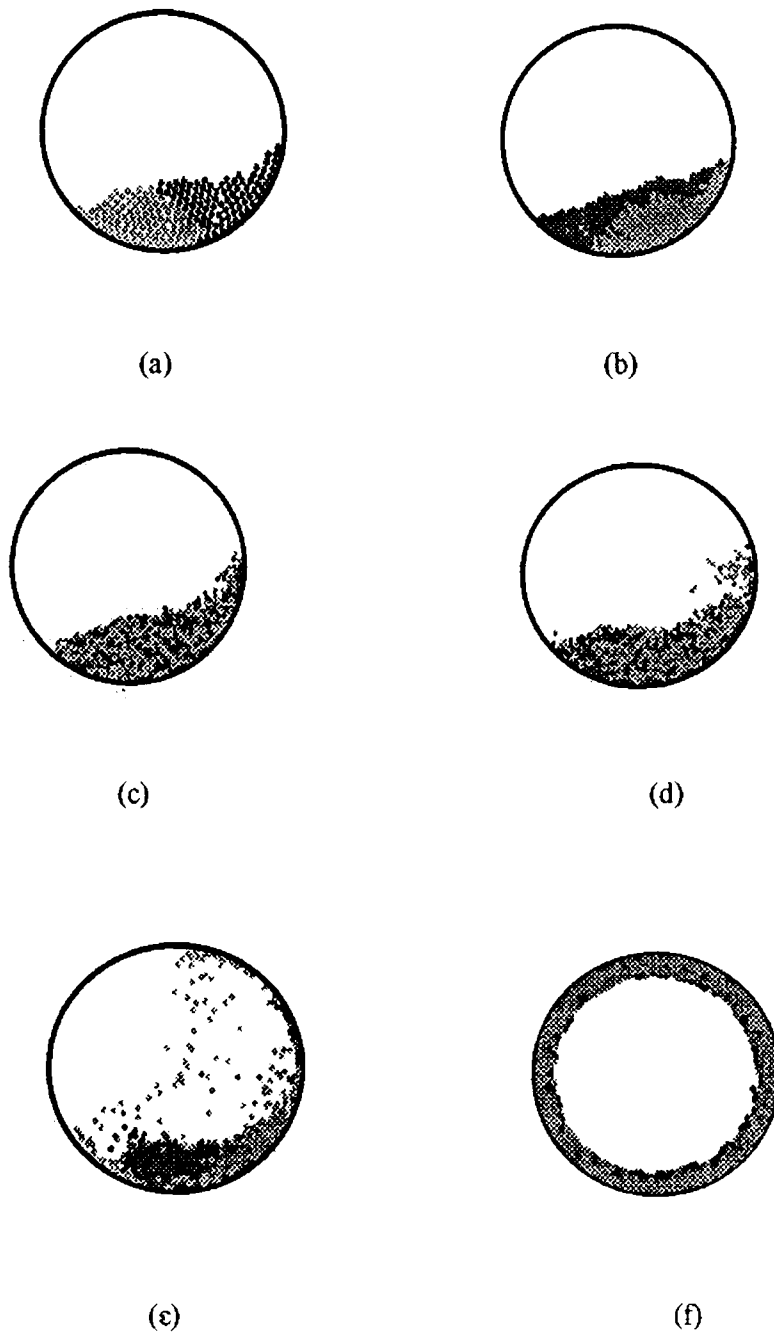
Figure 4.7:   Six different modes of motion obtained through DEM simulation

4.4.1 Slipping mode

Figures 4.8 (a) and (b) show the profile of granular solid bed and the corresponding velocity profile when the rotational velocity of the cylinder was maintained at 4 rpm. These plots were obtained after the cylinder had undergone 10 rotations while reaching the steady state. It can be clearly seen from the velocity profile that, the granular solid bed remains nearly stationary as evidenced by a look of movement of particles. The fact that the particles were almost stationary was also verified through the Figure 4.8 (a) where it is clearly visible that mixing of particles was absent and the solid bed was equivalent to a packed bed at an elevated position. This mode of granular solids motion was further confirmed by plotting the dynamic angle of repose and the total kinetic energy of the granular solid bed with respect to time as shown in Figure 4.8(c) and Figure 4.8(d)
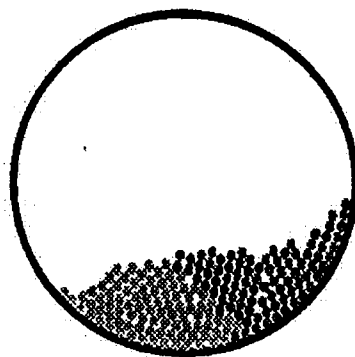
Figure 4.8(a): Granular bed in slipping mode
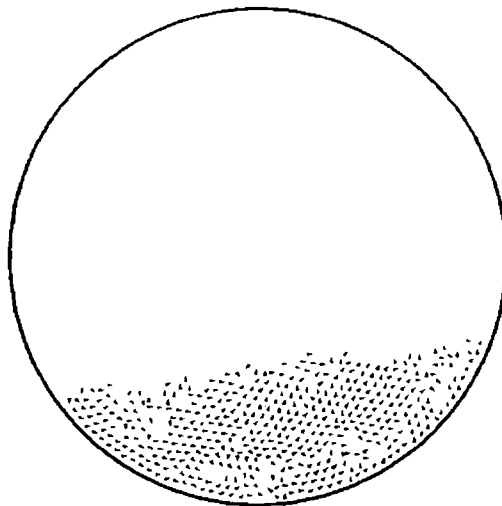
Figure 4.8 (b): The velocity profile in slipping mode
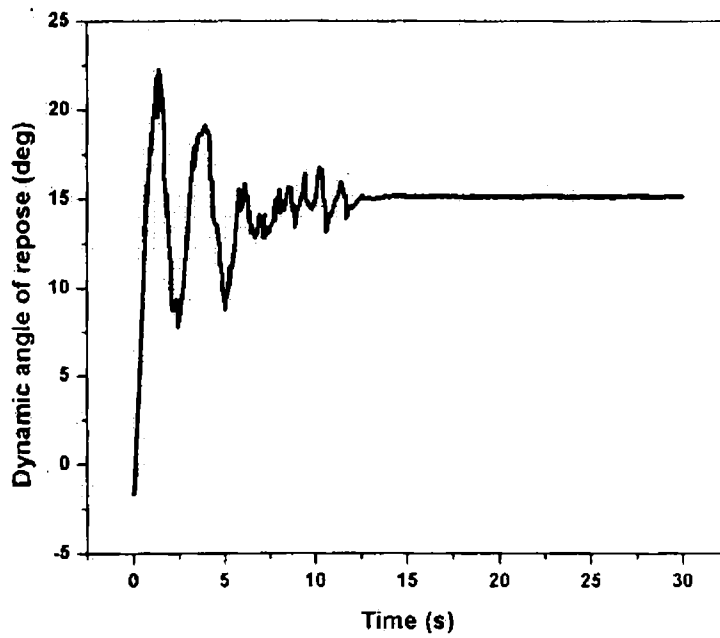
Figure 4.8(c) : Dynamic angle of repose of the granular solid bed at 4 rpm
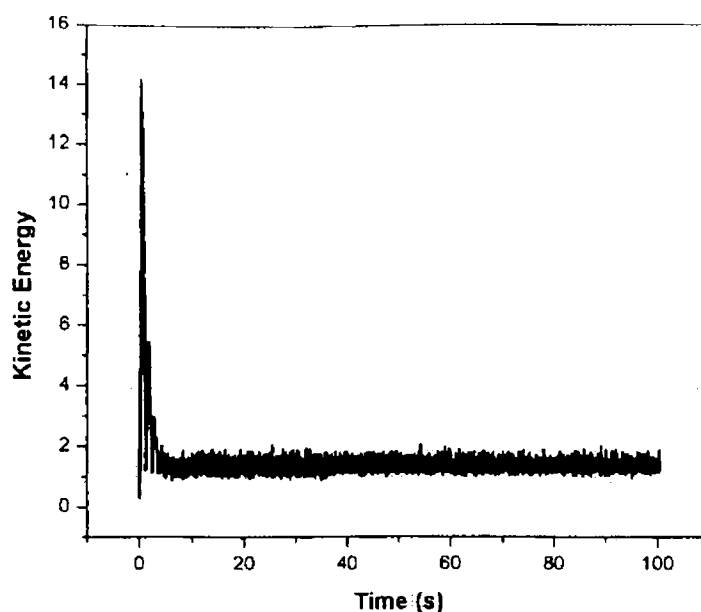
Figure 4.8 (d): Kinetic energy of the granular solid bed at 4 rpm

4.4.2 Slumping mode

As the rotational velocity of the cylinder was increased further, the slumping of the granular bed commences. For most of the time, the entire granular bed rotates at the same rotational velocity, thus undergoing solid body rotation. Further an avalanche is triggered when the bed surface reaches the static angle of repose Θ_s. During the avalanche, material from the upper part of the bed surface slides rapidly down. At the end of avalanche period the bed surface was inclined at a lesser angle Θ_d called the dynamic angle of repose. Solid body rotation of the whole bed ensues, until the surface inclination again reaches the angle Θ_s when avalanching occurs and the cycle is repeated. Davidson et al (2000) has given the following relationship for characterizing the slumping cycle time:

$$t_{13} = t_{12} + \frac{(\Theta_s - \Theta_d)\pi}{180\omega}$$

(4.7)

where t_{12} is the avalanche time, t_{13} is the total cycle time and ω is the rotational velocity of the cylinder. The schematic view of one slumping cycle is shown in the Figure 4.9 (a) to 4.9 (c).
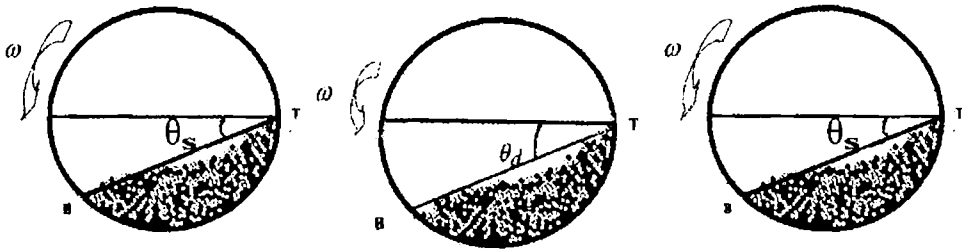
Figure:4.9 :   Cyclic slumping or avalanching

           (a) Initial stage of a slump at an angle θ_s

           (b) Final stage of a slump at an angle θ_d and

           (c) Initial stage of the next slump at an angle at θ_s.
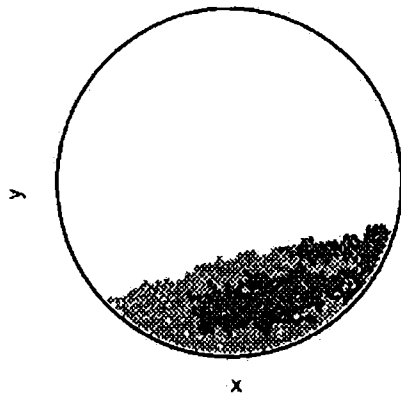
Figure 4.9(d):   The granular solid bed profile at the beginning of avalanching in slumping mode

It has been shown by Henein (1983a) that the slumping frequency is dependent on the rotational speed, particle size and cylinder diameter. The slumping mode of the granular solid bed motion is shown in Figures 4.9 (d) where the rotational velocity of the cylinder is kept at 10 rpm. Figure 4.10 (a) and 4.10(b) shows the velocity profile of the granular solid bed at the beginning of avalanching of the surface particles and the end of the avalanching of the particles respectively, in the slumping mode.
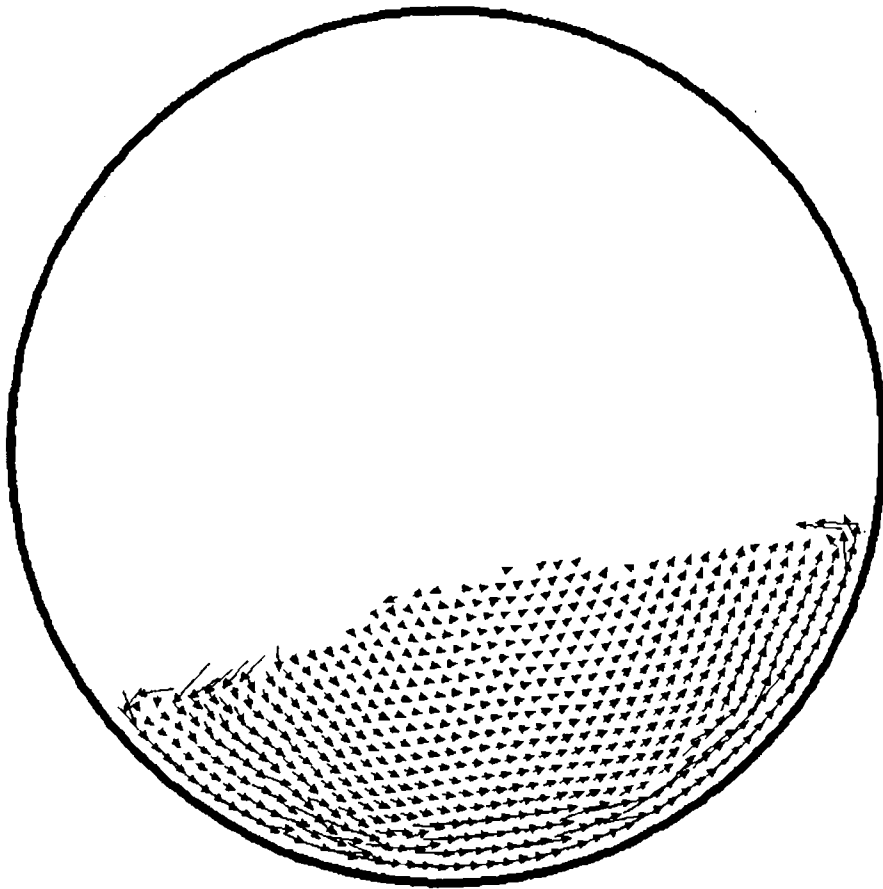
Figure 4.10(a): Vector plot of the granular solid bed during solid body rotation in slumping mode
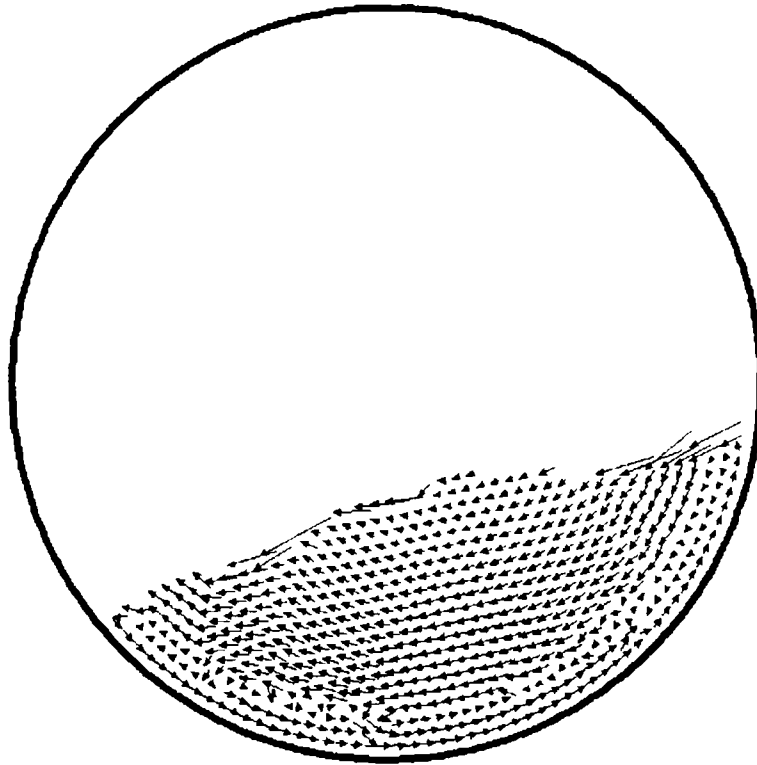
Figure 4.10 (b)   Vector plot of the granular solid bed at the beginning of avalanching in slumping mode

The trajectory of a single particle in the slumping mode is shown in figure 4.10 (c), which shows that, the particles will have much movement. The corresponding kinetic energy distribution and the dynamic angle of repose variation are shown in Figures 4.10 (d) and 4.10(e). The angles Θ_s and Θ_d are found to be approximately 17.5^0 and 15.1^0 and the avalanching duration is found to be around 3s and the predicted cycle time based on equation (4.7) turns out to be 3.3s which agrees with the predicted value of 4s given by Davidson et al (2000) for the same process parameters.
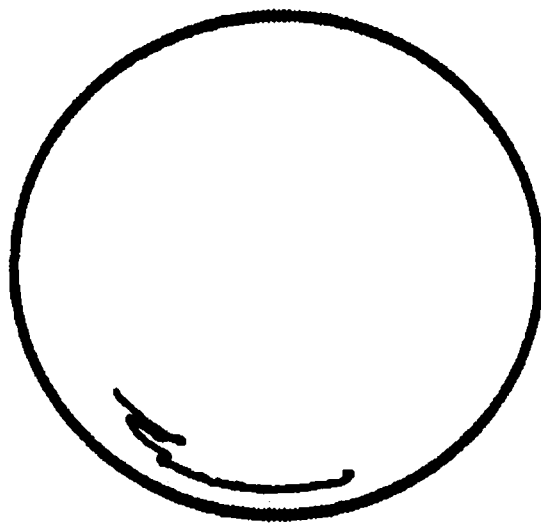
Figure 4.10(c): Trajectory of a single particle in slumping mode.
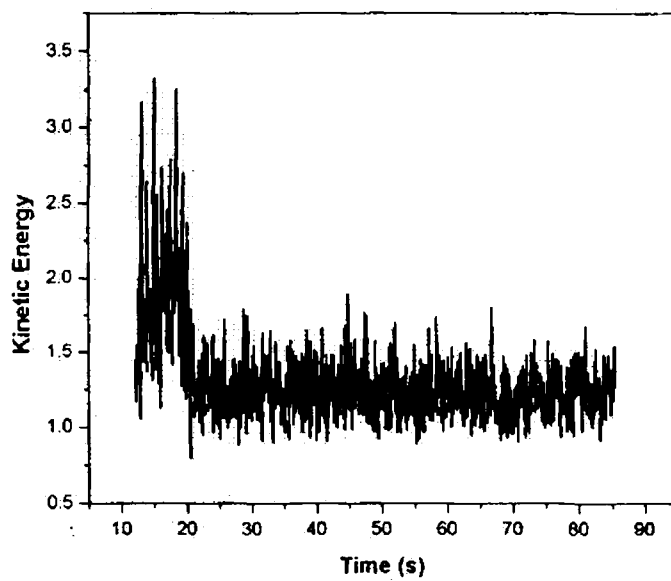
Figure 4.10(d): Kinetic energy distribution during slumping mode
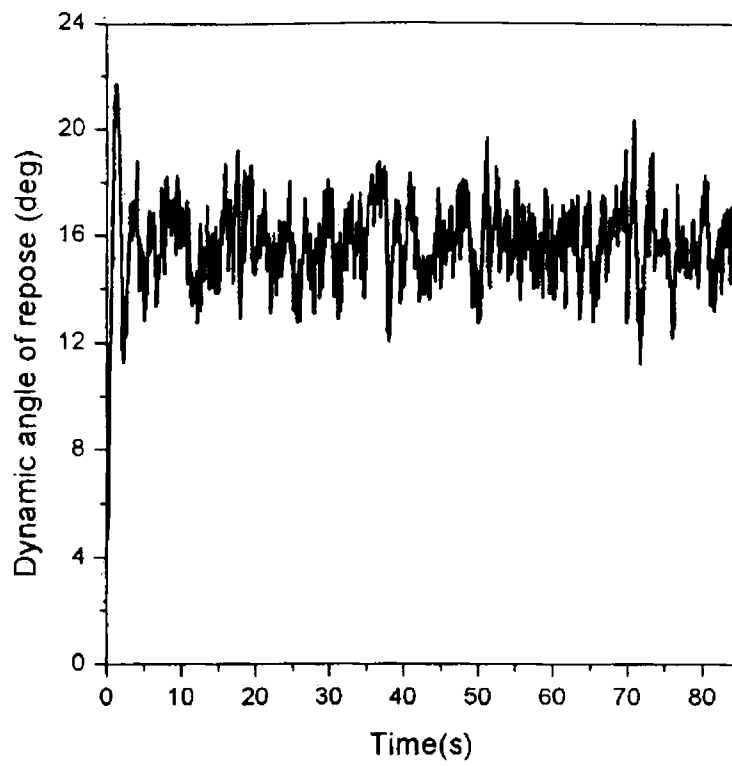
Figure 4.10(e): Dynamic angle of repose with respect to time during slumping mode.

4.4.3 Rolling mode

As the rotational speed of the cylinder increases further, a transition to the rolling mode takes place. This type of motion is characterized by a uniform static flow of a particle layer on the surface (active layer) while the larger part of the bed (plug flow region) is transported upwards by solid body rotation with the rotational speed of the wall. The bed surface is nearly level. This type of motion enables good intermixing and hence this mode has been investigated extensively in the literature.
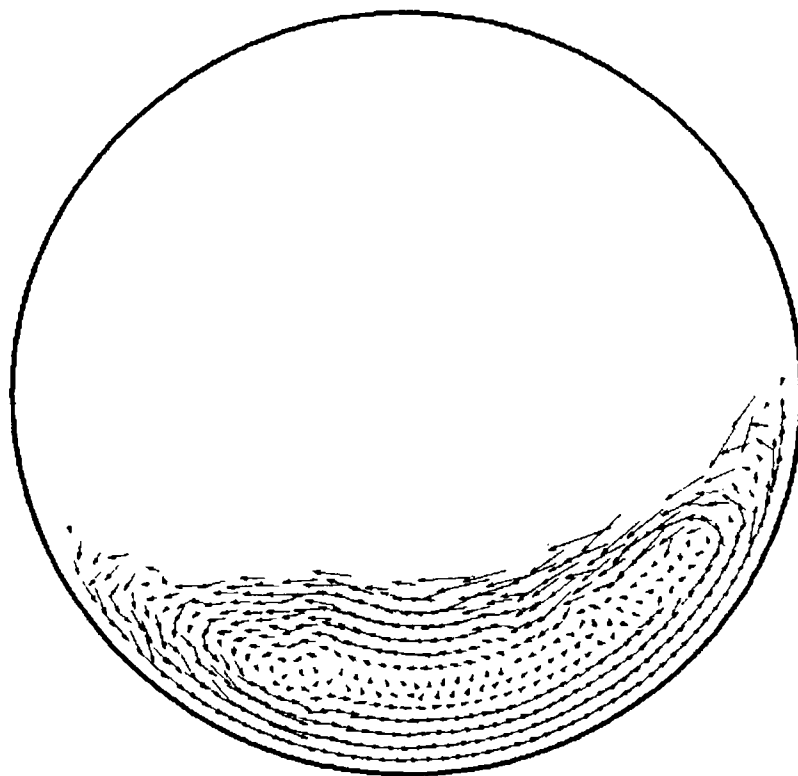
Figure 4.11 (a): Velocity profile of the rolling bed

Figure 4.11 (a) depicts the velocity profile of the granular solid bed after 10 rotations, with the rotational speed of the cylinder set at 15 rpm. The active layer is clearly visible in the picture. A small stagnation zone can also be observed and the bulk of the granular solids move with the cylinder wall.

Figure 4.11(b) shows the profile of the granular solid bed after 10 rotations and as can be observed significant intermixing of particles has occurred. Figure 4.11(c) shows the kinetic energy distribution and Figure 4.11(d) depicts the variation of dynamic angle of repose. The trajectory of a single particle shown in figure 4.11 (e), describes the path of the particle in the rolling mode.
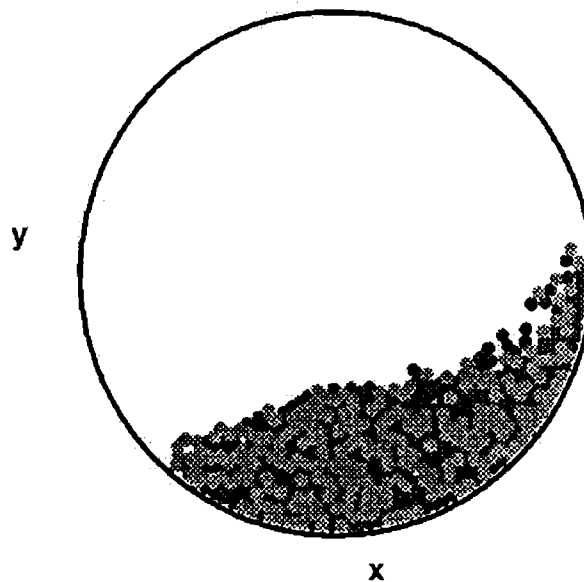
Figure 4.11 (b):   Granular solid bed during rolling mode
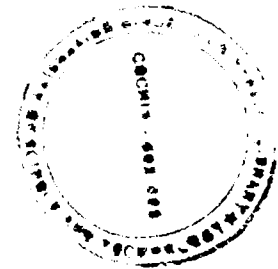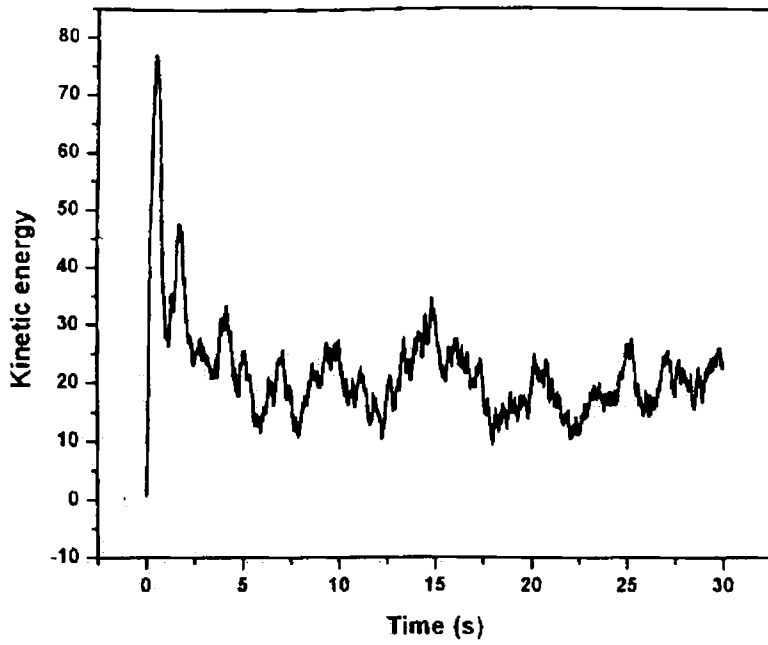
Figure 4.11 (c):   Kinetic energy distribution
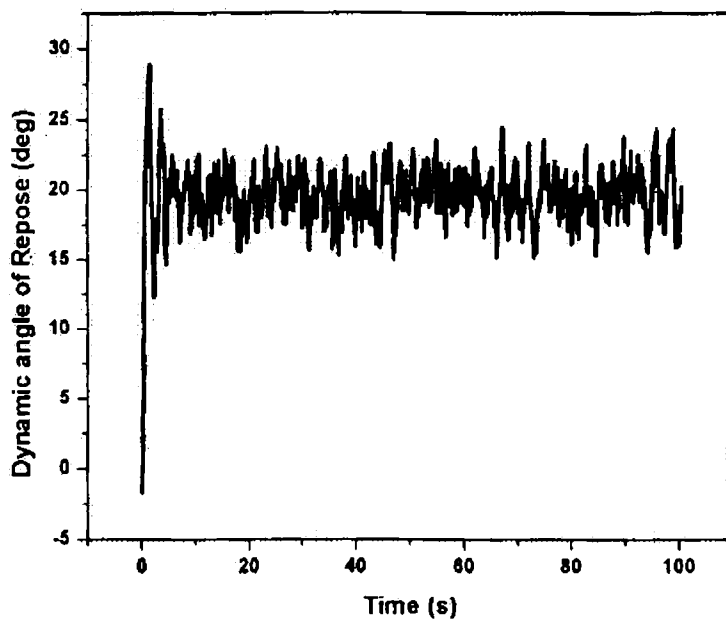
Figure 4.11(d):   Dynamic angle of repose with respect to time.
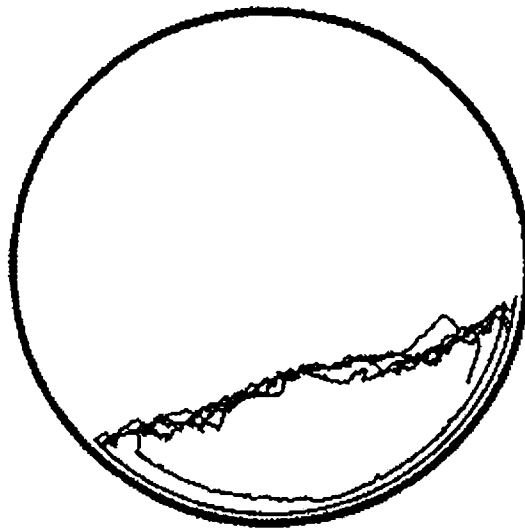
Figure 4.11 (e) :   Trajectory of a single particle in rolling mode.

4.4.4 Cascading

As the rotational speed further increases, the bed surface begins to arch and cascading sets in. The granular solid bed is almost kidney shaped and the height of the arch of the kidney-shaped bed increases with increasing rotational speed. The results obtained from the simulation data when the rotating speed of the cylinder is increased to 30 rpm is shown in Figures 4.12 (a). The corresponding trajectory of a single particle, vector plot, kinetic energy distribution and dynamic angle of repose obtained through simulation are shown in figures 4.12 (b) to 4.12 (e) respectively.
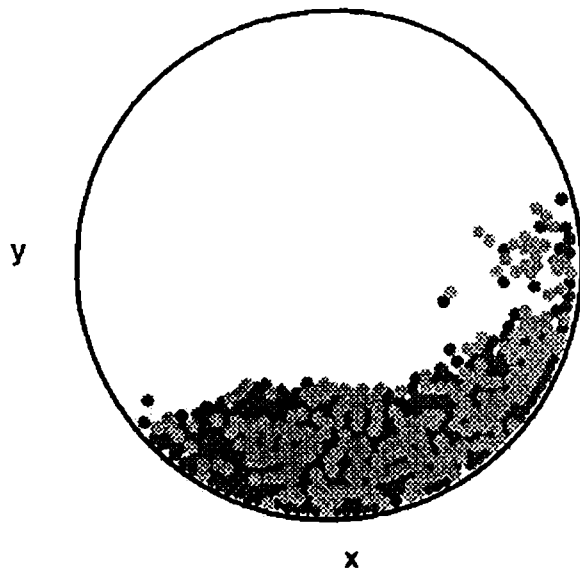
Figure 4.12 (a): Granular solid bed during cascading mode
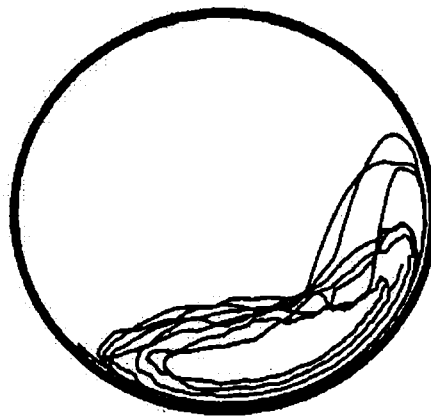
Figure 4.12 (b) : Trajectory of a single particle in cascading mode
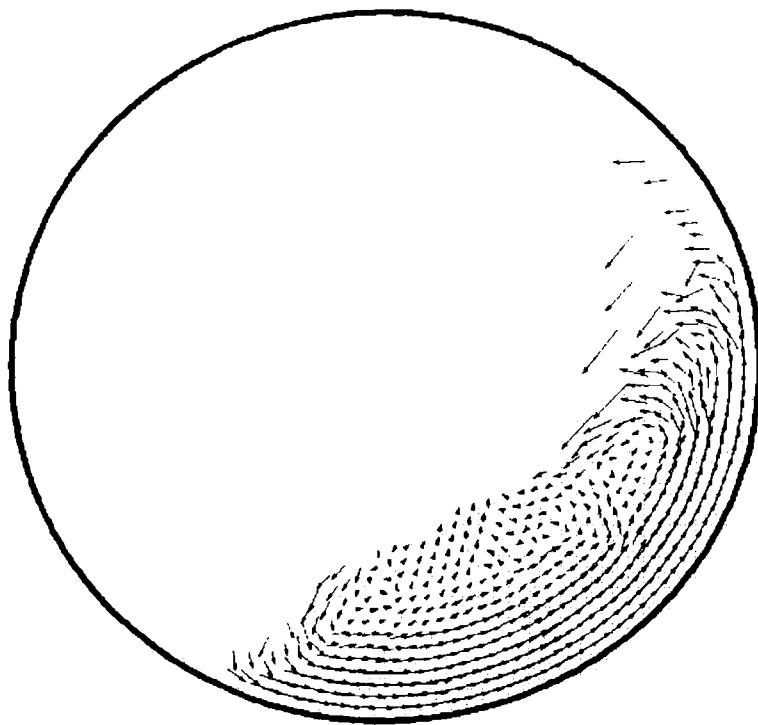
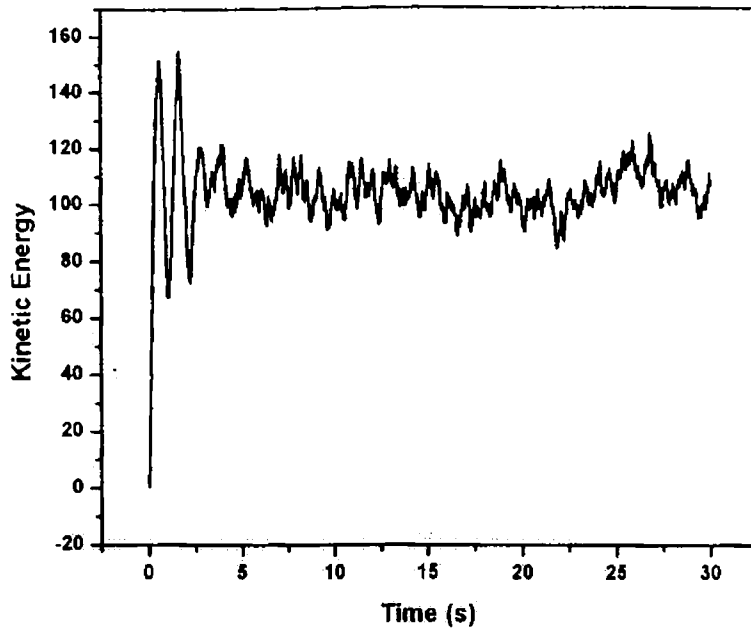**Figure 4.12 (c):** Velocity profile of the cascading mode

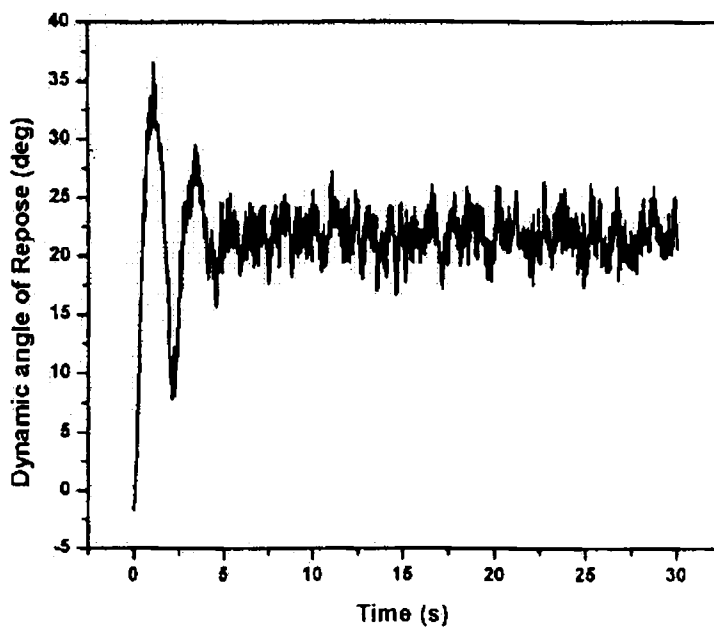**Figure 4.12 (d):** Kinetic energy distribution

Figure 4. 12 (e): Dynamic angle of repose with respect to time.

4.4.5   Cataracting mode

As the rotational speed increases, the cascading motion is so strongly pronounced that individual particles detach from the bed and are thrown off into free space of the cylinder. The release of particles from the solid bed to the free surface is the characteristic feature of cataracting motion. The simulated results of the cataracting mode of the granular solid bed are shown in Figures 4.13 (a). The corresponding figures for the velocity profile is shown in figure 4.13(b). The trajectory of a single particle is depicted in figure 4.13 (c), kinetic energy distribution is given in figure 4.13 (d). The rotational speed of the cylinder is 35 rpm.
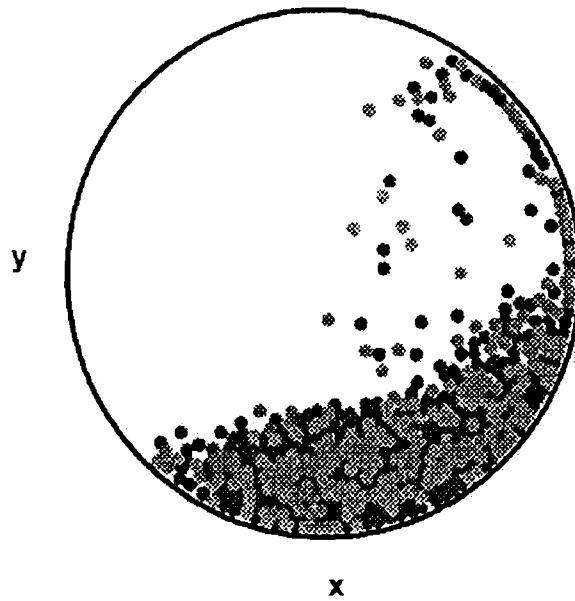

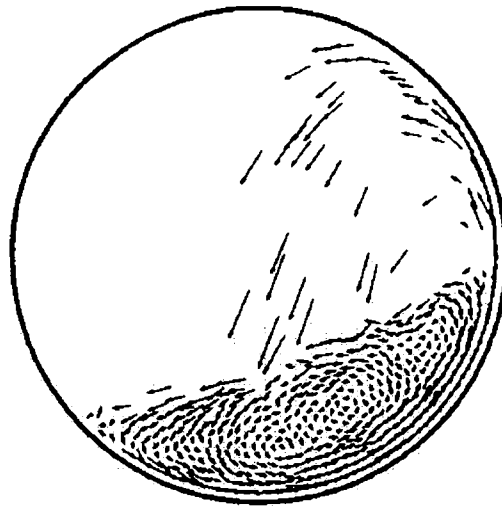**Figure 4. 13 (a) :   Granular solid bed during cataracting mode**

Figure 4.13 (b) :   Velocity profile of the cataracting mode
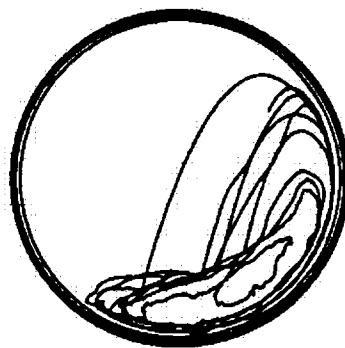

Figure 4.13 (c):   Trajectory of a single particle in cataracting mode.
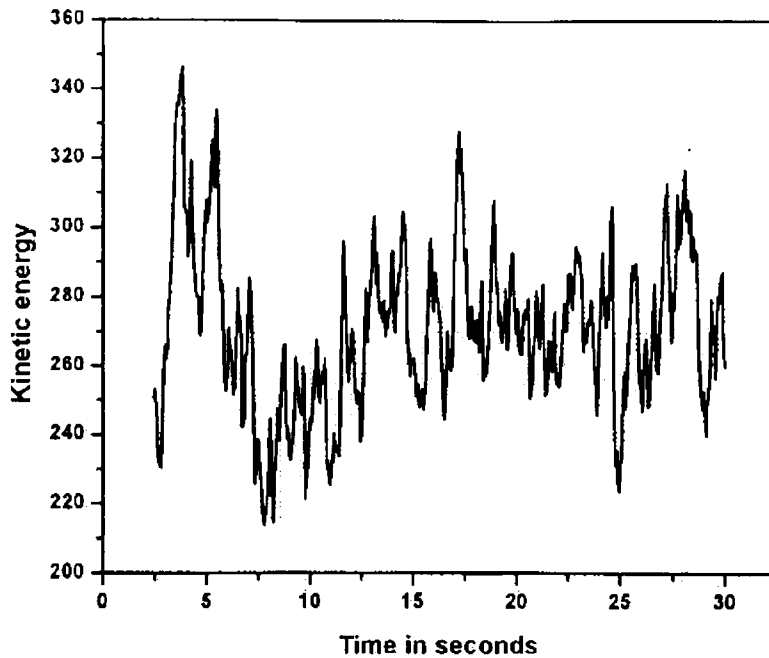
Figure 4.13 (d) : Kinetic energy distribution

4.4.6 Centrifuging

With increasing rotational speed, the number of particles thrown off from the bed increases and the length of trajectories also increase. With further increase in the rotational speed, some of the particles begin to adhere to the wall and after a few rotations the whole solid bed rotates with the cylinder wall as a uniform film. This type of mode is known as centrifuging and is usually obtained at high rotational speeds. Typical plots of the granular solid bed, velocity profile, trajectory of a single particle and kinetic energy distribution of the centrifuging motion when the rotational speed of the cylinder is set at 80 rpm are shown in the following series of figures 4.14 (a) to 4.14 (d).
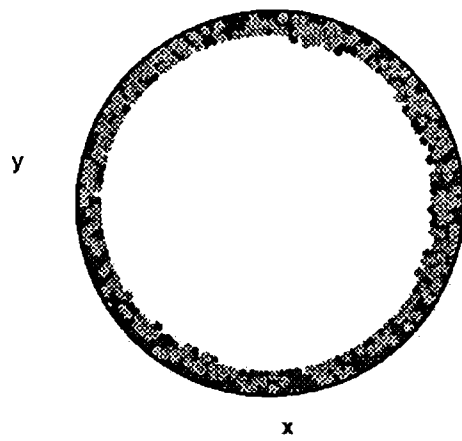
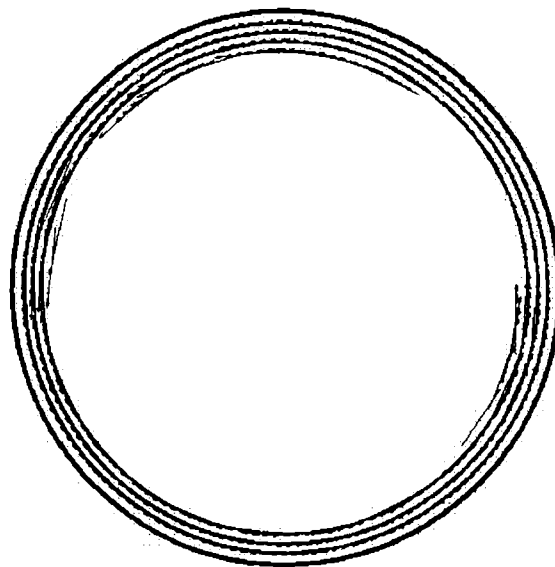**Figure 4.14 (a):** Granular solid bed during centrifuging mode

Figure 4.14 (b): Velocity profile of the centrifuging mode
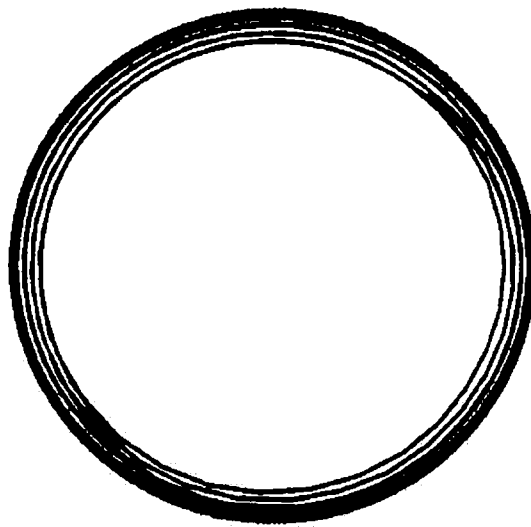
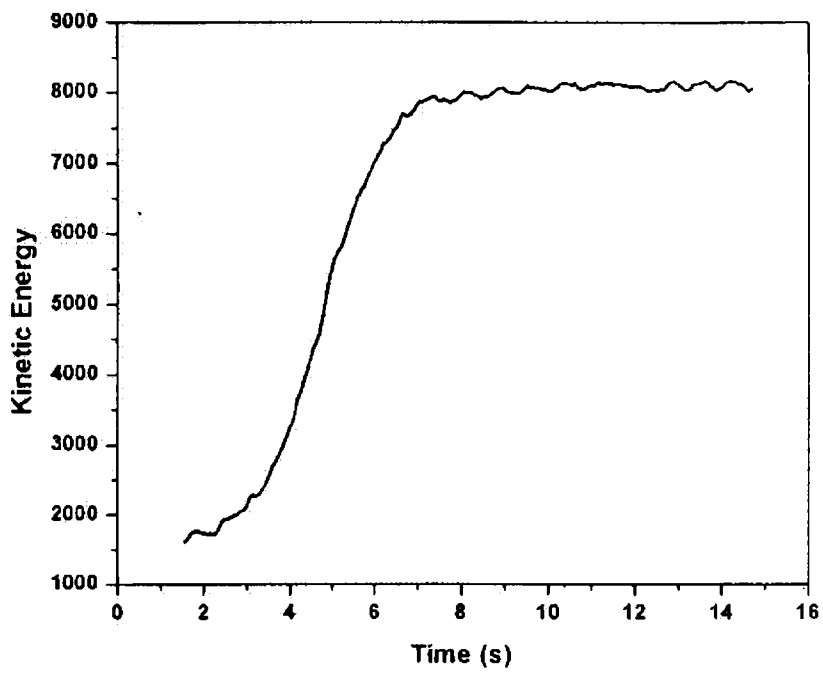**Figure 4.14 (c):**   Trajectory of a single particle in centrifuging mode.

Figure 4.14 (d):   Kinetic energy distribution

Figures 4.15 (a) to 4.15 (f) shows the vector plots of various stages which lead to the centrifuging mode.

Figure 4.15 (a):   Vector plot of centrifuging motion after 1 rotation

Figure 4.15 (b):   Vector plot of centrifuging motion after 2 rotations

Figure 4.15 (c):   Vector plot of centrifuging motion after 3 rotations
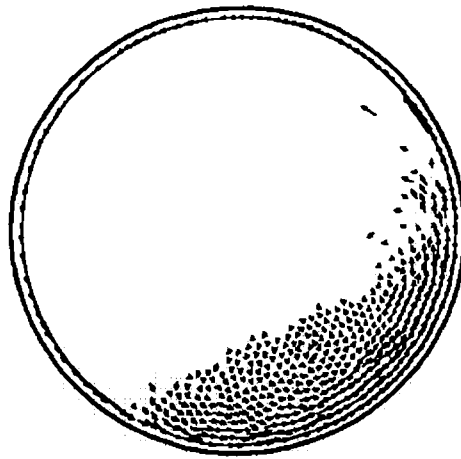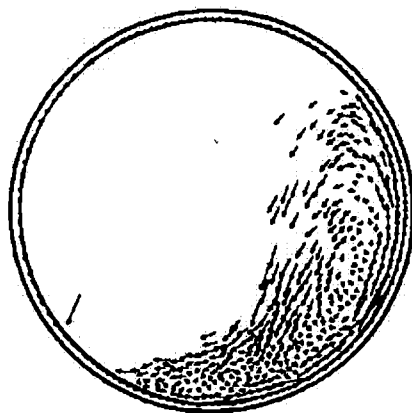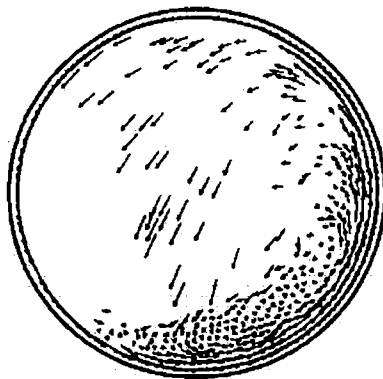

Figure 4.15 (d):   Vector plot of centrifuging motion after 5 rotations
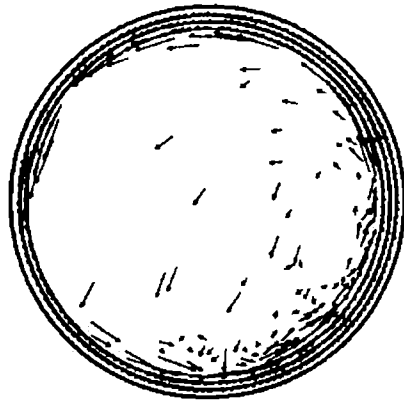
Figure 4.15 (e): Vector plot of centrifuging motion after 7 rotations
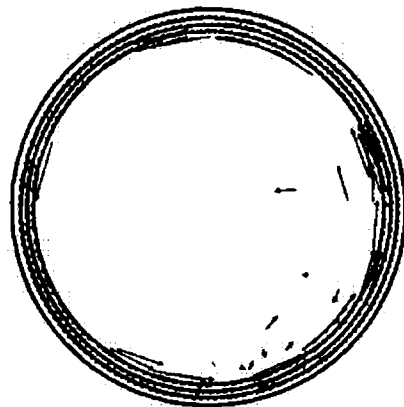
Figure 4.15(f): Vector plot of centrifuging motion after 9 rotations

The dynamics of granular solid bed at different rotational speeds are presented in Figures 4.16 (a) to 4.16(e) after 2, 4, 6, 8, 10 rotations. It can be clearly seen from the Figures that good mixing occurs only in the rolling and cascading modes. Since Cascading, Cataracting and Centrifuging motions are less preferable modes of operations for rotating cylinders, further studies are confined only to investigating the rolling mode.

5 rpm

10 rpm

15 rpm

20 rpm

25 rpm

30 rpm
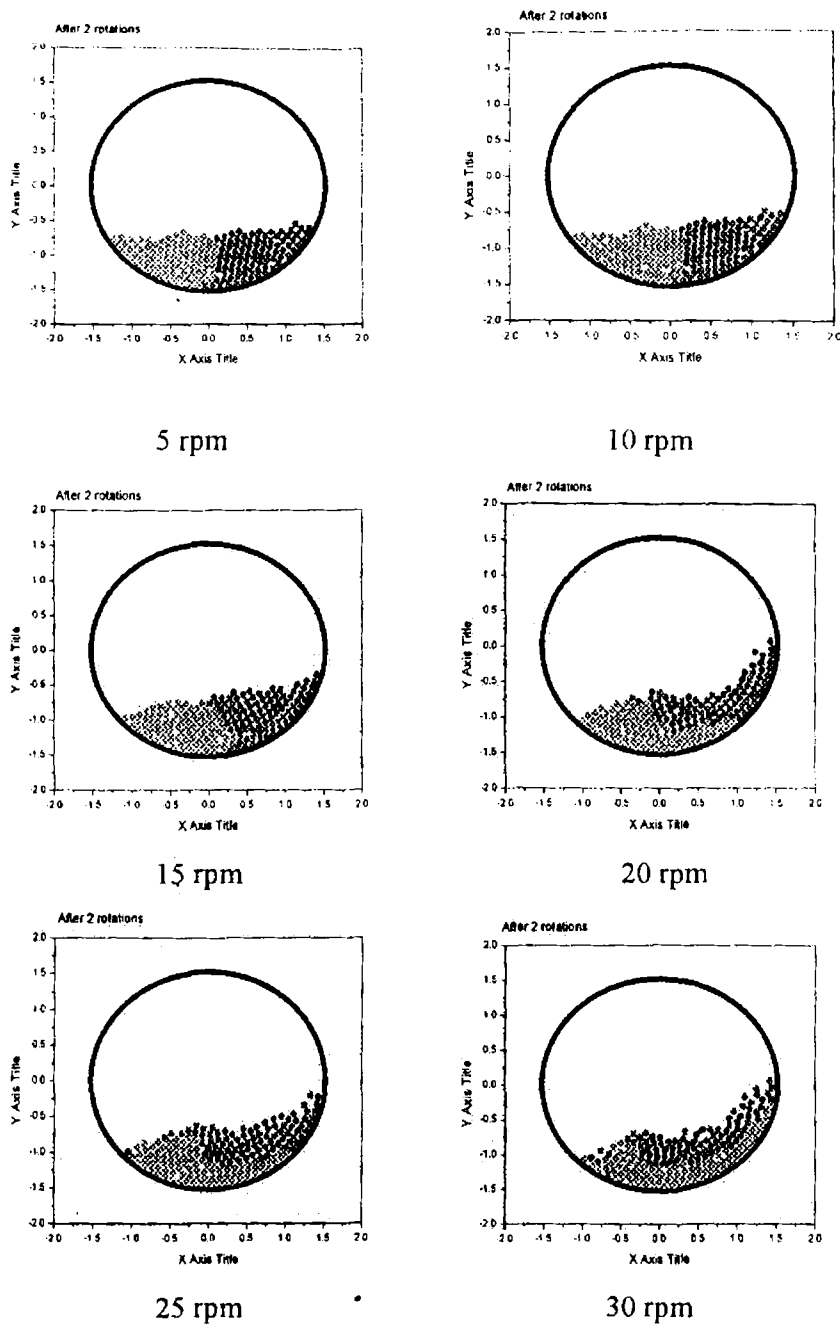
Figure 4.16 (a): After 2 rotations with different rotational speed

5 rpm

10 rpm

15 rpm

20 rpm
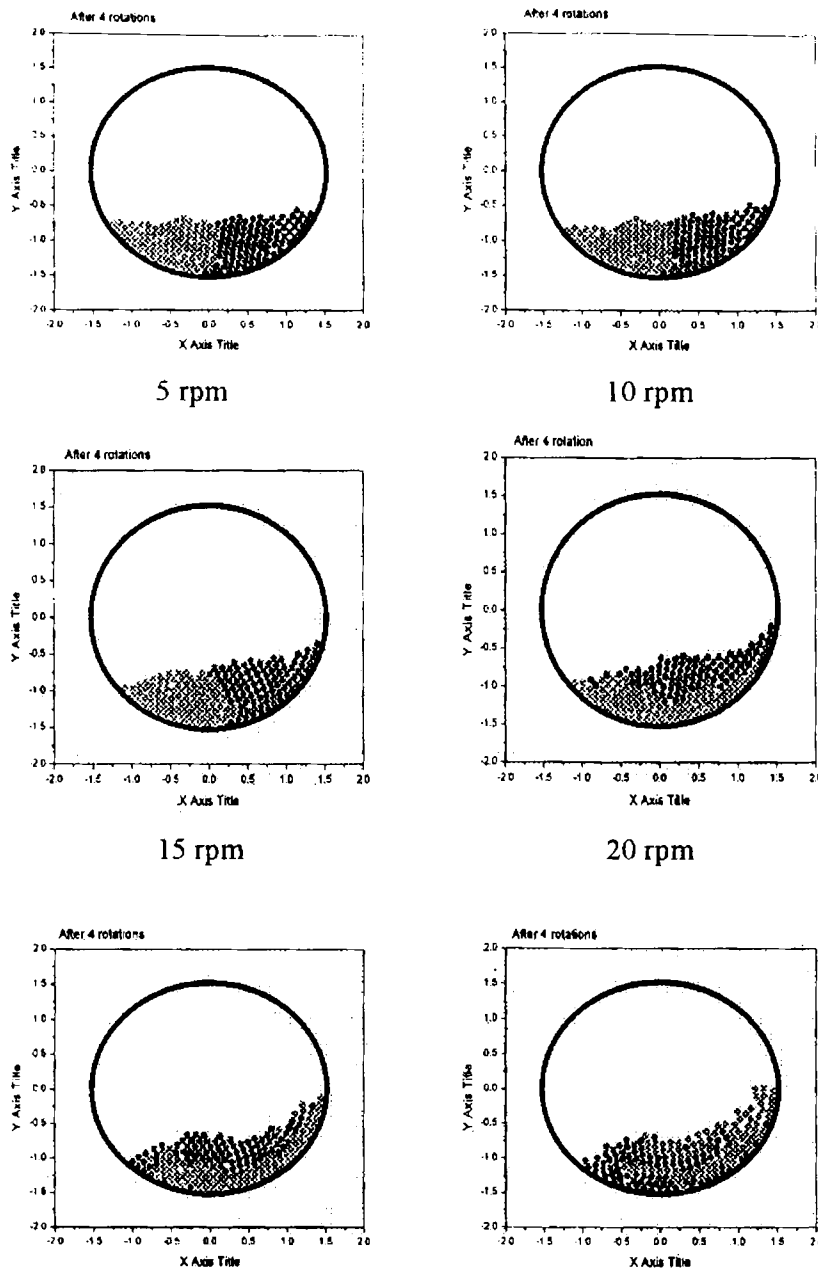
Figure 4.16 (b): After 4 rotations with different rotational speed

5 rpm

10 rpm

15 rpm

20 rpm

25 rpm

30 rpm
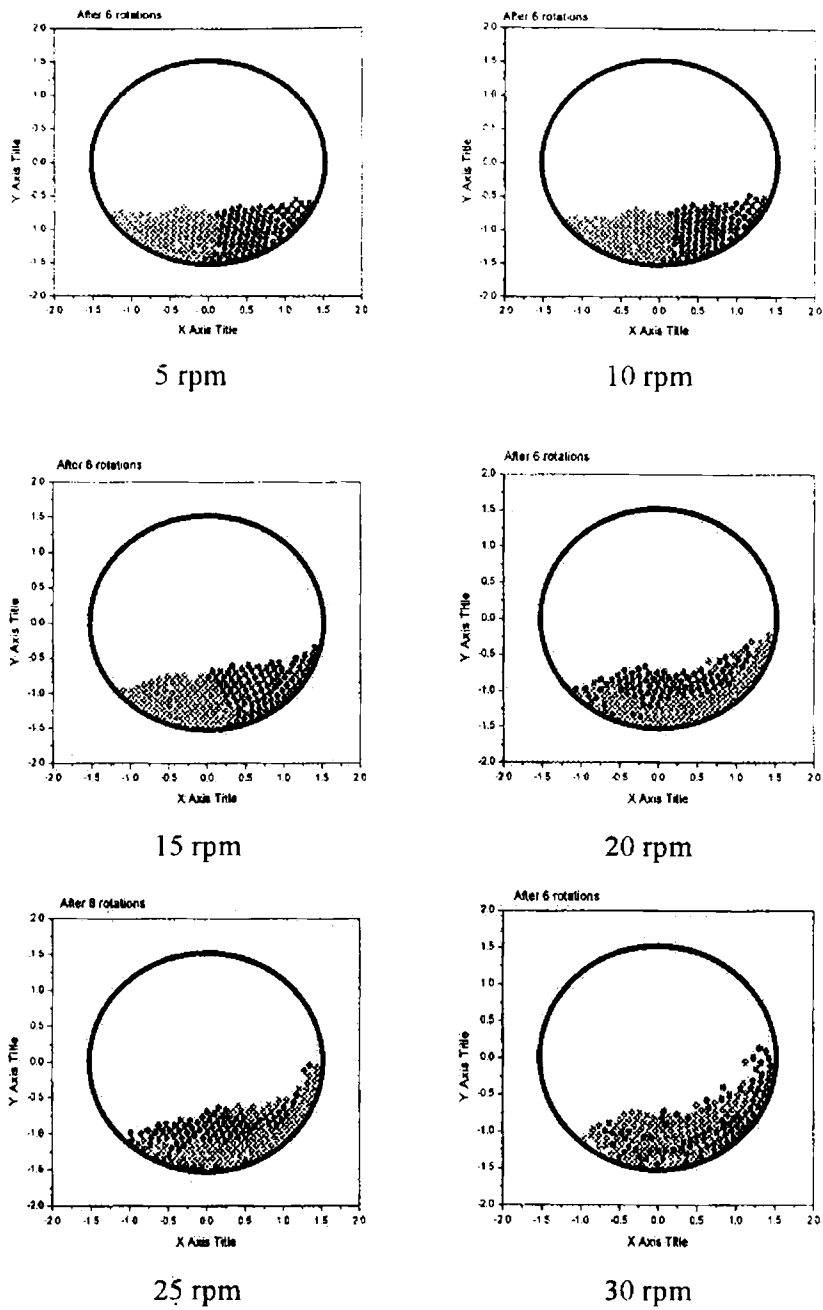
Figure 4.16 (c): After 6 rotations with different rotational speed

5 rpm

10 rpm

15 rpm

20 rpm

25 rpm

30 rpm
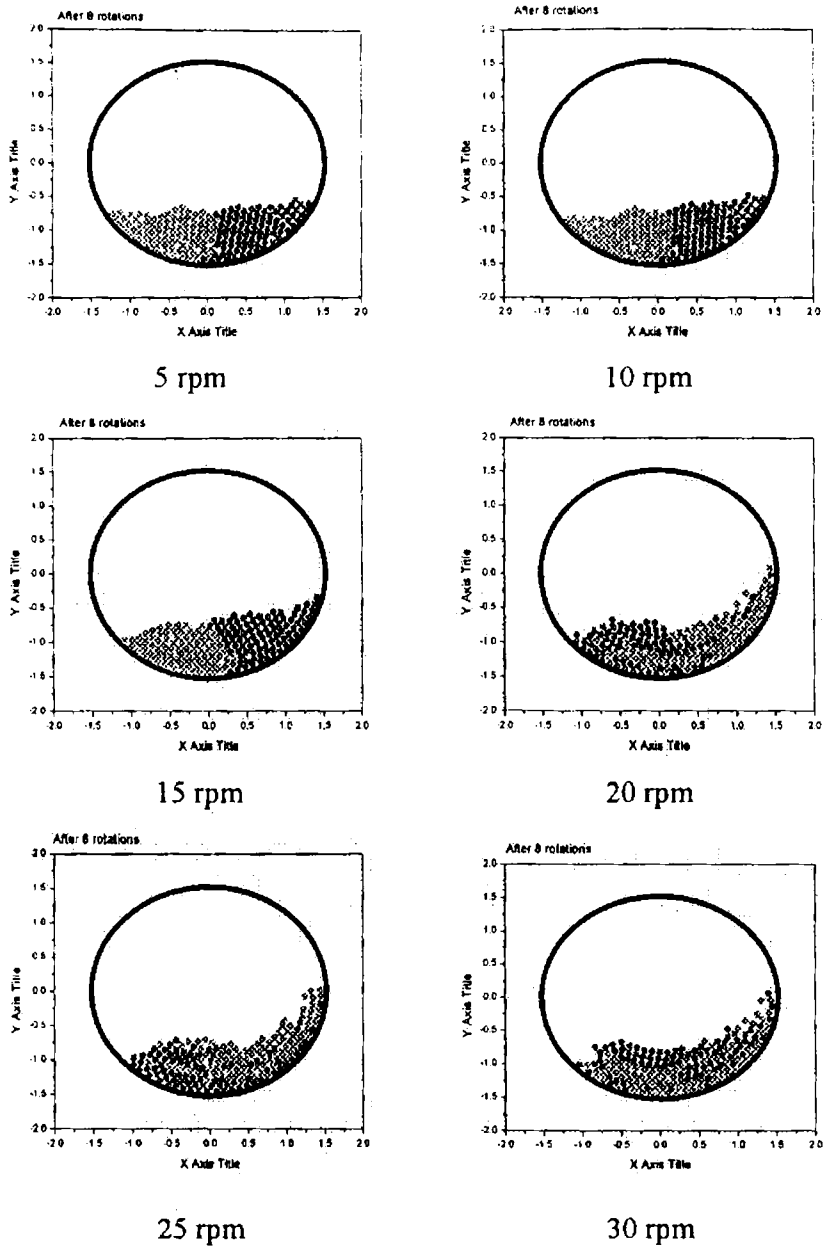
Figure 4.16 (d): After 8 rotations with different rotational speed

5 rpm

10 rpm

15 rpm

20 rpm

25 rpm

30 rpm
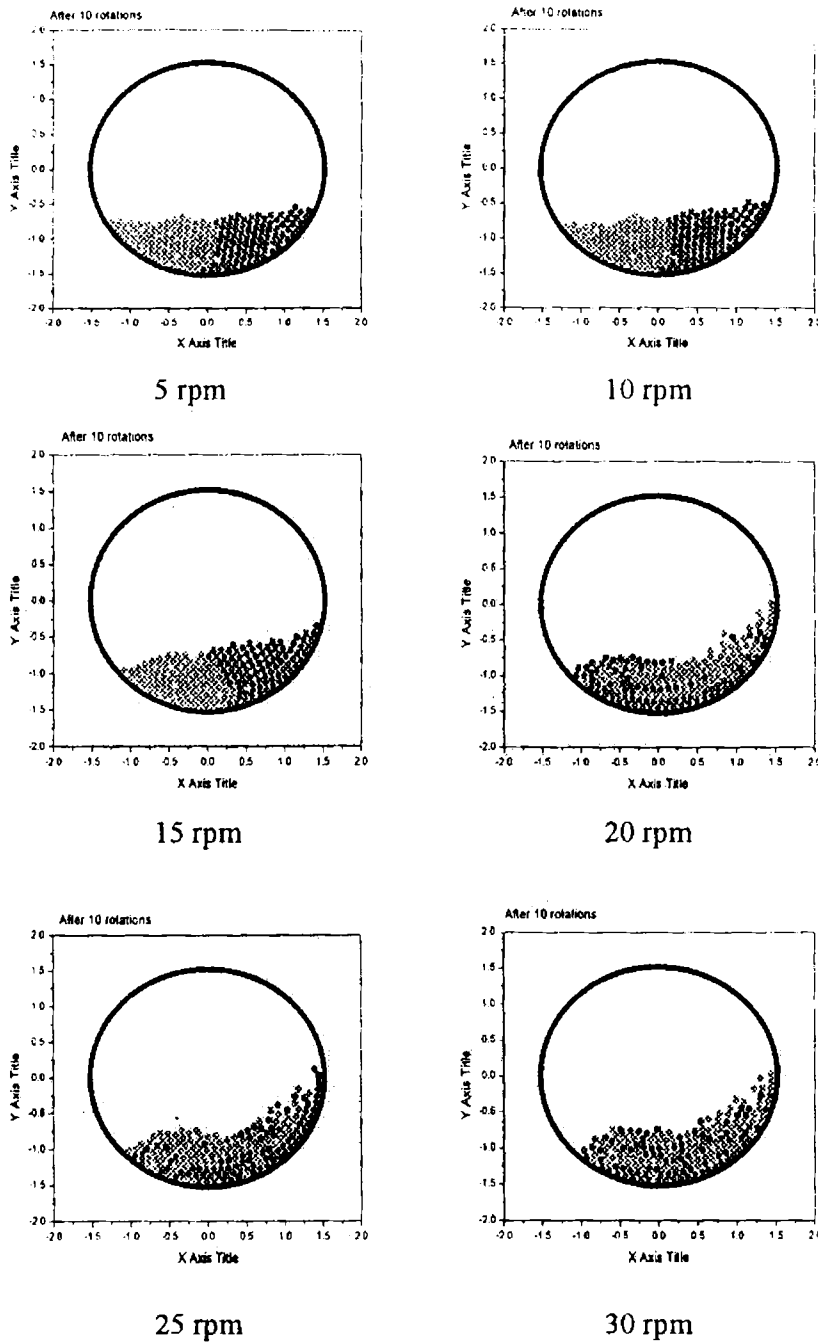
Figure 4.16 (e)   After 10 rotations with different rotational speed

4.5 Results and Discussion

4.5.1 Characterization of the Transition behaviour

Henein [1983a, 1983b] proposed the Froude number as a suitable parameter to define the transition from one mode to another. The Froude number is defined as

$$Fr = \frac{R\omega^2}{g} \tag{4.8}$$

where R, ω and g are the cylinder radius, rotational speed of the cylinder and acceleration due to gravity respectively. Henein's [1983a, 1983b] experiments showed that low values of Fr less than 10^{-5} are consistent with avalanching. Then there is a transition region where $10^{-5} < Fr < 10^{-4}$. Values of Fr more than 10^{-4} are consistent with the rolling mode. Mellmann [2001] developed mathematical models to predict the transition behaviour and he has presented the results as a bed behaviour diagram and he observed that the bed behaviour diagram depends strongly on the fill fraction and rotational speed. He also presented the Froude number values for transition behaviour. To confirm the transition values of the Froude number, simulation runs are made for the following operating parameters for simulating the transition behaviour of the granular solid bed from one mode to the next mode.

➢ Cylinder diameter 7.5 cm

➢ Particle size – 3 mm with density 1300 Kg/m^3

➢ Fill fraction 20% which corresponds to around 750 particles

➢ Rotational speed is varied from 1 rpm – 80 rpm

The simulations are carried out and by graphically observing the velocity profile for various rotational speeds and the Froude numbers are calculated using the equation $Fr = \dfrac{\omega^2 R}{g}$. And these values are tabulated in Table 4.2 along with the predicted values Mellmann [2001]. The values predicted by the simulation closely matches with the values predicted by Henein et al [1983a, 1983b] and Mellmann [2001].

Table 4.2   Froude numbers as predicted by simulation

Types of motion	Froude number as predicted by Mellmann [2001]	Froude number as predicted by the present simulation
Slipping	$0<Fr<10^{-4}$	3.4×10^{-4} (2 rpm)
Slumping	$10^{-5}<Fr<10^{-3}$	7.5×10^{-4} (3 rpm)
Rolling	$10^{-4}<Fr<10^{-2}$	5.3×10^{-3} (8 rpm)
Cascading	$10^{-3}<Fr<10^{-1}$	0.03 (20 rpm)
Cataracting	$10^{-1}<Fr<1$	0.20 (50 rpm)
Centrifuging	$Fr\geq1$	1.01 (110 rpm)

Davidson et al [2000] predicted the transition pattern from slumping to rolling by plotting the slump cycle time against $1/\omega$ and demonstrated a linear relationship between these variables. They also obtained the avalanche time t_{12} (explained in section 4.3.2) in the order of 1-2 s. To verify Davidson's results, the following methodology is adapted in the present work
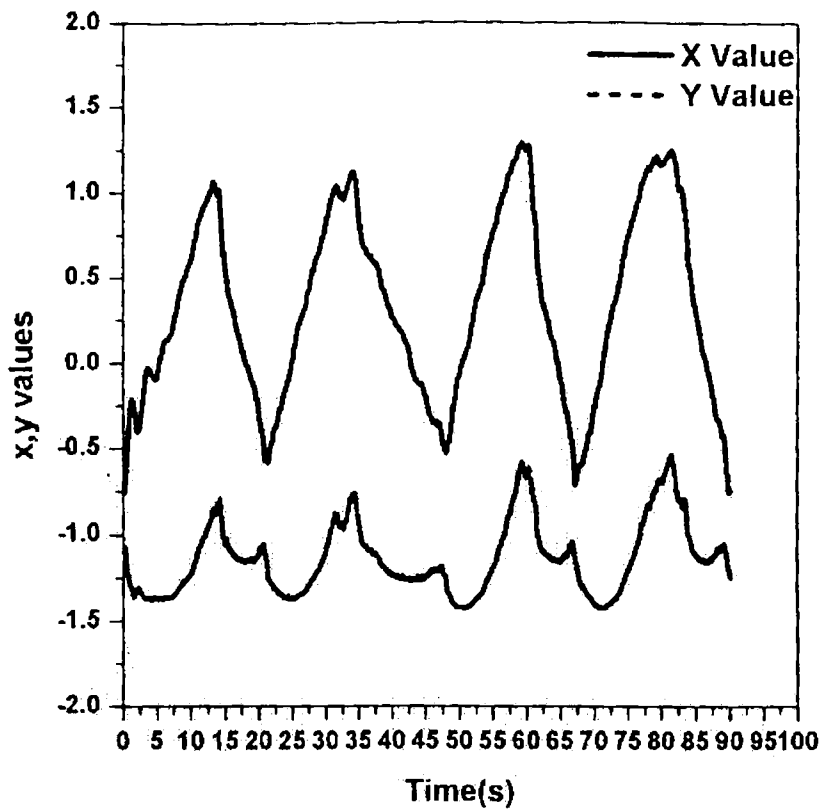
Figure 4.17:   Horizontal and vertical position of the particle with respect to time using DEM simulation.

From the trajectory plots as shown in the Figure 4.17, the slump cycle time is calculated as the difference between in time between consecutive maximum x-positions. This is calculated at various times for each representative particle and then they are averaged out. These results are plotted in the same way as that of Davidson [2000) and are shown in Figure 4.18 for various fill fractions.   The avalanche time is in the order of 0.5-0.8 s for the simulation runs.
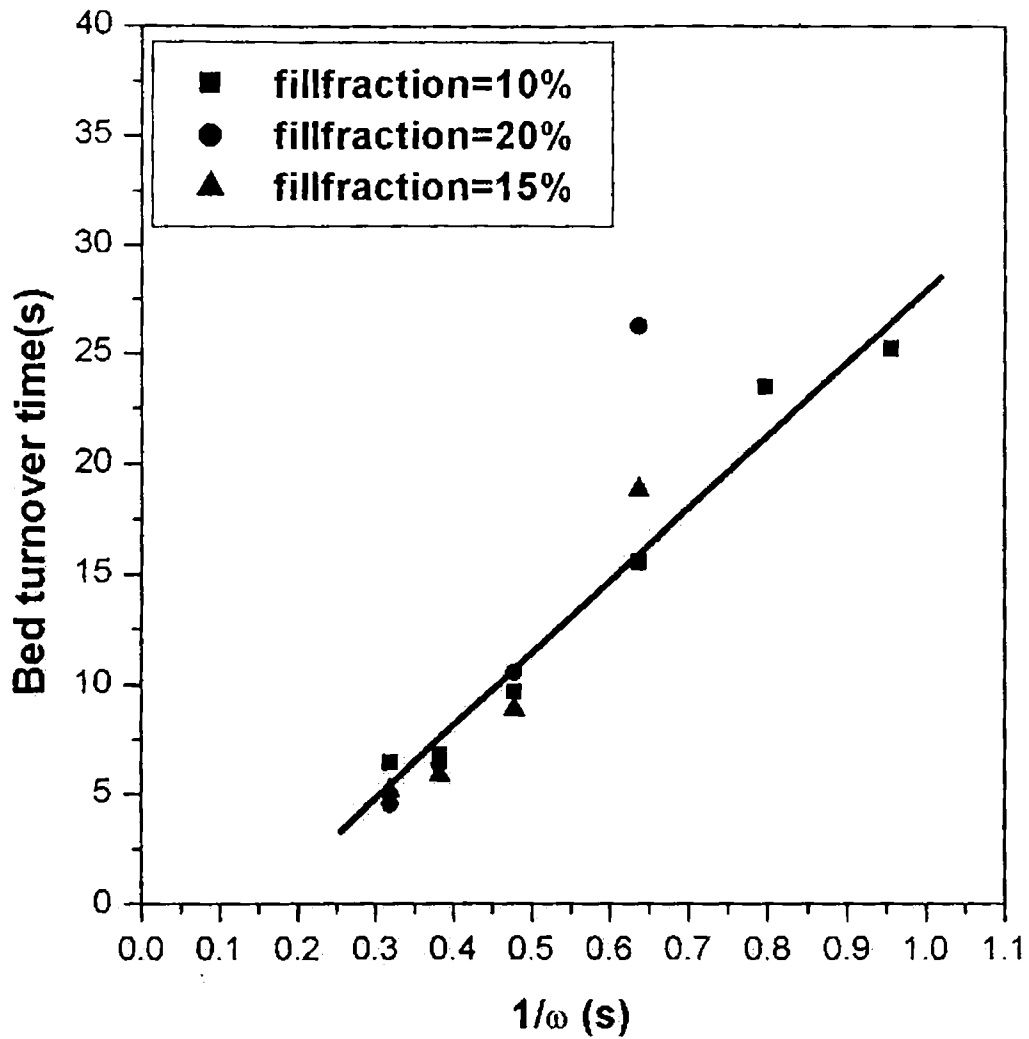
Figure 4.18:   Bed turn over time using DEM simulation

Ding *et al.*, [2002] presented theoretical models based on overall material balance and geometric parameters to calculate bed turnover time in both the slumping and rolling modes and they suggested that the transition form slumping to rolling occurs when the two turnover times are equal. According to Ding, [2002] the bed turnover during rolling mode is given as

$$(t_{br})_r = \frac{2\left[R^2 \arcsin\left(\dfrac{L}{R}\right) - Lh \right]}{\omega\left[L^2 - 2h\delta_m - \delta_m^2 \right]}$$

(4.9)

where ω is the rotational speed, L is the half chord length, R is the radius, h is the shortest distance between the drum center and bed surface and δ_m is the maximum depth of the active region.

The simulation to check this equation is carried out for the following process parameters;

Table 4.3:   Process parameters

Parameter	Assigned Value
Cylinder Radius	1.5 m
Particle Size	6 mm
Fill Fraction	10 %- 30 %
Rotational Speed	5 – 30 rpm

From the simulation data the values of L, h and δ_m are obtained and substituted in the equation 4.9 to obtain the bed turnover time $(t_{br})_r$. From the trajectory plots of the representative number of particles, the bed turnover time is calculated as $\left(t_{br}\right)_r$ as predicted by simulation $= \dfrac{\text{Simulation time}}{\text{Average no. of cycles}}$. For example, from the figure 4.17, we obtain $(t_{br})_r$ as predicted by simulation $=$

$\dfrac{90\,\text{s}}{9\,\text{cycles}} \approx 13s$. The predicted bed turnover time from simulation are presented in table 4.4, Along with the values obtained from equation (4.9).

From the table it can be observed that the simulation results are deviating from the results of Ding *et al* [2002]. The deviations may be due to the following reasons.

Results obtained by the present simulation are based on the transient analysis of the granular solid bed dynamics, whereas derivation by Ding *et al* [2002] is based on the steady state assumption and on the geometrical pattern of the granular solid bed.

Only uniform spherical particles are taken for the present simulation, where as the work of Ding *et al* [2002] is based on a particle size distribution and for a different cylinder diameter.

Table 4.4: Bed turnover time as predicted by equation 4.9 and by DEM simulation

Fill Fraction (%)	Angular Velocity (rpm)	$(t_{br})_r$ by equation 4.9 (s)	$(t_{br})_r$ by simulation (s)
10	15	1.17	13
15	20	0.931	11.1
20	20	1.105	9.5

4.5.2 Characterisation of active layer

Since active layer has been declared as the zone, that is responsible for the mixing of solids under going a rolling mode, several studies have been directed to characterizing the active layer depth.

Henein *et al.* [1983a,b] noted that the active layer depth decreased for smaller particles, decreased with increase in bed depth and increased with the

rotational velocity of the cylinder. Boateng [1993] found that the active layer proportion increased with increase in velocity and decreased with increased drum loading.

Recently Van Puyvelde *et al.* [2000] characterized the active layer depth based on their experimental results for various rotational speeds and fill fraction. They concluded that the only parameters, which affected the active layer percentage, were the cylinder loading and cylinder velocity. They also found out that particle sizes and cylinder diameter did not affect the active layer depth.

The active layer percentage as predicted by Van Puyvelde [2000] is given as

$$\%AL = 9.81\ln(N) + 0.438e^{0.08744(50-L)}$$
(4.10)

The simulation tests are carried out for the same process parameters Table 4.3. The active layer depth from the simulation runs are calculated as explained in section 4.3.4. The results are presented in Table 4.4:

Table 4.5: Percentage of Active layer both simulation and equation 4.10

Fill Fraction (%)	Rotational Speed (rpm)	% AL (Equation 4.10)	% AL (present study)
10	15	41	40
15	20	39	38
20	20	35	32.3
25	20	33.2	32.9
30	20	31.9	31.8

It is clearly evident that the DEM simulation carried out in this study is able to predict the active layer depth of granular solids undergoing in rolling motion accurately.

The variation of active layer depth with respect to the rotational speed and fill fractions are presented in Figures 4.19 and 4.20. It can be observed that active layer depth increases with rotational speed and decreases with fill fraction, which agrees well with results of Henein et al., [1983a, 1983b]
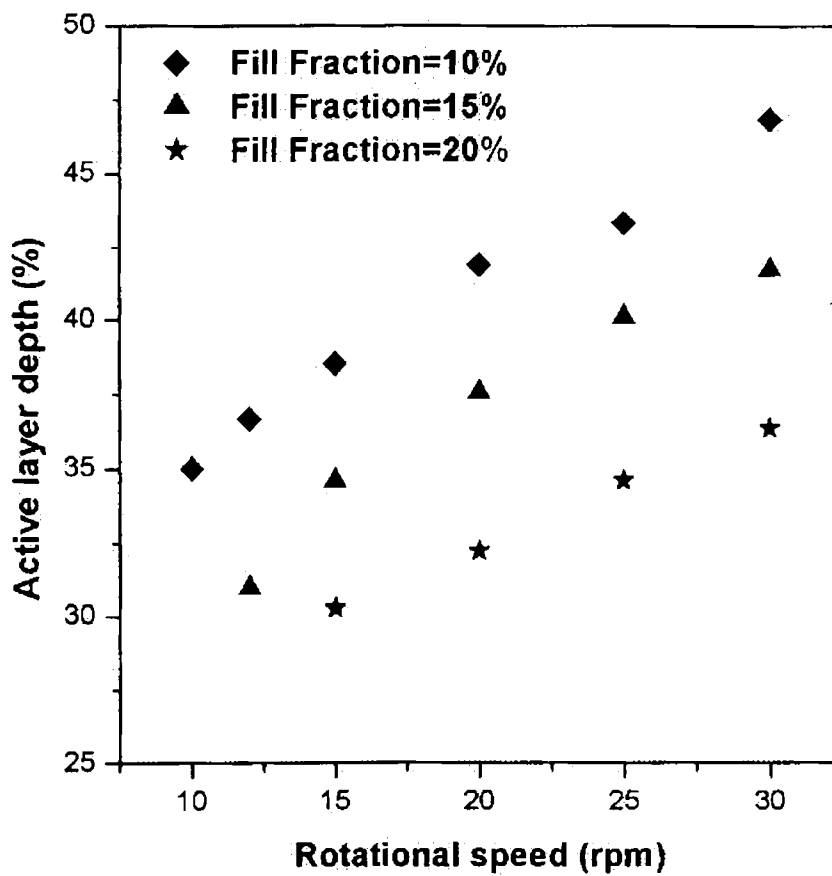
Figure 4.19:   Active layer depth vs rotational speed.
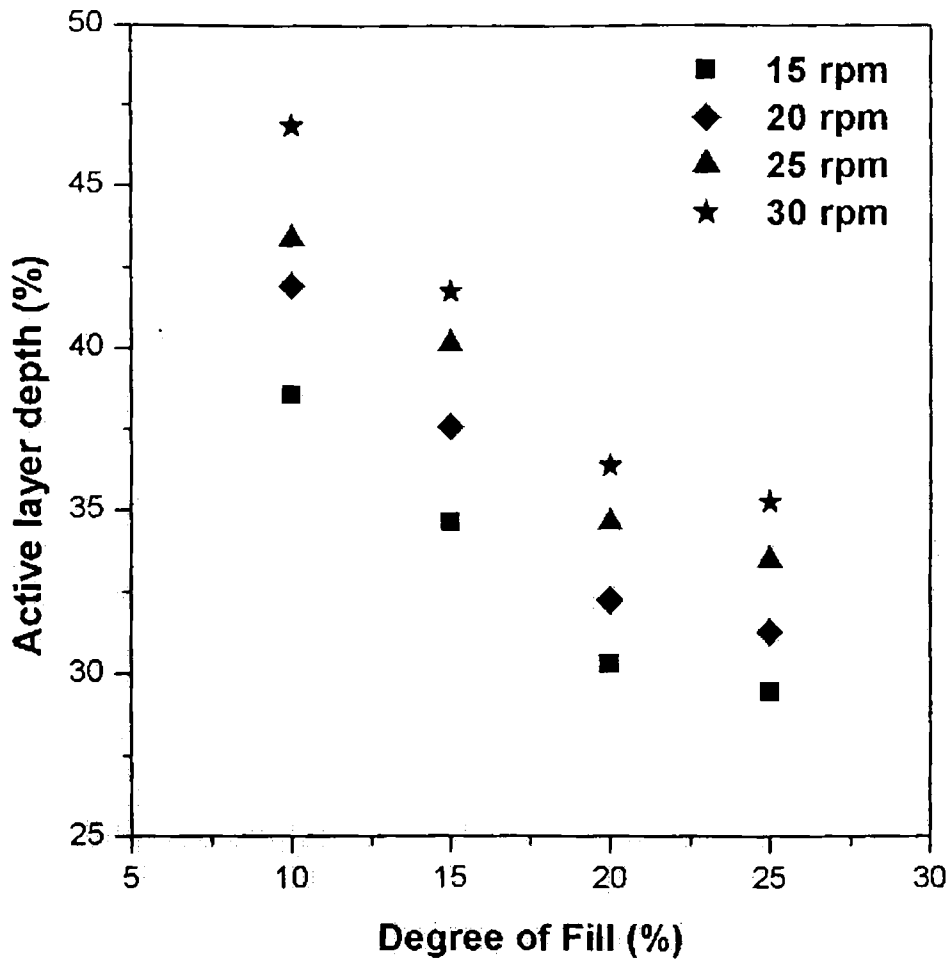
Figure 4.20: Active layer depth vs fill fraction

Increasing the percentage of fill signifies that although more material goes into shearing, the amount of material sheared is distributed over a longer chord length and hence smaller increment in thickness. This results in the observed decrease in percent active layer depth. The decreasing percent active layer depth with increased percent fill is therefore related to geometrical constraints.

4.5.3 Dynamic angle of repose

The variation of dynamic angle of repose with respect to rotational speed obtained through DEM simulation carried out in this work is plotted in Figure 4.21 for various fill fractions. It can be seen that the dynamic angle of repose increases linearly with the rotational speed.
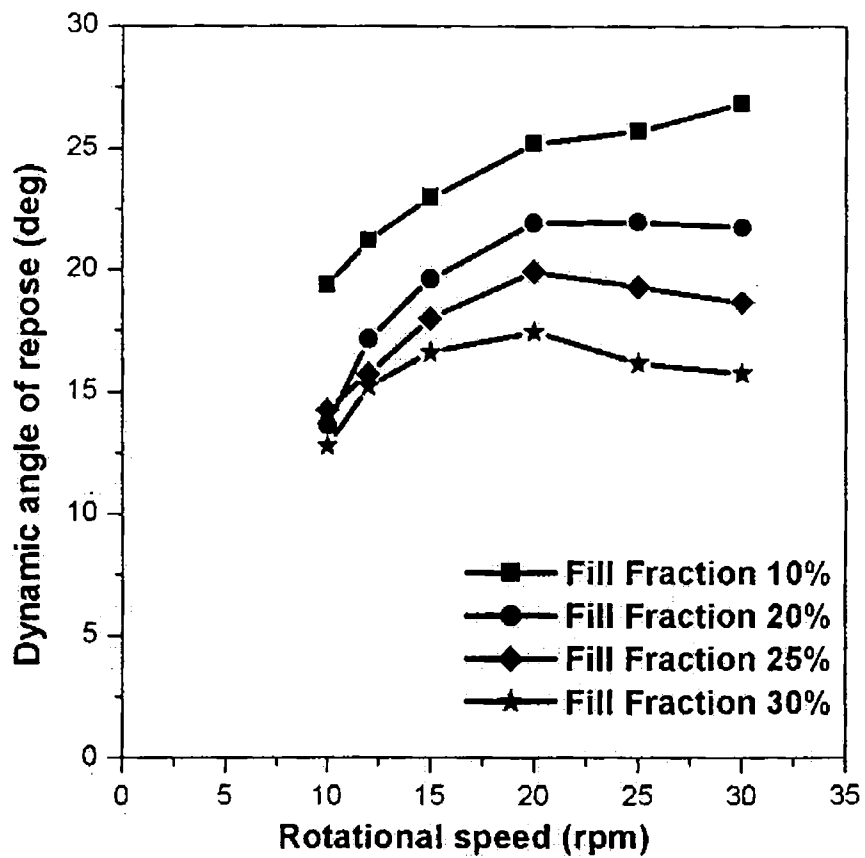

Figure 4.21:   Dynamic angle of repose vs rotational speed

To study the effect of friction between cylinder wall and granular particles, simulation runs were made by varying the coefficient of friction. The values of dynamic angle of repose are plotted in figure 4.22 for various values of coefficient

of friction. The dynamic angle of repose increases rapidly with an increase in the coefficient of friction but levels off for friction coefficients greater than 0.5. These simulation results agree very closely with the observations of Yamane *et al.*, [1998].
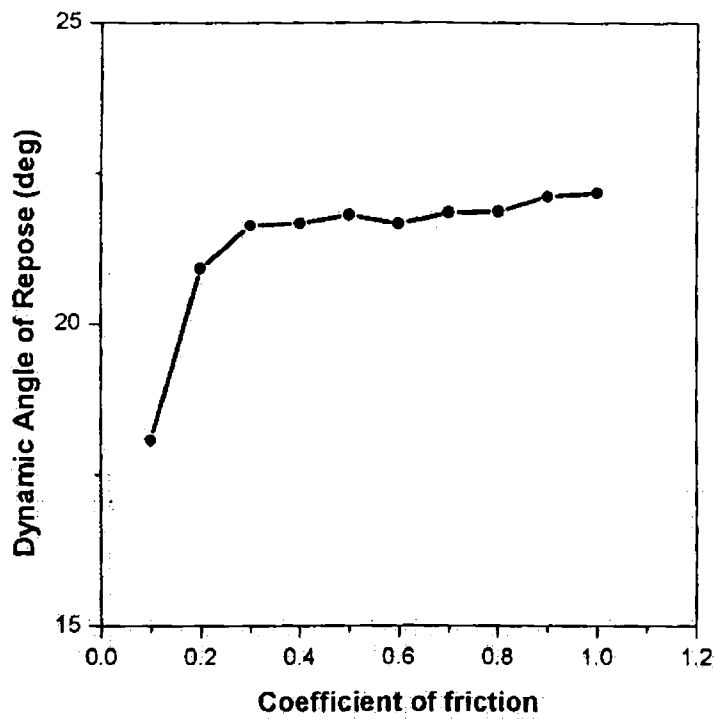
Figure 4.22: Dynamic angle of repose vs coefficient of friction

4.5.4 Surface velocity during granular motion

Particle velocity is one of the most important variables that affect individual particle dynamics. Boateng and Barr [1997] measured surface velocity with fibre optic probes and found that the velocity profiles which were roughly parabolic centered about the mid chord length, agrees with the previous experimental works by Singh [1978]. However, these symmetric profiles were not consistent among all the materials tested nor for the same material at different

rotation rates. Decreasing the fill percent at constant rotation rates, caused the velocity profiles to become skewed towards the base, meaning the particles accelerated beyond the mid chord position. MRI studies by Nagakawa *et al.* [1993] likewise showed roughly parabolic velocity profiles skewed towards the base of the cylinder. One such typical plot is shown in Figure 4.23 which clearly shows the parabolic velocity profile.

The maximum surface velocity is plotted against rotational speed in Figure 4.24 and it can. be seen that there is a linear relationship between these two quantities as predicted by Yamene *et al.*, [1998].

Normalised surface velcoity along the dimensionless distance along the surface layer (x/2L)
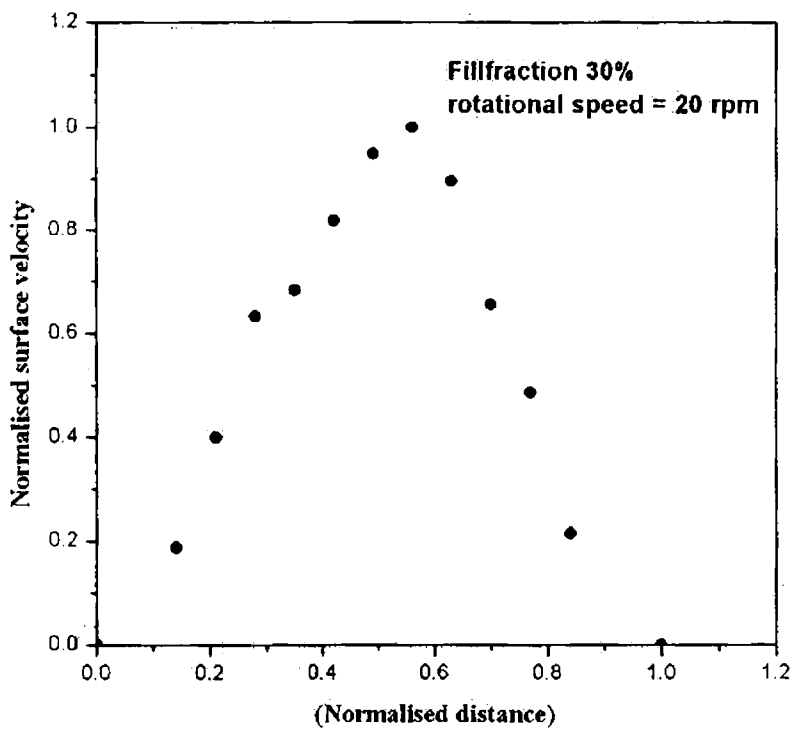
Figure 4.23 :   Normalised surface velocity along the chord length
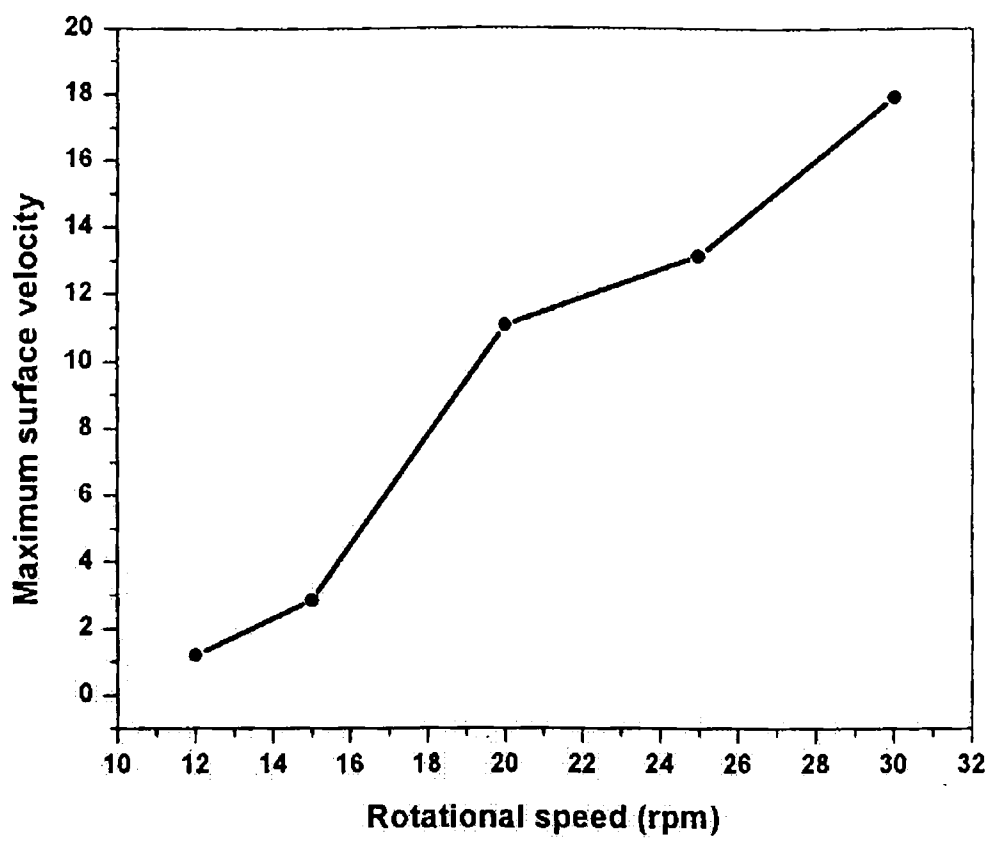
Figure 4.24: Maximum surface velocity vs rotational speed

4.6   Conclusion:

Using the software code DEMCYL presented in Chapter 3, the simulation of granular solids in the transverse plane of a horizontal rotating cylinder is carried out in this Chapter. The results obtained are presented both at the micro-level and macro-level.   The procedure to obtain individual particle velocities, their trajectories, velocity vector plots, dynamic angle of repose, surface layer velocities, active layer depth are presented. This is followed by results showing the six forms of solid body motion with respect to rotational speed along with trajectory plots and kinetic energy distribution for each mode.

For slumping mode, the slump cycle time is validated with the results of Davidson *et al.*,[2000]. Prediction of the transition behaviour based on Froude number from simulation is compared with the results of Mellmann [2001] and the agreement is found to be satisfactory. The bed turnover time against the frequency $\dfrac{1}{\omega}$ for various fill fractions demonstrated a linear relationship as predicted by Davidson *et al.*, [2000].

The active layer depth obtained through simulation are compared with the active layer depth predicted by Van Puyvelde *et al.*, [2000a] and the agreement is found to be very good. It has also been found that active layer depth does not depend on the particle size and cylinder diameter as observed by Van Puyvelde [2000a].

It has also been found that the active layer depth increases with rotational speed and decreases with degree of fill as predicted by Henein *et al.*,[1983a, 1983b]. The surface velocity profiles showed a parabolic nature and the maximum surface velocity increased with rotational speed in a linear way as predicted by Yamane *et al.* [1998]

The dynamic angle of repose is found to increase with the increase in rotational speed. The dynamic angle of repose is also found to increase with coefficient of friction, but after a value of 0.5 for coefficient of friction is almost constant as predicted by Yamane *et al.* [1998].

CHAPTER 5

MIXING AND SEGREGATION BEHAVIOUR OF GRANULAR MATERIALS IN A ROTATING CYLINDER

5.1 Introduction

Mixing and segregation of granular particles having different material properties such as particle size, density, shape, surface roughness is one of the important operations performed in horizontal rotating cylinders. They significantly contribute towards heat and mass transfer and chemical reactions and thereby play a major role in the productivity and product quality of the final product. In order to improve the efficiency of mixing, it is important to understand the particle behaviour in any mixing apparatus.

Several experimental studies have been directed towards investigation of mixing and segregation behaviour of granular solids in a horizontal cylinder slowly rotated about its axis, for example the work of Oyama [1939], Weidenbaun and Bonilla [1955] and Roseman and Donald [1962]. In general, experiments were performed in a cylinder that was closed at both ends and rotated in a batch mode, at various rotational speeds resulting in slumping, rolling or cascading modes of bed motion.

Hogg and Fuersteanu [1972] described the mixing in the transverse section of rolling bed as a combination of the convective and diffusive mixing mechanisms. Lehmberg et al., [1977] measured the dynamics of mixing of solids in an

experimental drum of diameter 310 mm and they mixed 0.80 mm sand having a mixture containing 90% as white and 10% as black. They used a rotational speed of 2 rpm and found that the bed was fully mixed after 42 rotations. However, they did not quantify the mixing rate. Woodle and Munro [1993] studied the mixing rate from a statistical point of view and found the rate of mixing to be constant until the bed became fully mixed. Boateng and Barr [1996] devised a model for the mixing and segregation using granular mechanics.

Experimental measurements of radial mixing of mono-sized particles of equal density are reported in a slumping bed by Clement *et al.* [1995] and Metcalfe *et al.* [1995], and in a rolling bed by Khakhar *et al.* [1997a]: (i) Clement *et al.* [1995] used a video camera to track the motion of a single particle of diameter 1.5 mm in a short cylinder having a diameter160 mm and depth 15 mm. The particle was reported to move at random between different radial positions in the bed. (ii) Metcalfe *et al.* [1995] investigated the radial mixing of table salt of mean diameter 0.6 mm, rotated in a short cylinder having a diameter of 144 mm and of length 24 mm.

A simple model for the mixing process was proposed consisting of (a) a geometric part corresponding to transport of the slumping wedge from the top to the bottom of the bed, and (b) a dynamic part, assuming random mixing within the wedge. Good qualitative agreement was found between the model and experiment, but the model was found to consistently overestimate the mixing rate. (c) Khakhar *et al.* [1997a] used a video camera to investigate radial mixing in a thin cylinder, of diameter 69 mm and length 15 mm, between different colours of (i) sugar crystals of diameter 1 mm, and (ii) spherical sugar balls of diameter 1.8 mm. The rate of mixing per revolution was found to increase as the hold-up was decreased, and to be higher for spherical particles. Recently van Puuvede et al [2000a, 2000b] has carried out extensive set of experiments to predict the mixing rate and final amount of mixing of solids in a rotating drum.

As can be seen from the literature review, several models have been proposed but each model is limited to individual experimental conditions.. A unified mixing model which helps to analyze the effect of important process variables like cylinder size, particle size, particle density, rotational velocity of the cylinder and fill fraction on the mixing kinetics is absent.

A considerable amount of experimental work on particle segregation in partially filled rotating drums has been carried out in the last few decades. The main conclusions, which should form the basis for validation of a generalized model are;

- Segregation occurs in both radial and axial directions, but axial segregation proceeds slowly while radial segregation takes place rapidly (Roseman Donald [1962], Rogers and Clements [1971], Henein [1987], Pollard and Henein [1989], Wightman and Muzzio [1998]).

- In the transverse plane, fine, rough and dense particles are found by most workers to concentrate in the core region of the bed (Pollard and Heneein [1989], Rogers and Clements [1971]).

- Segregation in the transverse plane occurs mainly through percolation, random sieving and expulsion and trajectory mechanisms (Nityanand *et al.* [1986], Savage and Lun [1988], Boateng and Barr [1996]).

- There are some controversies regarding the kinetics of radial segregation. The results of Rogers and Clements [1971] and Cantelaube *et al.* [1997] showed that the kinetics of segregation was first-order while Nityanand *et al.* [1986] observed a zeroth order kinetics.

In parallel with the experimental work, mathematical modelling has also been carried out aiming with a view at understanding the kinetics and mechanism of particle segregation. These studies can be classified into the following two categories. The first category is the application of the Eulerian method, which treats the granular material as a continuum (Boateng and Barr [1996], Levitan [1998], Puri and Hyaakawa [1999]). The second category is the application of Lagrangian approach, which includes discrete element method, and Cellular automata approaches (Walton and Braun [1993], Yamane [1997], Cleary [1998] and Kitarev and Wolf [1999]). *These models help with interpreting some experimental observations. However quantitative agreement between model predictions and experiments has been rare in the published work.*

The effect of mass ratio on segregation has been investigated by Ristow [1994] using equal sized particles of different densities and he showed that the segregation velocity increased proportionally with the logarithm of the mass ratio of the particles.

Based on the earlier analysis carried out it is apparent that the particle size ratio and the rotational velocity of the drum are important variables in trying to predict the segregation behaviour. *Hence this work is directed towards checking the capability of the prediction of the mixing and segregation behaviour of granular materials in a horizontal rotating cylinder through the simulation code DEMCYL Further the effect of particle size, particle density and rotational velocity on the mixing and segregation behaviour is studied based on the simulation results. The simulation results are quantified in terms of mixing index, mixing rate, segregation index and percolation index*

5.2   Mixing curve, Segregation Index and Percolation index

5.2.1 Mixing curve

Using DEM simulation, the mixing process was simulated by drawing a mixing curve by relating the degree of mixing and the mixing time. As a first step, the particle bed was divided into two parts, particles in the upper part are coloured with black and lower particles are coloured with white as shown in Figure 5.1. The degree of mixing was calculated using these two sets of particles at each cycle of rotation from the initial state onwards. To get a better idea of how the degree of mixing varies over the solid bed, we divided the solid bed into different segments as shown in Figure 5.2. Each segment may have unequal areas. During the simulation, at the end of each iteration, the parameters corresponding to the solid materials belonging to each of the segments is computed separately and analysed.
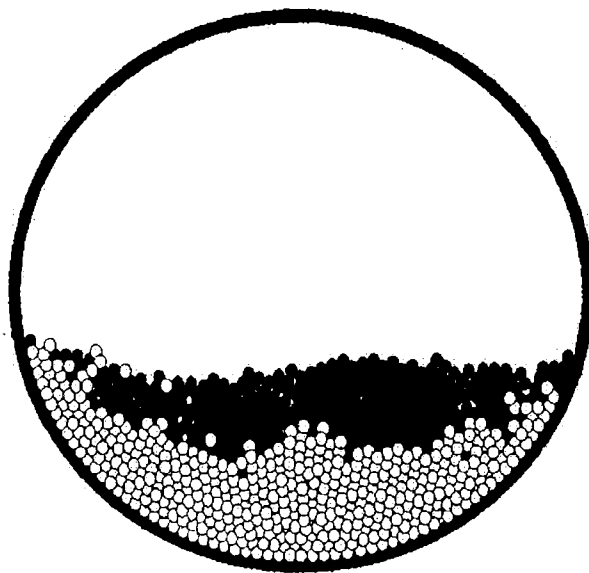

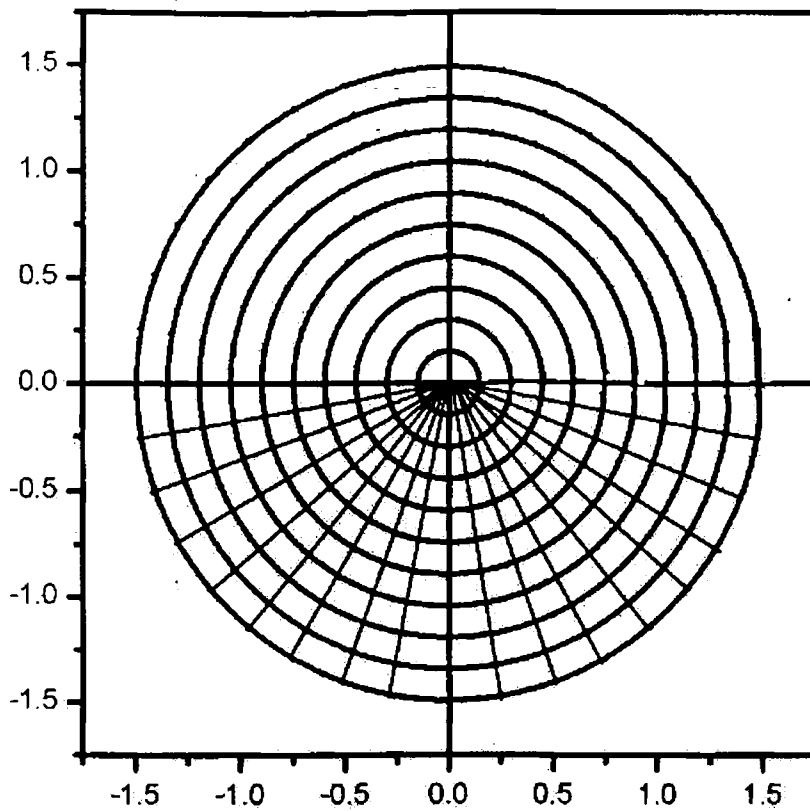**Figure 5.1:**   Initial particle distribution

Figure 5.2: The cross section of the cylinder divided into different segments.

The standard deviation for each set of particles in each segment (Muguruma *et al..*, [1997]) is given by

$$\sigma = \sqrt{\frac{\sum_{I=1}^{N}(f_i - \bar{f})^2}{N-1}} \tag{5.1}$$

where f_i denotes the volume fraction of black coloured particles in each segment i, $\bar{f}$ is the over all proportion of black coloured particles (Initially assumed

volume fraction) in each segment and N is the number of segments in which particles are occupied.

The degree of mixing is given by $\dfrac{\sigma}{\sigma_0}$, where σ_0 denotes the standard deviation obtained during the initial condition of totally unmixed state and is given by

$$\sigma_0 = \sqrt{\overline{f}(1-\overline{f})}. \tag{5.2}$$

When the granular bed is randomly mixed then the standard deviation, σ_0 is expressed as

$$\sigma_0 = \sqrt{\dfrac{\overline{f}(1-\overline{f})}{n}}, \tag{5.3}$$

where n is the total number of black coloured particles in each segment.

5.2.2 Segregation Index

When the cylinder is rotated with particles having different sizes, one has to take care of the degree of segregation. A similar procedure employed for calculating the mixing index was used to calculate segregation index also. The solid bed was divided into different segments as shown in Figure 5.2 each segment consisting both smaller and larger sized particles. The standard deviation for the fraction of small particles in each segment is given by

$$\sigma = \sqrt{\frac{\sum_{i=1}^{N}(f_i - \bar{f})^2}{N-1}}$$

(5.4)

where f_i is the volume fraction of smaller particles in each segment i, $\bar{f}$ is the over all proportion of smaller particles (initial volume fraction) and N is the number of segments in which particles are occupied.

The segregation index is given by $\dfrac{\sigma}{\sigma_0}$, where σ_0 denotes the standard deviation obtained during the initial condition of totally unmixed state and is given by

$$\sigma_0 = \sqrt{\bar{f}(1-\bar{f})}.$$

(5.5)

Porosity is one of the fundamental properties of a bed of granular materials (Ai-Bing Yu [1993], Alonso *et al.*, [1991], Ouchiyama and Tanaka [1984]. Prediction of porosity of a bed of granular materials helps in controlling the product quality at the optimum level. It is seen earlier from literature that porosity is intimately related to the particle size distribution. For the present study, the following methodology is adapted to calculate the porosity. After dividing the transverse plane of the cylinder into segments as shown in Figure 5.2, the number of particles inside each segment is identified and their total volume calculated. The porosity is defined as

$$\zeta_i = \frac{Volume\ of\ the\ segment\ i - Total\ volume\ of\ the\ particles\ in\ segment\ i}{Volume\ of\ the\ segment\ i}$$

5.2.3 Percolation Index

As the cylinder rotates the denser or smaller particles percolates inside to the central region of the solid bed creating a radial segregation. The magnitude of segregation depends on various factors such as rotational speed, particle size ratio, fill fraction and particle density. The degree of segregation can be expressed quantitatively in terms of a percolation index (Alonso *et al.*,[1991]). The Percolation index P_I is defined as;

$$P_I = \zeta \exp\left\{ -\frac{(1-\zeta)}{\zeta}\left[\left(1 + \frac{1}{1+v_C(d-1)}\right)^2 - 1 \right] \right\}$$

(5.6)

where ζ is the average porosity, v_C is the overall solid volume fraction of coarse or larger size particles in the bed and d is the size ratio of coarser to fine particles.

5.3 Mixing behaviour using DEMCYL

Since mixing and segregation are more pronounced in the rolling mode of solid bed motion in a rotating cylinder, the simulation code DEMCYL is run for the following process parameters to study the mixing behaviour of the granular solids.

➤ Cylinder radius= 1.5 m
➤ Particle size= 6 mm
➤ Fill Fraction = 0.30
➤ Rotational speed= 20-30 rpm

To identify the mixing process 50% of the particles are taken as black coloured particles and 50% as white coloured particles. The Figures 5.3 (a to c) shows the mixing pattern of the granular material after 15 rotations during rolling mode at three different rotational speeds viz., 20 rpm, 25 rpm and 30 rpm. It is evident from the figures that mixing behaviour is more pronounced for higher rotational speeds.
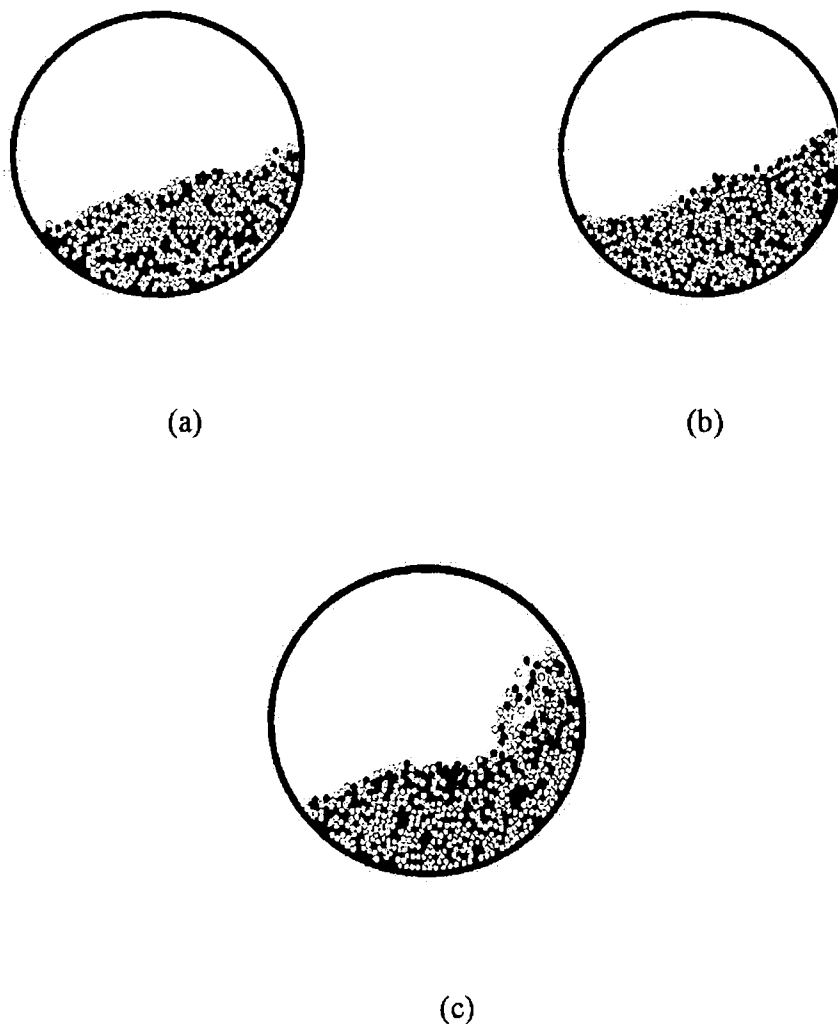

(a)   (b)

(c)

Figure5.3:   Mixing pattern after 15 rotations in rolling mode at rotational speeds (a) 20 rpm, (b) 25 rpm and (c) 30 rpm.

The Figures 5.4 (a to c) shows the trajectory of a single particle after 15 rotations during rolling mode at three different rotational speeds viz., 20 rpm, 25 rpm and 30 rpm. The rolling behaviour of the bed is shown clearly in Figure 5.4 (b) when the rotational speed is 25 rpm. In the cascading regime (Figure 5.4(c)), it can be observed that once the particle reaches the center of the bed it almost remains there.
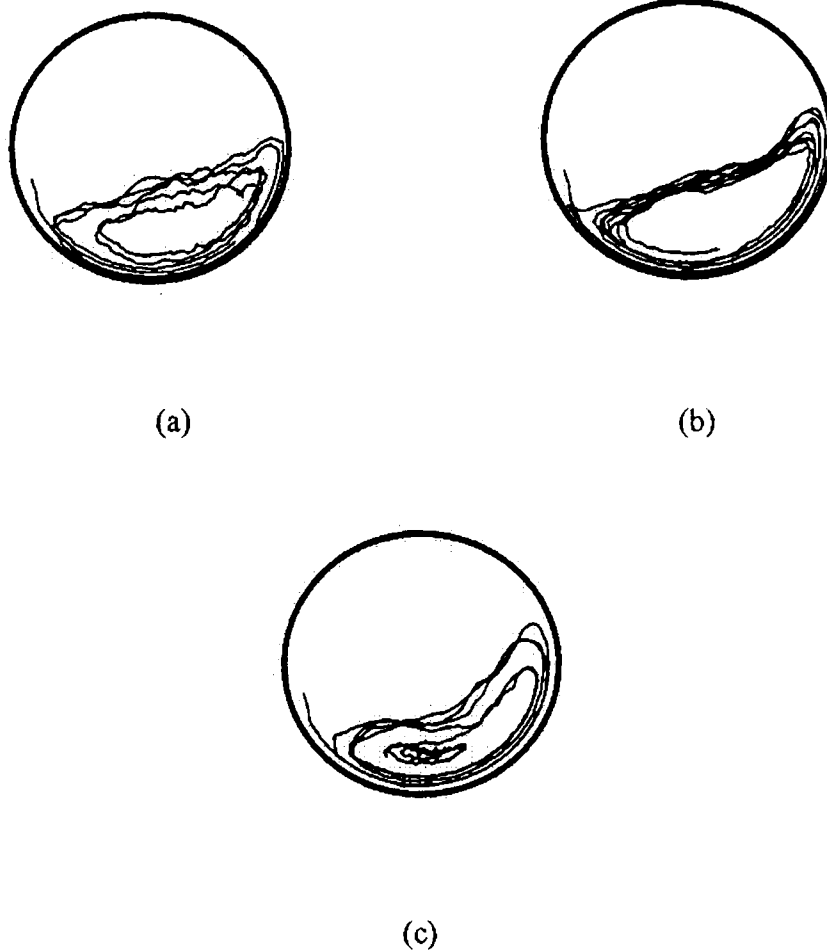

(a)   (b)

(c)

Figure5.4: Trajectory of a single particle after 15 rotations in rolling mode at rotational speeds 20 rpm, (b) 25 rpm and (c) 30 rpm.

Figures 5.5 shows the mixing curve obtained through the DEM simulation for a fill fraction of 30 % at rotational speeds of 20 rpm, 25 rpm and 30 rpm respectively.
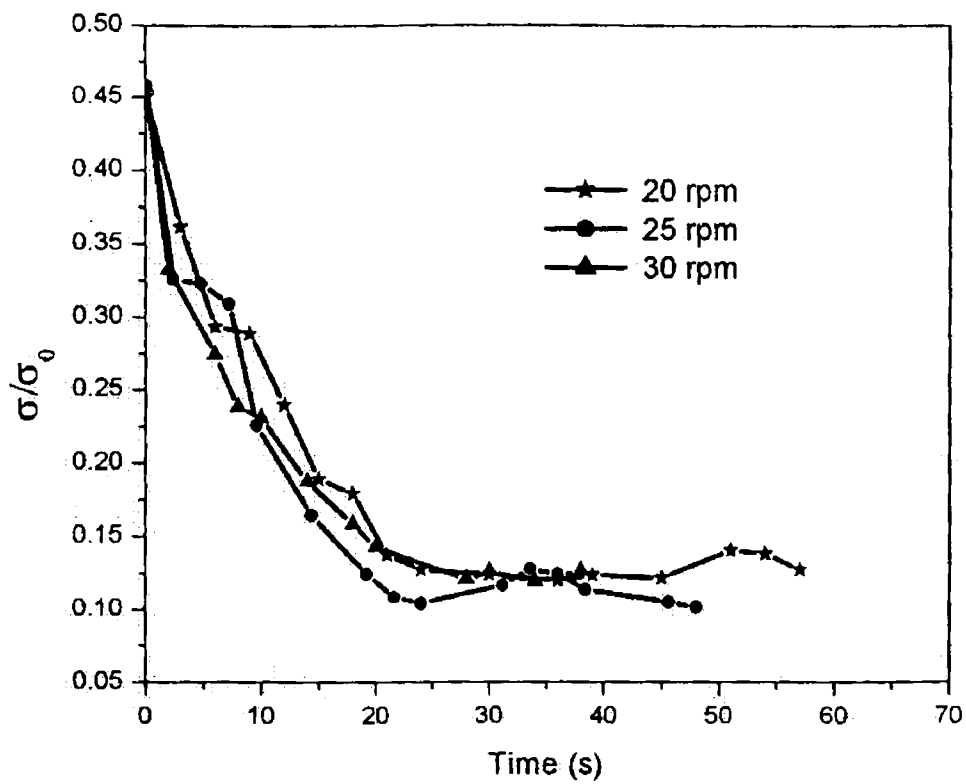

Figure 5.5: Mixing Curve for fill fraction 30%

It can be observed that the degree of mixing diminishes as the time of mixing increases. When the solid particles get mixed well then the degree of mixing becomes constant. A plot of degree of mixing on the natural logarithmic scale versus time is shown in Figure 5.6.
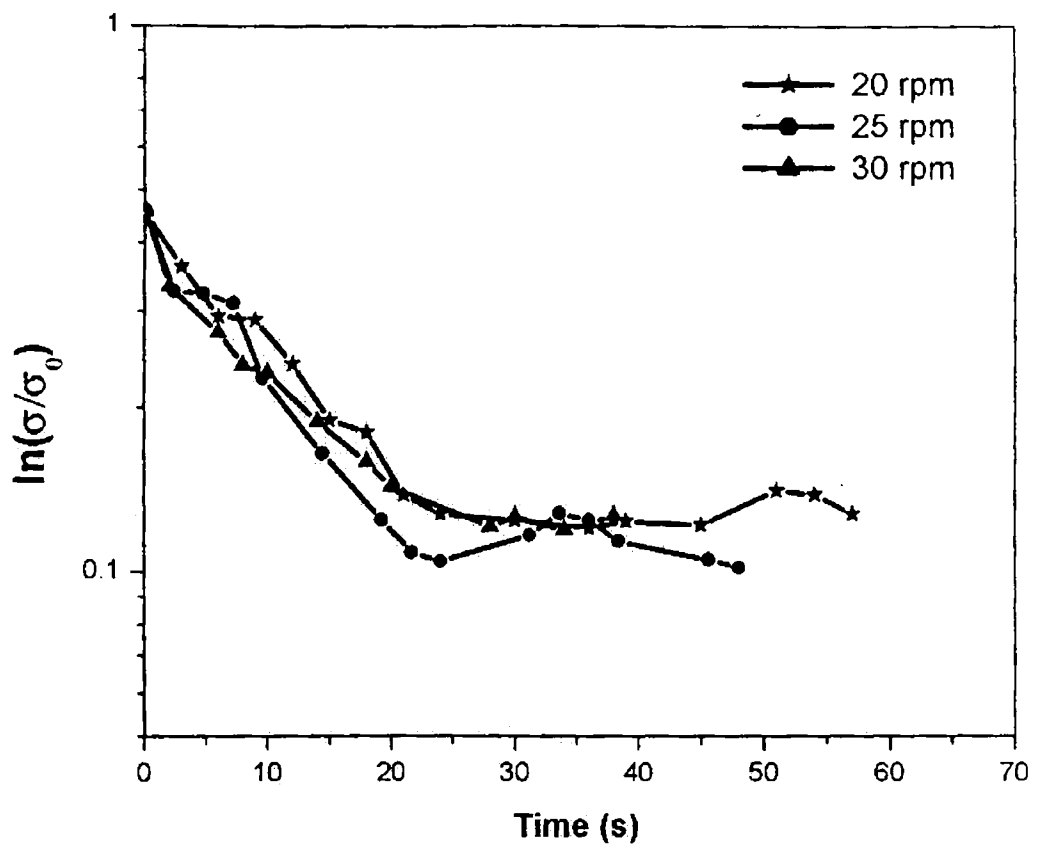
Figure 5.6: Degree of mixing on natural log scale vs time (fill fraction 30 %)

It can be observed that mixing process can be classified into two stages for non-adhesive particles; during the first stage, the term $\ln\left(\dfrac{\sigma}{\sigma_0}\right)$ decreases with the

slope $-\phi$ and in the second stage $\ln\left(\dfrac{\sigma}{\sigma_0}\right)$ takes the constant value of the random

mixture, which is given by $\ln\left(\dfrac{\sigma_r}{\sigma_0}\right)$.

The slope obtained through the mixing curve is termed as the *rate coefficient of mixing* denoted by ϕ and it indicates the effectiveness of a machine as a mixer. The rate coefficient of mixing and the corresponding mixing index are shown in Table 5.1 for different rotational speeds at a fill fraction of 30%. The relation between the rate coefficient of mixing and rotational speed is depicted in Figure 5.7. It is evident that ϕ increases linearly with rotational speed.
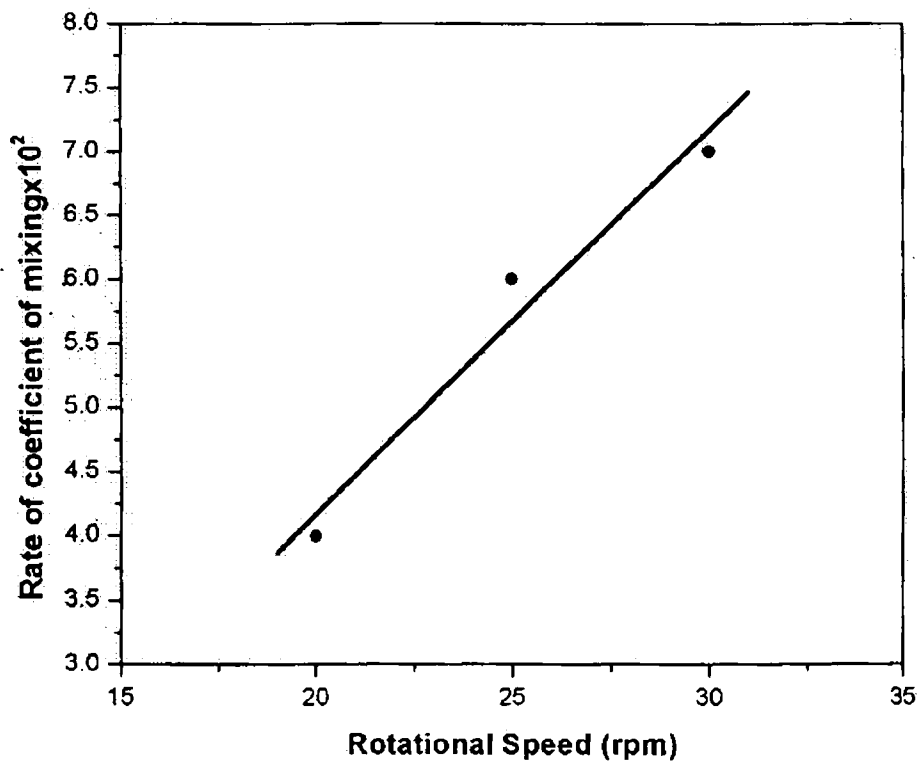

Figure 5.7: Rate of coefficient of mixing vs rotational speed

In Table 5.2 the values of rate coefficient of mixing and the mixing index are given for various fill fractions at two different rotational speeds. The relation between fill fraction and the mixing index is shown in Figure 5.8. At a rotational speed of 30 rpm, the mixing index decrease with increase in fill fraction but when the fill fraction becomes more than 25%, it remains constant.
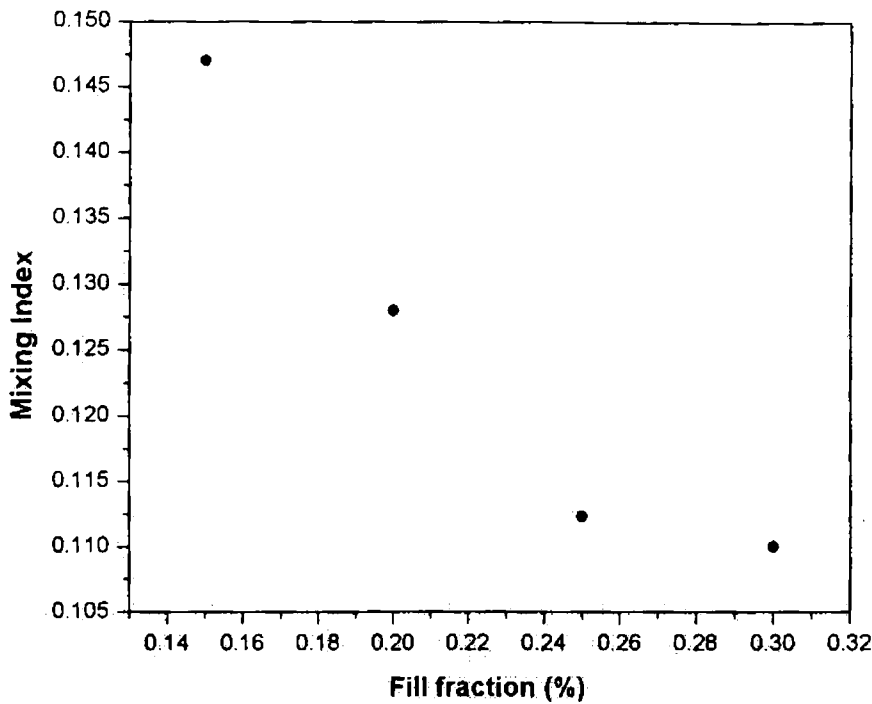

Figure 5.8: Mixing index vs fill fraction.

Table 5.1: Mixing parameters at fill fraction 30 %

Rotational Speed (rpm)	Rate Coefficient of Mixing (-)	Average Mixing Index (-)
20	.004	0.12
25	.006	0.11
30	.007	0.11

Table 5.2: Mixing parameters for different fill fractions

Fill Fraction (%)	Average Mixing Index (-) for 20 rpm	Average Mixing Index (-) for 30 rpm
15	0.15	0.16
20	0.13	0.14
25	0.11	0.12
30	0.12	0.11

5.4 Segregation behaviour using DEMCYL

The simulation code DEMCYL was run for the following process parameters to observe the segregation behaviour for the following process parameters

- ➤ Cylinder radius= 1.5 m
- ➤ Particle size = 4 -10 mm
- ➤ Particle density= 1300 Kg/m^3, 2500 Kg/m^3
- ➤ Fill Fraction = 0.30
- ➤ Rotational speed= 20-30 rpm

5.4.1 Effect of particle size ratio

Various combinations of particle sizes between 4 to 10 mm with density 1300kg/m^3 were chosen to check the segregation pattern for a rotational speed of 30 rpm. It was observed from DEM simulation that particle size ratios play an important role in forming segregation patterns. However, for some specific particle size ratios, segregation is generated while for other ratios of particles, the granular bed is well mixed even though it seems to have a very slight chance for segregation. For example, where for particles sizes 6mm and 10 mm, a perfect segregated bed is

obtained as shown in Figure 5.9 (b), while it was observed that for particle sizes 6mm and 8mm bed is perfectly well mixed. Similarly for particle sizes 5mm and 9mm, as shown in Figure 5.9 (a) a perfectly segregated bed is observed, where as for particle sizes 6mm and 9 mm, the bed is mixed without segregation. So the size ratio plays an important role in mixing and segregation of non-uniform particles.
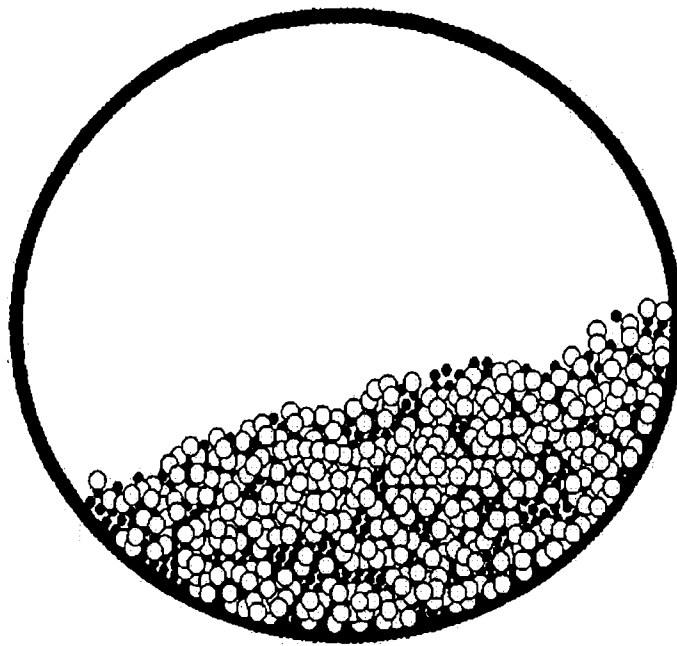

Figure 5.9 (a):   A Granular solid bed with 20 % of 6 mm and 80 % of 8 mm particles.
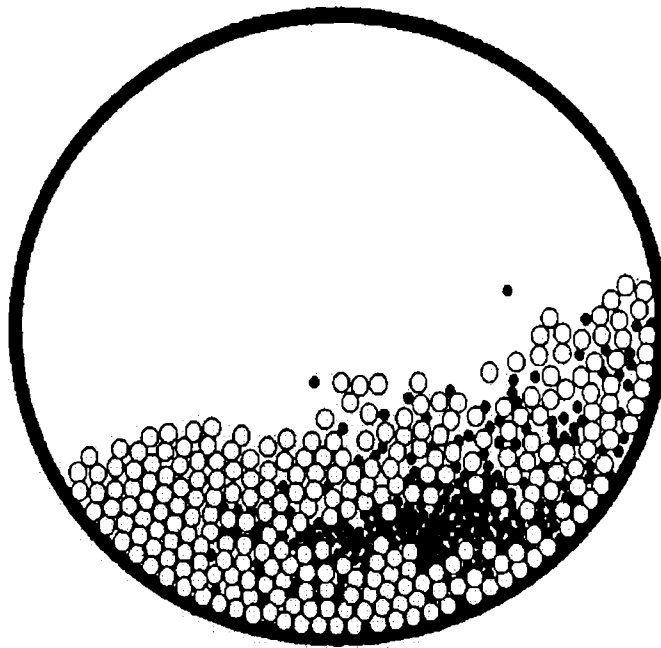
Figure 5.9 (b):   A Granular solid bed with 20 % of 6 mm and 80 % of
                        10 mm particles.

5.4.2 Effect of rotational speed

The effect of rotational speed on the segregation pattern is depicted in the Figures 5.10 to 5.13. The fill fraction was fixed at 30% and the volume fraction of 6 mm particles was taken as 20 % and volume fraction of 10 mm particles was taken as 80 %. The rotational speed of the cylinder is changed from 15 rpm to 100 rpm. The profiles of granular solid particles for each rotation from the figures, shows how the segregation mechanism takes place at various rotational speeds. These patterns agree well with the experimental results of Nityanand *et al.* [1986].
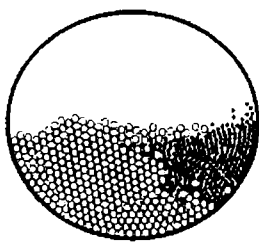
a (1 rotation)
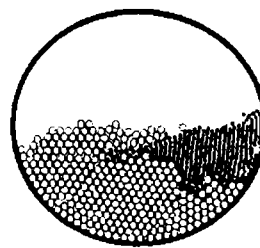
b (2 rotations)
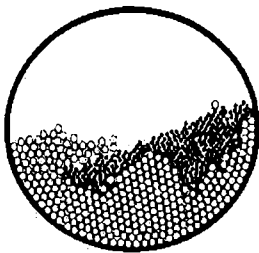
c (3 rotations)

d (4 rotations)

e (5 rotations)

f (6 rotations)

g (7 rotations)   h (9 rotations)

Figure 5.10 (a-h):   Segregation pattern formation for the first 9 rotations in the rolling mode.
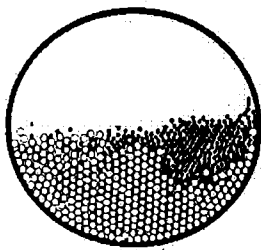
a (1 rotation)   b (2 rotations)
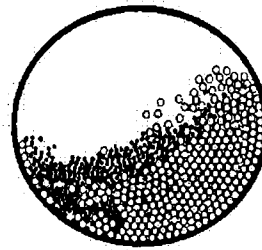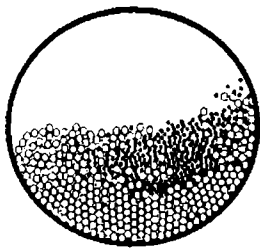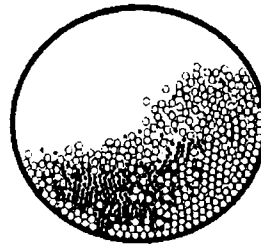
c (3 rotations)   d (4 rotations)
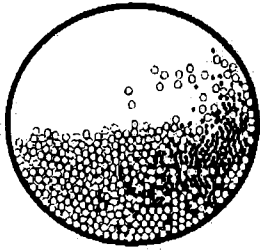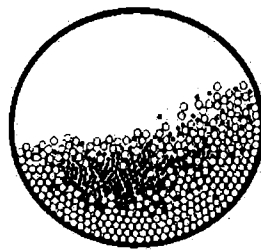
e (5 rotations)   f (6 rotations)
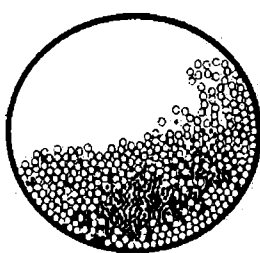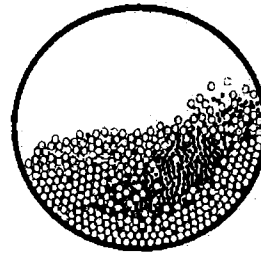
g (7 rotations)   h (8 rotations)

Figure 5.11 (a-h): Segregation pattern formation for the first 9 rotations in the cascading mode.

a (1 rotation)
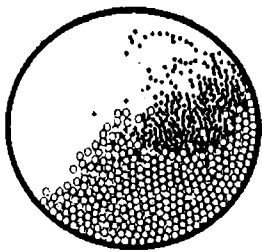
b (2 rotations)
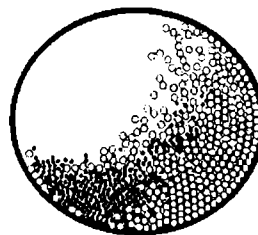
c (3 rotations)
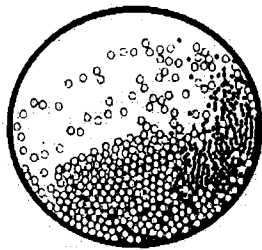
d (4 rotations)
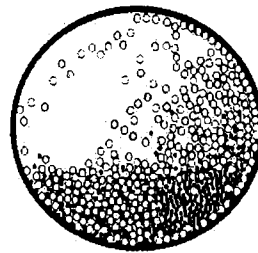
e (5 rotations)
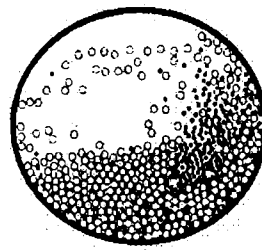
f (6 rotations)
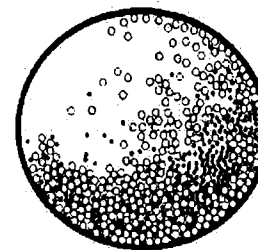
g (7 rotations)
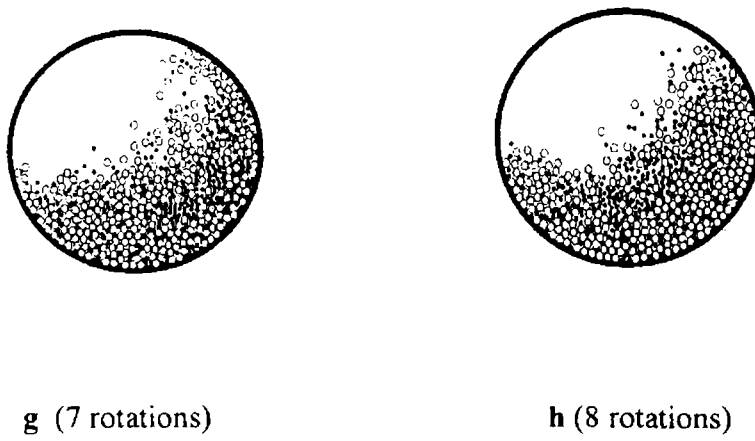
h (8 rotations)

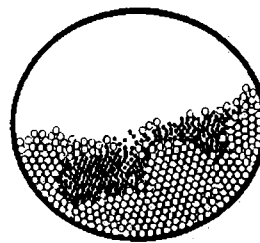**Figure 5.12 (a-h):** Segregation pattern formation for the first 9 rotations in the cataracting mode.
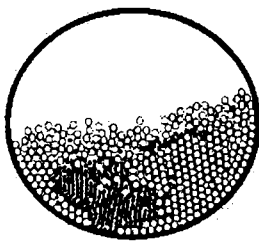

a (1 rotation)

b (2 rotations)
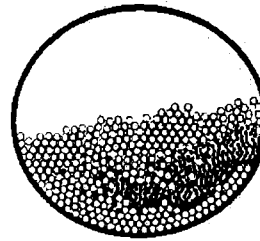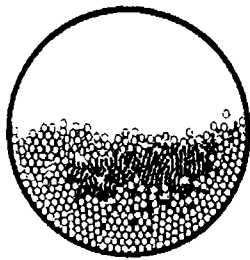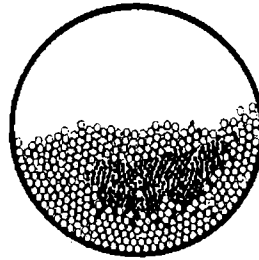

c (3 rotations)
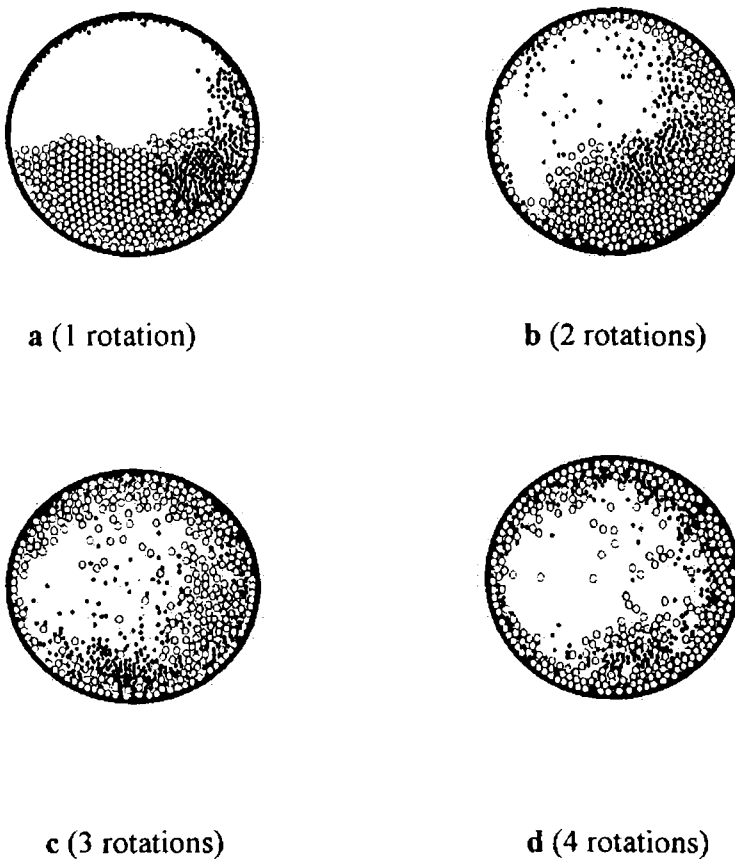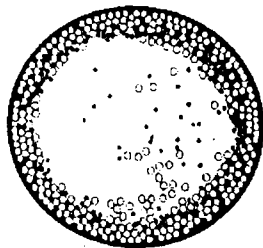
d (4 rotations)
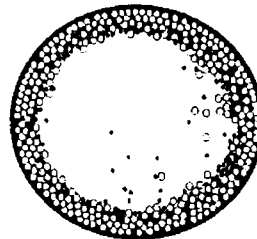
e (5 rotations)   f (6 rotations)
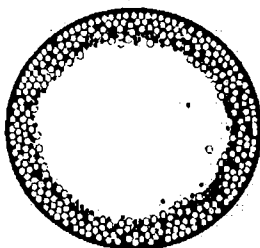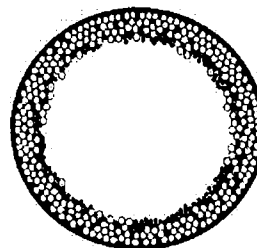
g (7 rotations)   h (8 rotations)

Figure 5.13 (a-h) :   Segregation pattern formation for the first 9 rotations in the centrifuging mode.

When the mode of granular material motion is cascading, particles will be almost well mixed and no radial segregation is observed. At higher rotational speeds the smaller particles segregate to the walls of the cylinder. This phenomenon has been termed as reverse segregation by Nityanand *et al.* [1986] to differentiate from the segregation core associated with rolling and slumping modes. The differences occurring in the segregation patterns in the rolling mode compared with the centrifuging mode may be due to the differences in the bed behaviour.

5.4.3   Effect of volume fraction of finer particles

To study the effect of volume fraction of finer (smaller) particles, DEMCYL is used to simulate the granular dynamics of two different sized particles having 30 % of fill fraction with volume fraction of finer particles changing from 10 % to 50 %. The rotational speed of the cylinder is set at 30 rpm. The segregated granular bed after 10 rotations are shown in Figures 5.14 to 5. 17. The size of the core increases with increase in volume fraction of finer particles.
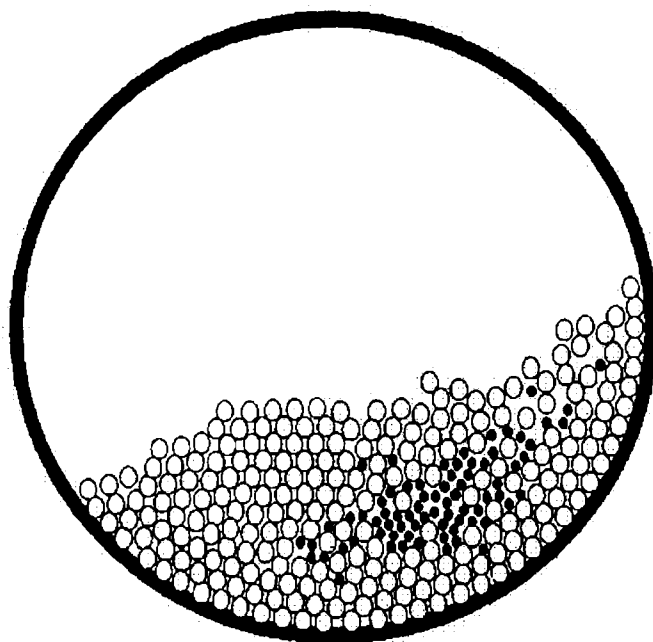
Figure 5.14:   Segregated solid bed of 10% of smaller particles and 90% of larger particles
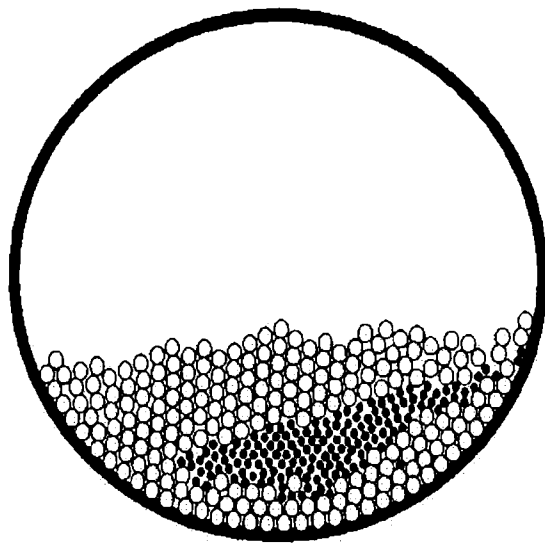
Figure 5.15:   Segregated solid bed of 20% of smaller particles and 80% of larger particles
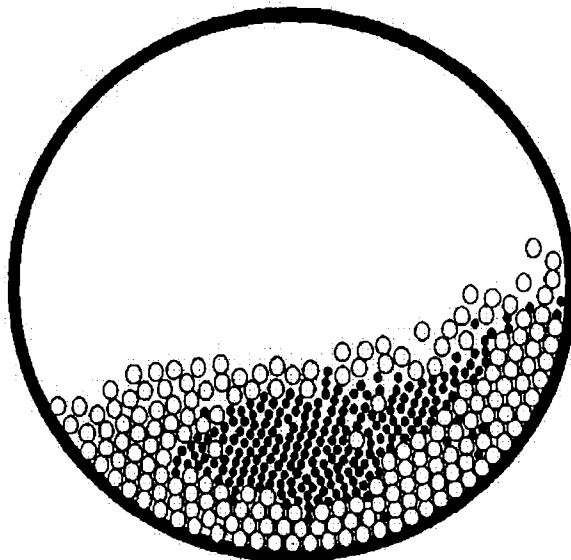
Figure 5.16:   Segregated solid bed of 30% of smaller particles and 70% of larger particles
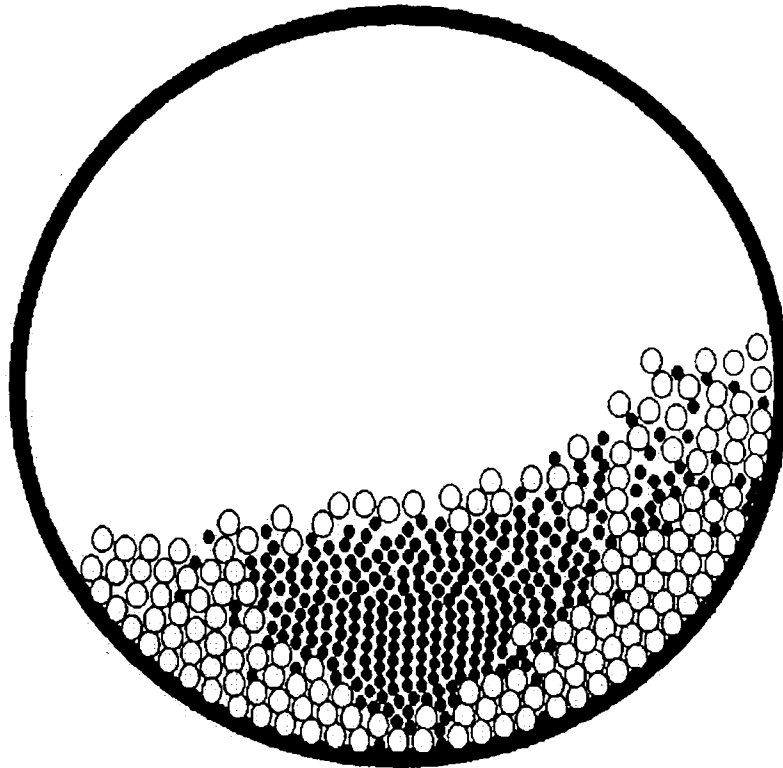
Figure 5.17: Segregated solid bed of 40% of smaller particles and 60% of larger particles

The percolation index was computed for granular solid bed consisting of volume fractions of two different sized particles. The values of percolation index is plotted against volume fraction of smaller particles as shown in Figure 5.18. The volume fractions of smaller particles was varied from 10 % to 50 %. It can be observed that percolation index decreases with increase in volume fraction of finer particles as expected.
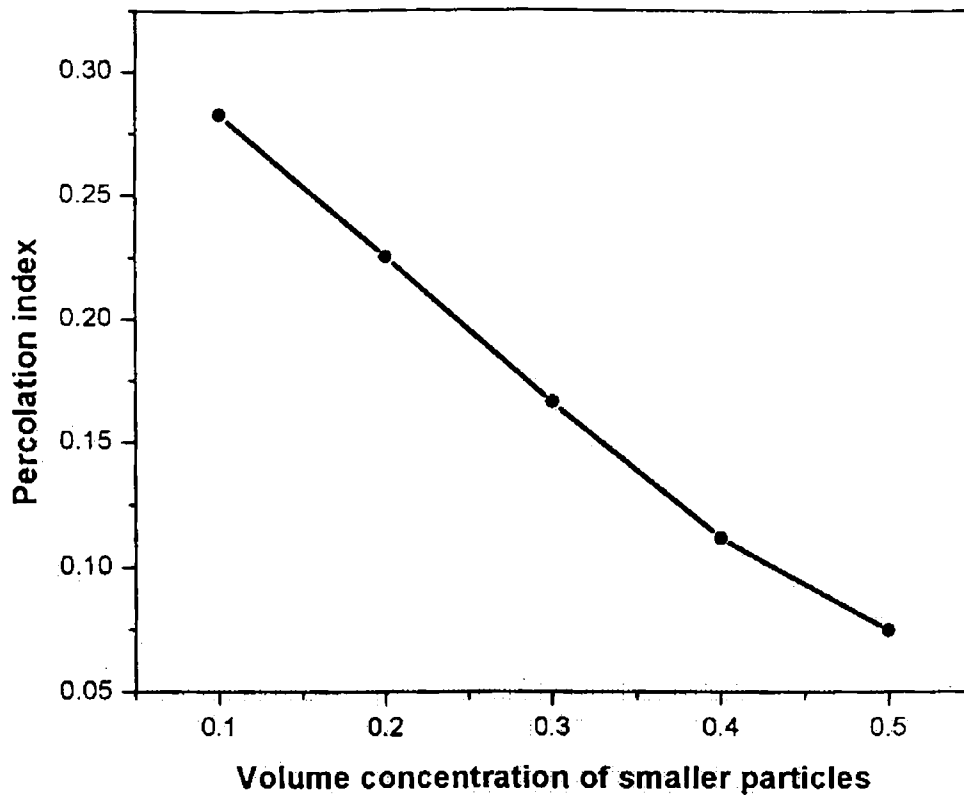
Figure 5.18: Percolation index vs volume fraction of smaller particles

5.4.4: Effect of particle density

The effect of particle density was studied using DEMCYL by simulating the granular bed with two different particle densities namely; 2500 kg/m^3 and 1300 kg/m^3. It is found that the denser particles forms an inner core in the granular bed as predicted by Ristow [1994]. The simulated figure is shown in Figure 5.19, where particles with 2500 kg/m^3 density are coloured with black and particles with 1300 kg/m^3 are coloured white.
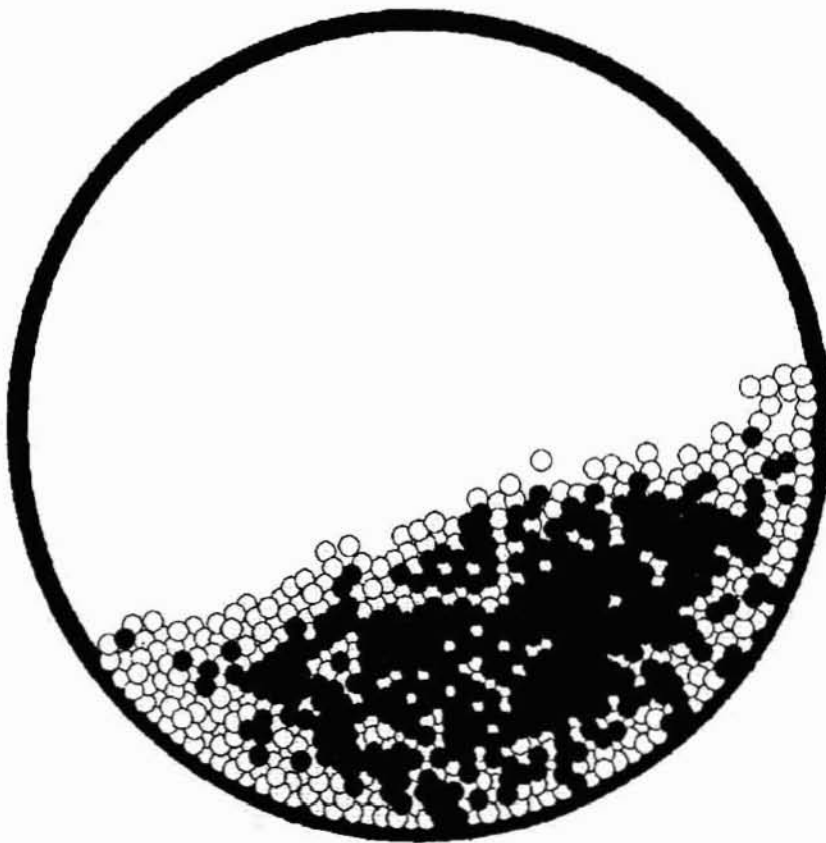
Figure 5.19: Segregation of denser particles.

5.5 Conclusion

In this Chapter an analysis of mixing and segregation in the transverse direction for different particle sizes, different particle densities, different volumetric concentrations and their size ratios is analysed using DEM simulation. The effect of fill fraction and rotational speed on the transverse mixing behaviour is presented in the form of a mixing index and mixing kinetics curve. The segregation pattern obtained by the simulation of the granular solid bed with respect to the rotational speed of the cylinder is presented as graphs. From the results of the numerical experiments through computer simulation, the macro parameters such as mixing index, percolation index, and segregation index are obtained.

CHAPTER 6

CONCLUSIONS

This Chapter summarises the significant contributions made towards interpreting the complex macroscopic behaviour of the granular bed motion in a horizontal rotating cylinder through a model based on DEM. Also, further work required to enhance our understanding and predictive capabilities of the model developed in this work is presented.

6.1   Conclusions

The motion of granular solids in the cross section of a horizontal rotating cylinder is simulated in this work by a theoretical model based on Discrete Element Method. The salient features of the present theoretical model are;

(a) There are no empirical parameters in the model
(b) There are no assumptions or any artificial boundary conditions are imposed at the boundaries as in the case with continuum models

The influence of the two important process variables namely; the fills fraction and rotational speed on the various regimes of granular solid bed motion is simulated in this work. The transition behaviour of the granular solids motion for the six different modes are predicted with the Froude Number as the basis and the results have been validated with the results reported by Mellmann [2001] and the agreement is found to be very good.

The criteria for the transition behaviour between slumping and rolling modes are quantified using the bed turn over time. The bed turn over time against

$\dfrac{1}{\omega}$, where ω is the angular speed in rad/s of the rotating cylinder showed a linear

relationship as predicted by Davidson *et al.*, [2000].

The depth active layer obtained through simulation are compared with the results predicted by Van Puyvelde *et al.*, [2000a] and the agreement is found to be very good. It has also been observed that the active layer depth does not depend on the particle size and cylinder diameter as observed by Van Puyvelde [2000a].

It has also been found that the active layer depth increases with rotational speed and decreases with degree of fill as predicted by Henein *et al.*,[1983a, 1983b]. Increasing the percentage of fill signifies that although excess material goes into shearing, the amount of material sheared is distributed over a longer chord length and hence the smaller increment in thickness. This behaviour leads to results in the observed decrease in percent active layer depth. The decreasing active layer depth with increased percent fill is therefore related to geometrical constraints.

The surface velocity profiles computed from the simulation results of this work showed a parabolic nature and the maximum surface velocity increased with rotational speed in a linear manner as predicted by Yamane *et al.* [1998].

The simulation code has been used to study the mixing and segregation behaviour of the granular solids at the cross section of the horizontal rotating cylinder. The mixing behaviour has been quantified in terms of a mixing index and a rate coefficient of mixing. It is observed that the rate coefficient of mixing increases with the rotational speed and the mixing index decreases with fill fraction at a given rotational speed.

The segregation behaviour of granular solids is simulated for a

(a) Granular solid bed comprising of different sized particles with varying volume fraction of finer sized particles

(b) Granular solid bed comprising of equal sized particles but with varying density. .

It is observed that the finer particles form an inner core and the predicted extent of the segregated core agrees with the experimental results reported by Henein [1983a]. Further denser particles formed an inner segregation core as observed by Ristow *et al.*, [1994].

The intensity of segregation intensity is quantified in terms of a percolation index. Other important conclusions are;

(a) A mathematical model for the granular solid bed dynamics based on first principles has developed and validated with the widely reported experimental results.

(b) It is found that fill fraction, rotational speed and particle size are the most sensitive parameters governing the flow behaviour.

(c) The depth of the active layer depth increases with increase in rotational speed. The coefficient of dynamic friction determines the dynamic angle of repose. The dynamic angle of repose increases with increase in the coefficient of dynamic friction up to a value of 0.5 and for higher values of friction coefficient, the dynamic angle of repose remains constant.

(d) The DEM model developed in this work is capable of quantitative predictions of concentration profiles of particles and the extent of segregation in the cross section of the rotating cylinder.

Finally it can be concluded that the present mathematical model is able to predict accurately particle concentration profile, velocity profiles, surface velocity profiles, active layer depth, individual particle trajectories, dynamic angle of repose, bed turn over time etc., thus providing a reliable and comprehensive model for the design, optimisation and interpretation of complex phenomena encounter in granular solids motion in horizontal cylinders.

6.2 Future Scope

1. The mathematical model should be extended to incorporate mass diffusion terms in the active layer, temperature effect due to heterogeneous reactions, so that it will enhance our knowledge on hot spots, product quality etc.

2. The simulation based on the mathematical model developed should be carried out in a more systematic way to study the effect of the following process variables directly relevant of scale up and real life problems involving rotary systems with granular solids

   i.   Cylinder diameter

   ii.   Continuous particle size distribution

   iii. Various particle shapes.

Nomenclature

a_i	Acceleration vector of the particle
A	Area of cross section of the solid bed
AL	Active layer
d	Size ratio of larger to smaller particles
$dp(i)$	Diameter of the particle i
d_{cij}	Position vector between the center of the contact area with the center of particle i
D	Distance between the centers of particle i and particle j
f	Volume fraction of black coloured particles
f_i	Over all proportion of smaller particles initially
f_{wi}	Percentage of particles of size $dp(i)$
F_{ij}	Force acting on the contact area between particle i and particle j
$F_{i,contact}$	Sum of direct contact forces acting on particle i
$F_{i,external}$	Sum of all external forces acting on Particle i.
$F_{i,gravity}$	Force of gravity acting on particle, i
$F_{n,ij}$	Normal component of the contact force between particle i and j
$F_{n,ij,dissipation}$	Normal energy dissipation force between particle i and particle j
$F_{n,ij,elastic}$	Normal elastic repulsion force between particle i and particle j
$F_{t,ij}$	Tangential component of the contact force between particle i and particle j.
$F_{t,ij,dynamic}$	Tangential dynamic friction force between particle i and particle j

$F_{t,ij,dissipation}$	Tangential dissipation force between particle i and particle j
$F_{t,ij,static}$	Tangential static friction force between particle i and particle j
Fr	Rotational Froude number
g	Acceleration due to gravity
h	Shortest distance between the cylinder center and the bed surface
h_{ij}	Depth of he overlap between particle i and particle j
H	Actual solid Bed
k	Spring stiffness coefficient
$k_{n,ij}$	Normal spring stiffness coefficient
KE	Total kinetic energy
I_i	Inertial tensor acting on particle i
I_{1i}, I_{2i}, I_{3i}	Components of inertial tensor acting on particle i
L	Half chord length of the bed surface
m_i	Mass of the particle, i
m_1, m_2	Slopes made by the particle i at its maximum and minimum x-position
n	Number of collision particle
n_c	Critical rotational speed of the cylinder
n_{ij}	Unit normal vector through the center of the overlap area between particle i and particle j
$np(i)$	Number of particles of size range $dp(i)$
N	Number of Particles
P_I	Percolation index
rpm	Rotations per minute
R	Cylinder radius

R_i	Radius of particle i
t_{ij}	Unit tangential vector through the center of the overlap area between particle i and particle j
$(t_{br})_r$	Bed turnover time in rolling mode
t_{12}	Avalanche time
t_{13}	Total cycle time
Δt	Time step
t	Time
T_c	Time of contact
T_i	Sum of all torques acting on particle i
T_{ij}	Torque acting on contact area between particle i and particle j
$T_{i,contact}$	Sum of all torques caused by contact forces acting on the particle i
$T_{i,fluid}$	Sum of all torques caused by anti-symmetric fluid drag forces
ΔT_c	Critical time step
$v_{t,ij}$	Tangential relative velocity vector between particle i and particle j
$\langle v \rangle$	Fluctuation of velocity
$\bar{v}$	Average velocity of particles in the segment
v_c	Overall solid volume fraction of larger particles in the bed
$\langle v_P \rangle$	Granular temperature
v	Volume concentration of solids
v^*	Minimum possible void fraction
v_{cij}	Velocity of particle I at the contact point of the particle i and particle j
v_{ij}	The relative velocity of the contact point between particle i and particle j

v_i	Velocity vector of the particle I
v_{nij}	Normal relative velocity vector between particle i and particle j
V_i	Volume of the particle i
Vs	Axial Solids Velocity
V_{xi}	x-component velocity of particle i
V_{yi}	y-Component velocity of particle i
x_i	Position vector of the particle i
x_{cij}	Position vector of the center of the overlap area between particle i and particle j
z	Dynamic angle of repose in slumping mode

ω	Angular velocity of the cylinder
β	Slope of the cylinder
ε	Dynamic angle of Repose
θ	Bed depth in angular measure
ψ	Exponent determined by dimensional analysis
θ_i	Angular displacement of Particle i
$\bar{\lambda}$	Dilation Factor
$\delta_{t,ij}$	Tangential relative velocity vector between particle i and particle j
η	Damping coefficient
μ	Friction coefficient
γ_n	Normal dissipation coefficient
Θ	Dynamic angle of repose
Θ_d	Dynamic angle of repose in slumping mode

Θ_s	Static angle of repose in slumping mode
ω	Angular velocity of the cylinder
δ_m	Maximum depth of the active region
ρ_i	Density of the Particle i
σ	Standard deviation for each set of particle in each segment
γ_t	Tangential dissipation coefficient
$\dfrac{\sigma}{\sigma_0}$	Degree of mixing
σ_0	Standard deviation obtained during the initial conditon of totally unmixed state
σ_r	Standard deviation for a random mixture of particles
ξ	Porosity

Bibliography

1. Abu Zaid. S. and G. Ahmadi, "Analysis of rapid shear flows of granular materials by a kinetic model including frictional losses", *Powder. Technol.* 77, 7 (1993).

2. Adams M. J. and B. J. Briscoe, *Deterministic micromechanical modelling of failure or flow in discrete planes of densely packed particle assemblies: Introductory principles*, A. Mehta, Editor, Granular Matter, Springer Verlag, 259, 1993.

3. Agrawala S, R. K. Rajamani, P. Songfack and B. K. Mishra, "Mechanics of media motion in tumbling mills with 3D Discrete Element Method", *Min. Eng.* 10(2), 215 (1997).

4. Ai-Bing Yu, Nicholas Standish and Arnold McLean, "Porosity calculation of binary mixtures of non spherical particles", *J. Am. Ceram. Soc.* 76(11), 2813 (1993).

5. Algis Dzingys and Bernhard Peters, "An approach to simulate the motion of spherical and non-spherical fuel particles in combustion chambers", *Granular. Matter* 3, 231 (2001).

6. Alonso M., M. Satoh and K. Miyanami, "Optimum combination of size ratio, density ratio and concentration to minimize free surface segregation", *Powder Technol.* 68, 145 (1991).

7. Allen M. P. and Tildseley D. F., *Computer Simulation of Liquids*, Clarenden Press, Oxford, 1987.

8. Ang, H. M., M. W. Sze, and M. O. Tade, "Residence time distribution for a cold model rotary kiln", The AUSIMM Proc. 1, 11 (1998).

9. Aoki K. M. and T. Akiyama, "Simulation studies of pressure and density wave propagations in vertically vibrated beds of granules", *Phys. Rev. E* 52(3), 3288 (1995).

10. Asmar B. N, P. A. Langston, A. J. Matchett and J. K. Walters, "Validation tests on a distinct element method of vibrating cohesive particle systems". *Comp. and Chem. Eng.* **26**, 785 (2002).

11. Bagnold R. A., "Experiments on a gravity-free dispersion of large solids spheres in Newtonian fluid under shear", *Proc. R. Soc. London* **A225**, 49 (1954).

12. Bak, P., C. Tang and K. Wiesenfeld, "Self-organized criticality: an explanation of 1/f noise", Phys. Rev. Lett. **59**, 381 (1987).

13. Baumann G., *Modelle und Computer simulationen granularer Materie*, PhD thesis, University of Duisburg, Duisburg, Germany (1997).

14. Baxter G. W. and R. P. Behringer, "Cellular automata models of granular flow", *Phys. Rev. A.* **42**, 1017 (1990).

15. Baxter G. W. and R. P. Behringer, "Cellular automata models for the flow of granular materials", *Physica D* **51**, 465 (1991).

16. Behringer R. P., "The Dynamics of flowing sand", *Nonlinear Science Today* **3**, 1 (1993).

17. Behringer R. P., "Mixed Predictions", *Nature* **374**, 15 (1995).

18. Bideau D. and A. Hansen, Eds., *"Disorder and Granular Media"*, Random Materials and Processes Series, Elsevier Science Publishers B. V., Amsterdam, North-Holland, 1993.

19. Boateng A. A, *"Rotary kiln transport phenomena"*, Ph. D thesis, University of British Columbia, Canada, 1993.

20. Boateng A. A and P. V. Barr, "Modelling of particle mixing and segregation in the transverse plane of the rotary kiln", *Chem. Eng. Sci.* **51**, 4167 (1996).

21. Boateng and P. V. Barr, "Granular flow behaviour in the transverse plane of a partially filled rotating cylinder", *J. Fluid Mech.*, **330**, 233 (1997).

22. Bridgwater J., "Fundamental powder mixing mechanisms", *Powder. Technol.* **15**, 213 (1976).

23. Bridgwater J., W. S. Foo and D. J. Stephens, "Particle mixing and segregation in failure zones-theory and experiment", *Powder. Technol.* **41**, 147 (1985).

24. Bridgewater J., "Particle technology", *Chem. Eng. Sci.* **50**, 4081 (1995).

25. Broadbent, C.J., P. Knight, S.T. Keningley, D.J. Parker and J Bridgwater, "A phenomenological study of a batch mixer using a positron camera", *Powder. Technol.* **76**, 317 (1993).

26. Camp P.J. and M. P. Allen, "Hard ellipsoid rod-plate mixtures: Onsager theory and computer dimulation", *Physica A* **229**, 210 (1996).

27. Campbell. C. S. and C. E. Brennen, "Computer simulation of granular shear flows", *J. Fluid Mech.* **151**, 167 (1985).

28. Campbell. C. S., "Rapid granular flows", *Annu. Rev. Fluid Mech.*, **22**, 57 (1990).

29. Cantelauble F., D. Bideau and S. Roux, "Kinetics of segregation of granular media in a two-dimensional rotating drum", *Powder Technol.* **93**, 1 (1997).

30. Caram H. and D. C. Hong, "Random walk approach to granular flows", *Phys. Rev. Lett.* **67**, 828 (1991).

31. Caram, H. and D. C. Hong, "Diffusing void model for granular flow", *Mod. Phys. Lett. B* **6**, 761 (1992).

32. Chakraborty S., P. R Nott and J. Ravi Prakash, "Änalysis of radial segregation of granular mixtures in a rotating drum", *Eur. Phys. J. E.*, **1** 265 (2000).

33. Chaterjee, A., Mukhopadhyay, P.K., Srivastava, M.P and Sathe, A.V., "Flow of materials in rotary kilns used for sponge iron manufacture, Part 1: effect of some operational variables", *Metall. Trans. B* **14B**, 375 (1983).

34. Cleary, P. W., "The filling of dragline buckets", *Math. Eng. in Ind.*, **7**, 1 (1998a).

35. Cleary, P. W., " Predicting charge motion, power draw, segregation and wear in ball mills using discrete element methods", *Min. Eng.* **11**, 1061 (1998b).

36.   Cleary, P. W., Metcalfe, G., Liffman, K., "How well do discrete element granular flow models capture the essentials of mixing processes?" *Appl. Math. Modelling* **22**, 995 (1998).

37.   Cleary, P. W., "DEM simulation of industrial particle flows: case studies of dragline excavators, mixing in tumblers and centrifugal mills", *Powder. Technol.* **109**, 83 (2000).

38.   Cleary, P. W., " Modelling comminution devices using DEM ". *Int .J. Num. Analy. Meth. in geomechanics* **25**, 83 (2001).

39.   Clement E., Rajchenbach J and Duran J., "Mixing of granular material in a bidimensional rotating drum", *Europhys. Lett.* **30**, 7 (1995).

40.   Coulomb C., in *Memoir de Mathematique et de Phy-sique* 7, Academie des, 1773.

41.   Cundall P. A. and O. D. L. Strack, "A discrete numerical model for granular assemblies", *Geotechnique* **29**, 47 (1979).

42.   Davidson J. F., D. M. Scott, P. A. Bird, O. Herbet, A. A. Powell and H. V. M Ramsay, "Granular motion in a rotary kiln: the transition from avalanching to rolling", *KONA powder and particle* **18**, 149 (2000).

43.   Davies, T. R. H, "Large Debris flow: A macro-viscous phenomenon", *Acta Mech.* **63**, 161 (1986).

44.   de Jong, G. de J., *"Lower bound collapse theorem and lack of normality of strain rate to yield surface for soils"*, Rheology of soil mech. Symp., Grenoble, 69, 1964.

45.   Devillard P., "Scaling behaviour of size segregation (Brazil Nuts)", *J. Phys. 1 France* **51**, 369 (1990).

46.   Ding Y. L., R. N. Forster, J. P. K. Seville, D. J. Parker, "Solids motion in the rolling mode rotating drums operated at low to medium rotational speeds", *Chem. Eng. Sci.* **56**, 1769 (2001).

47. Ding Y. L., R. Forster, J. P. K. Seville and D. J. Parker, "Granular motion in rotating cylinders, bed turnover time and slumping-rolling transition", *Powder. Technol* **124**, 18 (2002).

48. Du, Y., H. Li and L. P. Kadanoff, "Breakdown of hydrodynamics in a one-dimensional system of inelasatic particles", *Phys. Rev. Lett.* **74**, 1268 (1995).

49. Dury C. M. and Ristow G. H, "Boundary effect on the angle of repose in rotating cylinders, "*Phy. Rev. E.* **57**, 4491 (1998).

50. Enni B. J., J. Green, and R. Davies, "The legacy of neglect in the U.S.," *Chem. Eng. Prog.* **90**, 32 (1994).

51. Fan L. T., Y. M. Chen, F. S. Lai, "Recent developments in solids mixing", *Powder. Technol.* **61**, 255 (1990).

52. Faraday M., "On a peculiar class of acoustical figures; and on certain forms assumed by groups of particles upon vibrating elastic surfaces", *Phil. Trans. R. Soc. London* **52**, 299 (1831).

53. Fitt, A. D. and P. Wilmott, Cellular-automaton model for segregation of a two-species granular flow", *Phys. Rev. A* **45**, 2383 (1992).

54. Form W., N. Ito and G. A. Kohring, "Vectorized and parallelized algorithms for multi-million particle MD-simulation", *Int. J. Mod. Phys. C* **4**, 1085 (1993).

55. Gilkman E., I. Kelson, N. V. Doan and H. Tietzet, "An optimized algorithm for molecular dynamics simulation of large-scale systems", *J. Comp. Phys.* **124**, 85 (1996).

56. Grest G. S., B. Dunweg and K. Kremer, "Vectorized link cell Fortran code for molecular dynamics simulations for large number of particles", *Computer phys. Comm.* **55**, 269 (1989).

57. Gu Z. H, P. C. Arnold and A. G. McLean, "Prediction of the flow rate of bulk solids from mass flow bins with conical hoppers", *Powder. Technol.* **72**, 157 (1992).

58. Haff P. K., *Discrete Mechanics*, In A. Mehta, editor, Granular matter, Springer-verlag, 141 1993.

59. Hawkesworth, M.R., G. Jonkers, N. L. Jeffries, J.F. Crilly, P. Fowles and D.J. Parker, "Non-medical applications of a positron camera", *Nucl. Instrum. Meth. A* **310**, 423 (1991).

60. Hayakawa H., H. Nishimori, S. Sasa, and Y. H. Taguchi, "Dynamics of granular matter", *Jpn. J. Appl. Phys.* **34**, 397 (1995).

61. Henein H., J. K. Brimacombe and A. P. Watkinson, "Experimental study of transverse bed motion in rotary kilns", *Met. Trans. B*, **14B**, 191 (1983a).

62. Henein H., J. K. Brimacombe and A. P. Watkinson, " The modelling of transverse solids motion in rotary kilns", *Met. Trans. B* **14B,** 207 (1983b).

63. Henein H., J. K. Brimacombe and A. P. Watkinson, "An experimental study of segregation in rotary kilns, *Met. Trans. B* **16B,** 763 (1985).

64. Henein H., *Radial segregation in rotary kilns: a review*, in Forrest-Holden, M. J., (Ed.), Rotary Kiln Technology, World Cement Publication, London, 34, 1987.

65. Hiseman, M.J.P., D.I. Wilson and J. Bridgwater, "Positron emission particle tracking studies of powder mixing in a planetary mixer", *Proc. of Frontiers in Ind. Proc. Tomography*, Delft (1997).

66. Hogg R, D. S. Cahn, T. W. Healy and D. W. Fuerstenau, "Diffusional mixing in an ideal system", *Chem. Eng. Sci.* **21**, 1025 (1966).

67. Hogg R. and D. W. Fuerstenau, "Transverse mixing in rotating cylinders", *Powder. Technol.* **6,** 139 (1972).

68. Hogue C. and D. Newland, "Efficient computer computation of moving granular particles", *Powder. Technol.* **78**, 51 (1994).

69. Hong, D. C., "Dynamic model for granular assembly", *Int. J. Mod. Phys. B* 7, 1929 (1993).

70.   Hoomans B. P. B., J. A. M. Kuipers, W. J. Briels and W. P. M. Van Swaiij, "Discrete particle simualiton of bubble and slug formation in two-dimensional gas-fluidised bed: A hard sphere approach", *Chem. Eng. Sci.* **51**, 99 (1996).

71.   Jaeger H. M. and S. R. Nagel, "The physics of the granular state", *Science* **255**, 1523 (1992).

72.   Jaeger, H. M., J. B. Knight, C. H. Liu, and S. R. Nagel, "What is shaking in the sand box", *Mater. Res. Bull.* **19**, 25 (1994).

73.   Jaeger H. M., S. R. Nagel, and R. P. Behringer, "The Physics of Granular Materials", *Physics Today* **4**, 32 (1996a).

74.   Jaeger H. M., S. R. Nagel and R. P. Behringer., "Granular solids, liquids and glasses", *Rev. Mod. Phys.* **68**, 1259 (1996b).

75.   Johnson P. C. and R. Jackson, "Frictional-collisional constitutive relations for granular materials, with application relations to plane shearing, *J. Fluid Mech.* **176**, 67 (1987).

76.   Jones, J.R. and J.Bridgwater, "A case of particle mixing in a ploughshare mixer using positron emission particle tracking", *Int. J. Miner. Processing* **53**, 29 (1998).

77.   Khakhar D. V, J. J McCarthy, T Shinbrot, J. M. Ottino., "Transverse flow and mixing of granular materials in a rotating cylinder", *Phys. Fluids* **9**, 31 (1997a).

78.   Khakhar D. V, J. M. Ottino and J. J McCarthy, "Radial segregation of granular mixtures in rotating cylinders", *Phy. Fluids* **9**, 3600 (1997b) .

79.   Kitarev V and D. Wolf, "A cellular automata for grains in a rotating drum", *Comput. Phys. Comm.* **121**, 303 (1999).

80.   Knowlton T. M., J. W. Carson, G. E. Klinzing, and W. C. Yang, "The importance of storage, transfer, and collection", *Chem. Eng. Prog.* **90**, 44 (1994).

81.   Kohring G. A, "Studies of diffusional mixing in rotational drums via computer simulations", *J. Phys. I France* **5**, 1551 (1995).

82. Kopf A., W. Paul and B. Dunweg, "Multiple time step integrators and momentum conservation", *Comp. Phy. Comm.* **101**, 1 (1997).

83. Kornilovsky A. N., D. R. Kingdom and A. A. Harms, "Pellet dynamics of fuel pellets in suspension", *Ann. Nucl. Energ.* **23**, 171 (1996).

84. Kumaran V., "Velocity distribution function for a dilute granular material in shear flow", *J. Fluid Mech.* **340**, 319 (1997).

85. Lacey P.M., "Developments in the theory of particle mixing", *J. Appl. Chem.* **4**, 257 (1954).

86. Landau L. D. and E. M. Lifshitz, *Mechanics, Volume 1 of the course of Theoretical physics*, Pergamon Press, 1960.

87. Laurent, B., D. J. Parker, and J. Bridgwater, "Motion in a particle bed stirred by a single blade", *AIChE J.* **46**, 1723 (2000)..

88. Lee J. and H. J. Hermann, "Angle of repose and angle of marginal stability: Molecular dynamics of granular particles", *J. Phys. A* **26**, 373 (1993).

89. Lehmberg J., M. Hehl and K. Schugerl, "Transverse mixing and heat transfer in horizontal rotary drum reactors", *Powder. Technol.* **18**, 149 (1977).

90. Levitan B., "Segregation and coarsening of granular mixture in a rotating tube", *Physica A* **249**, 386 (1998).

91. Lubachevsky B. D., "How to simulate billiards and similar systems", *J.Comp. Physics* **94**, 255 (1991).

92. Lubachevsky B. D., V. Privman and S. C. Roy, "Casting pearls ballistically: efficient massively parallel simulation of particle depositions", *J. Comp. Physics* **126**, 152 (1996).

93. Luding S., J. Duran, E. Clement and J. Rajchenbach, "Simulation of dense granular flow: Dynamic arches and spin organization", *J. Phys. I France* **6**, 823 (1996).

94. Lun, C. K. K. and A. A. Bent, "Numerical simulation of inelastic frictional spheres in simple shear flow", *J. Fluid Mech.* **258**, 335 (1994).

95. Mandl. G and R. F. Luque , "Fully developed plastic shear flow of granular materials", Geotechnique **20**, 277 (1970).

96. McCarthy J. J., J. M. Ottino, J. Eduardo wolf, G. Metcalfe and T. Shinbort, "Mixing of granular materials in slowly rotated containers", *AIChE J.* **42**, 3351 (1996).

97. McNamara, S. and W. R. Young. " Inelastic collaps and clumping in a one-dimensional granular medium ", *Phys. Fluids A* **4**, 496 (1992).

98. McNamara, S. and W. R. Young. "Kinetics of a one-dimensional granular medium in a quasielastic limit", *Phys. Fluids A* **5**, 34 (1993).

99. McNamara, S. and W. R. Young, " Dynamics of a freely evolving, two-dimensional granular medium ", *Phys. Rev. E* **53**, 5089 (1996).

100. McTait, G.E., *"Residence times and solid flows in rotary kilns"*, PhD thesis, Dept. Chem. Engg., University of Cambridge, 1998.

101. Mehta, A., Ed., *"Granular Matter: An Interdisciplinary Approach"*, Springer, New York, 1994.

102. Mellmann J., "The transverse motion of solids in rotating cylinders–forms of motion and transition behaviour *Powder. Technol.* **118**, 251 (2001).

103. Metcalfe, G., J. M. Ottino, J.J. McCarthy and T. Shinbrot, "Avalanche mixing of granular solids ", *Nature* **374**, 39 (1995).

104. Mindlin R. D., "Compliance of elastic bodies in contact", *J. appl. Mech.* **71(3)**, 259 (1949).

105. Mishra B. K. and R. K. Rajamani, "The discrete element method for the simulation of ball mills", *Appl. Math. Modeling* **16**, 598 (1992).

106. Muguruma Y., T. Tanaka, S. Kawatake and Y. Tsuji, "Discrete particle simulation of a rotary vessel mixer with baffles", *Powder Technol* **93**, 261 (1997).

107. Nakagawa, M., E.K. Jeong, E. Fukushima, A. Caprihan and S. A. Altobelli, "Non-invasive measurement of granular flows by magnetic resonance imaging", *Exp. in Fluids* **60**, 54 (1993).

108. Nedderman, R.M., *"Statics and Kinematics of Granular Materials"*, Cambridge University Press, 1992.

109. Newmark N. M and F. Asce, "A method of computation for structural dynamics", *J. Eng. Mech. Div. Proc ASCE(EM3.* **85**, 67 (1959).

110. Nityanand N., B. Manley and H. Henein, "An analysis of radial segregation for different sized spherical solids in rotary cylinders", *Met. Trans. B* **17B**, 247 (1986).

111. Ouchiyam N. and T. Tanaka, "Porosity estimation of random packings of spherical particles", *Am. Chem. Soc.* **23**, 490 (1984).

112. Ottino J. M., *"The kinematics of Mixing, Stretching, Chaos, and Transport"*, Cambridge Univ. Press, Cambridge, 1989.

113. Ovensen J. H., H. G. Petersen and J. W. Perram, "Comparison of two methods for solving linear equations occurring in molecular dynamics applications", *Comp. Phy. Comm.* **94**, 1(1996).

114. Oyama, Y., (Japanese), "Mixing of solids", *Bull. Inst. Phys. Chem. Res. Jpn. Rep.* **18**, 600(1939). English translation 1958, *Adv. Chem. Eng.* **2**, 211 (1958).

115. Parker, D.J., P.A. McNeil, M.R. Hawkesworth, P. Fowles and C.J. BroadBent, C.J, "Positron emission particle tracking - a technique for studying flow within engineering equipment", *Nucl. Instrum. Meth. A* **236**, 592 (1993).

116. Parker, D.J., P.A. McNeil, T. D. Fryer, P. Fowles, C.J. Broadbent and M.R. Hawkesworth., "Industrial positron-based imaging: principles and applications", *Nucl. Instrum. Meth. A* **348**, 583 (1994).

117. Parker, D.J., J.P.K. Seville, T.W. Martin, and A.E. Dijkstra, "Positron emission particle tracking studies of spherical particle motion in rotating drums", *Chem. Eng. Sci.* **52**, 2011 (1997).

118. Perron J. and R.T. Bui, "Rotary cylinders: Solid transport prediction by dimensional and rheological analysis", *Can. J. Chem. Eng.* **68**, 61 (1990).

119. Pershin V. R. and G. A. Mineav, "Modelling the mixing of a granular material in a cross section of a smooth rotating drum", *Theor. Found. Chem. Eng.* **23**, 249 (1989).

120. Polderman H. G., J. Boom, E. De Hilster and A. M. Scott, "Solids flow velocity profiles in mass flow hoppers", *Chem., Eng. Sci.* **42**, 737 (1987).

121. Pollard B. L. and H. Henein, "Kinetics of radial segregation of difference sized irregular particles in rotary cylinders", *Can. Met. Quart.* **28**, 29 (1989).

122. Poux M., P. Fayolle, J. Bertrand, D. Bridoux and J. Bousquet, "Some practical rules applied to agitated systems", *Powder. Technol.* **68**, 214 (1991).

123. Puri S. and H. Hayakawa, "Dynamical behaviour of rotated granular mixtures", *Physica A* **270**, 115 (1999).

124. Rajamani R. K., B. K. Mishra, R. Venugopal and A. Dutta, "Discrete element analysis of tumbling mills", *Powder. Technol.* **109**, 105 (2000).

125. Rajchenbach J., "Flow in powders: from discrete avalanches to continuous regime", *Phys. Rev. Lett.* **65**, 2221 (1990).

126. Reynolds O., On the dilatancy of media composed of rigid particles in contact with experimental illustrations", *Philos. Mag.* **20**, 469 (1885).

127. Ristow G. H., "Particle mass segregation in a two-dimensional rotating drum" *Europhys. Lett.* **28**, 97 (1994).

128. Ristow G. H., "Dynamics of granular materials in a rotating drum", *Europhys. Lett.* **34**, 263 (1996).

129. Rogers A. and J. A. Clements, "The examination of segregation of granular materials in a tumbling mixer", *Powder Technol.* **5**, 167 (1971).

130. Rosato A., K. J. Strandburg, F. Prinz and R. H. Swendsen, "Why the brazil nuts are on top: size segregation of particular matter by shaking", *Phys. Rev. Lett.* **58**, 1038 (1987).

131. Roscoe. K. H., "The influence of strains in soil mechanics", *Geotechnique* **20**, 129 (1970).

132. Roseman, B. and M.B. Donald, "Mixing and de-mixing of solid particles part 2: effects of varying the operating conditions of a horizontal drum mixer", *Brit. Chem. Eng.* **7**, 823 (1962).

133. Runesson. K and L. Nilsson, "Finite element modeling of the gravitational flow of a granular material", *Bulk solids* **6**, 877 (1986).

134. Rutgers R., "Longitudinal mixing of granular material flowing through a rotary cylinder: part I–Description and theoretical", *Chem. Eng. Sci.* **20**, 1079 (1965).

135. Sadd M. H., Q. Tai and A. Shukla, "Contact law effects on wave propagation in particulate materials using distinct element modelling", *Int. J. Non-Linear Mech.* **28**, 251 (1993).

136. Sai, P.S.T., A.D Damodaran,. and G.D Surender,.., Prediction of axial velocity profiles and solids hold-up in a rotary kiln, *Can. J. Chem. Eng.* **70**, 438 (1992).

137. Sai, P.S.T., K. Sankaran, Z.G. Philip, V. Suresh, A.D. Damodaran, and G.D. Surender, "Residence time distribution and material flow studies in a rotary kiln", *Met. Trans. B* **21B**, 1990 (1990).

138. Satoh A, "Molecular dynamics simulations on internal structures of normal shock waves in Lennard-Jones liquids", *ASME J. Fluid Mech.* **117**, 97 (1995a).

139. Satoh A, "Stability of computer algorithms used in molecular dynamics simulations", *ASME J. Fluid Mech.* **117**, 531 (1995b).

140. Savage S B, "Gravity flow of cohesionless granular materials in chutes and channels", *J. Fluid Mech.* **92**, 53 (1979).

141. Savage S. B. and C. K. K. Lun, "Particle size segregation in inclined chute flow of dry cohesionless granular materials," *J. Fluid Mech.* **189**, 311 (1988).

142. Savage S. B., "Streaming motions in a bed of vibrationally fluidized dry granular material", *J. Fluid Mech.* **194**, 457 (1988).

143. Seaman, W. C., "Passage of solids through Rotary Kilns: Factors Affecting Time of Passage", *Chem. Eng. Prog.* **47**, 508 (1951).

144. Shida K, R. Suzuki and T. Kawai, "Numerical error of total energy: Dependence on time step", *Comp. Phys. Comm.* **102**, 59 (1997).

145. Singh D. K., *"A fundamental study of the mixing of solid particles"*, University of Rochester, Rochester, 1978.

146. Spencer, A. J. M., "A theory of the kinematics of ideal soils under plane strain conditions", *J. Mech. Phys. Solids* **12**, 337 (1964).

147. Spurling R. J., *"Granular flow in an inclined rotating cylinder: steady state and transients"*, University of Cambridge, Dept. of Chem. Eng., (2000).

148. Sriram V. and P. S. T. Sai, "Transient response of granular bed motion in rotary kiln", *Can. J. Chem. Eng.* **77**, 597 (1999).

149. Sullivan J. D., C.G. Maier and O.C. Ralston, "Passage of solid particles through rotary cylindrical kilns", *US Bureau of Mines, Technical Papers* **384**, 1 (1927).

150. Sundaram S. and L.R. Collins, "Numerical considerations in simulating a turbulent suspension of finite-volume particles", *J. Comp. Phys.* **124**, 337 (1996).

151. Thompson P. A and G. S. Grest, "Granular flow: Friction and the dilatancy transition", *Phy. Rev. Lett.* **67**, 1751 (1991).

152. Tsuji Y., T. Kawaguchi and T. Tanaka, "Discrete particle simulation of two-dimensional fluidized bed", *Powder. Technol.* **77**, 79 (1993).

153. Van Gunsteren. W. F. and H. J. C. Berendsen, "Algorithm for macromolecular dynamics and constraint dynamics", *Mole. Phys.* **34**, 1311 (1977).

154. Van Puyvelde D R., B. R. Young, M. A. Wilson and S. J. Schmidt, Experimental determination of transverse mixing kinetics in a rolling drum by image analysis", *Powder. Technol.* **106**, 183 (1999).

155. Van Puyvelde D. R., B. R. Young M. A. Wilson and S. J. Schmidt, "Modelling transverse mixing in a rolling drum", *Can. J. Chem. Eng.* 78, 635 (2000a).

156. Van Puyvelde D R., B R Young, M A Wilson and S J Schmidt, "Modelling transverse segregation of particulate solids in a rolling drum", *Trans. I Chem.* 78, 643 (2000b).

157. Walton O. R. and R. L. Braun, *"Proceedings of the Joint DOE/NSF Workshop on the Flow of Particulates and Fluids"*, 29 September–1 October, Ithaca, New York. 131(1993).

158. Weidenbaum, S.S. and C.F. Bonilla, "A fundamental study of the mixing of particulate Solids", *Chem. Eng. Prog.* 51, 27 (1955).

159. Woodle G. R. and J. M. Munro, "Particle-motion and mixing in a rotary kiln", *Powder. Technol.* 76, 241 (1993).

160. Yamane K., T. Sato, T. Tanaka and Y. Tsuji, "Computer simulation of tablet motion in coating drum", *Pharm. Res.* 12, 1264 (1995).

161. Yang L. and B. Farouk, "Modelling of solid particle flow and heat transfer in rotary kiln calciners", *J. Air Waste Manage. Assoc.* 47, 1189 (1997).

162. Yamane K., M. Nakagawa, S. A. Altobelli, T. Tanaka and Y. Tsuji, "Steady particulate flows in a horizontal rotating cylinder", *phys. Fluids* 10(6), 1419 (1998).

List of Publications

1. **V. Hema**, S. Savithri, G. D. Surender, "Numerical Simulation of Granular Material Motion in a Rotating Cylinder", Proceedings International Seminar on Mineral Processing Technology (MPT), 307 – 317, 2002.

2. **V. Hema**, S. Savithri, G. D. Surender, "Transition Behaviour of Solids Motion in a Rotating Cylinder through Discrete Element Simulation", Proceedings International Seminar on Mineral Technology (MPT), 138-143, 2003.

3. **V. Hema**, S. Savithri, G. D. Surender, "Mathematical Modelling of Granular Material Motion in a Rotating cylinder using Discrete Element Simulation", National Seminar on Science and Technology of Advanced Engineering Materials, 2003.

4. **V. Hema**, S. Savithri, G. D. Surender, "Dynamics of granular solids motion in the transverse plane of rotating cylinder", (communicated).

5. **V. Hema**, S. Savithri, G. D. Surender, "Mixing and segregation behaviour of granular materials in a rotating cylinder", (communicated).